Summer 8-18-2017

Characterization of Paper Dusting

Gregory K. Yum
University of Maine, gregory.yum@gmail.com

CHARACTERIZATION OF PAPER DUSTING

By

Gregory Yum

B.S. University of Maine, 2013

A THESIS

Submitted in Partial Fulfillment of the

Requirements for the Degree of

Master of Science

(in Chemical Engineering)

The Graduate School

The University of Maine

August 2017

Advisory Committee

Douglas Bousfield, Professor of Chemical and Biological Engineering, Advisor

Michael Mason, Professor of Chemical and Biological Engineering

Mehdi Tajvidi, Assistant Professor of School of Forest Resources

CHARACTERIZAITON OF PAPER DUSTING

By Gregory K. Yum

Advisor: Dr. Douglas W. Bousfield

An Abstract of the Thesis Presented
in Partial Fulfillment of the Requirements for the
Degree of Master of Science
(in Chemical Engineering)
August 2017

Dusting of paper in various printing and processing operations is a common problem. The dusting tendency of a paper is difficult to characterize with standard laboratory methods; there is currently no standard test available. As the trend to create grades with high filler content continues, the issue of dusting will remain important. The goal of this thesis was to explore various methods to characterize the dusting and linting in a laboratory environment with limited samples and time.

Techniques to cause and collect dust are compared that include a tape pull test, a bending test, and an abrasion test. Methods to collect dust are also compared that involve gravity settling of particles, electrostatic collection, and filter methods. The collected samples are imaged using an optical microscope and a flat bed scanner and analyzed using image analysis software. Six grades of commercial paper and three grades of handsheets with various filler loadings are compared and dust is collected from an industrial test and a laser printer.

In comparison with using gravity and electrostatic attraction, air filtration is found to be the best solution for collecting dust. The abrasion of paper against a rod gave the best repeatable results. The bending test measuring edge effects gives results that are significantly different between methods of cutting. The tests using the handsheets are conclusive in that increasing filler loading increases the dusting: all three methods agree with this expected result.

Dust collected from the back panel of a laser printer reveals that one commercial sample had low dusting and two samples had high dusting, compared to the other samples. Scanning electron microscope (SEM) and optical microscope images shows that both fibers and filler particles are present in the dust from the laser printer. No other tests found significant differences between the commercial samples. An increase in dust is found near the outer edges of the laser printer's guide rail. A test to measure edge effects showed an increase of dusting when paper is cut using the initial factory cut edges versus the edges of paper when cut by a standard benchtop paper cutter. The bending and abrasive test relates to industrial dust test results for particles over 40μm.

ACKNOWLEDGMENTS

I would first like to thank my advisor, Dr. Douglas W. Bousfield. Professor Bousfield has been my supervisor for many years, stretching well into my undergraduate career. He has always been a great advisor and was always willing to meet despite his busy schedule. I would like to acknowledge his hard work and dedication to the student of our department and that I appreciate everything that he has done.

I would like to thank my other two advisors, Dr. Michael Mason and Dr. Mehdi Tajvidi for their time spent being great advisers, for their assistance and for the irreplaceable experience that I have gained while working with them.

I would like to thank the sponsors of the Paper Surface Science Program for their assistance and the time spent working with us. I appreciate the representatives participating in the bi-annual meetings and their advice and assistance was always welcome.

I would like to thank my friend and colleague, Lisa Weeks, for all the time she spent giving advice, listening endlessly about my research and for her time spent managing the lab. Throughout all the hours spent working in the lab, she made the time in the west graduate lab a better place and I really want to thank her for all that she has done.

I would like to thank Amos Cline for his help in the lab. Amos was always willing to assist me with my project and I enjoyed the conversations that we had about science, physic and the information around this project.

Lastly, I would like to thank the graduate students in Chemical Engineering who made the time spent in Jenness Hall an enjoyable place to be.

TABLE OF CONTENTS

ACKNOWLEDGMENTS ii

LIST OF TABLES vi

LIST OF FIGURES viii

1. INTRODUCTION 1

1.1. Motivation 1

1.2. Dust and Linting 1

1.3. Paper Making Process 2

1.4. Particle Properties 3

1.5. Printing Process 4

1.6. Paper Parameters Linked with Dusting 5

1.7. Current Linting and Dust Testing Equipment 7

1.8. Thesis Summary 10

2. DUST TEST EQUIPMENT DESIGN 11

2.1. Introduction 11

2.2. Image Capture Methods 11

2.3. Particle Analysis 13

2.4. Particle Collection Methods 20

2.5. Testing Method 1: Paper Dust Tester 22

2.6. Testing Method 2: Tape Test 29

2.7. Summary 32

3. DUSTING RESULTS FROM FILLER LOADING PARAMETERS 33

3.1. Introduction 33

3.2. Experimental 33

3.2.1. Study 1-3: Dusting Tests from Test Method 1 34

3.2.2. Study 4: Tape Tests 36

3.2.3. Comparison Tests 37

3.3. Results and Discussion 39

3.3.1 Results for Comparison Tests 40

3.3.2. Results from Bending Test 45

3.3.3. Results from Edges Effect Test 47

3.3.4. Results from Abrasive Test 50

3.3.5. Results from Tape Pull Test 52

3.3.6. Correlations 54

3.4. Discussion 55

3.5. Conclusions 56

4. CONCLUSIONS AND FUTURE WORK 58

4.1. Concluding Remarks 58

4.2. Future Work 59

REFERENCES 63

APPENDIX A. SLITTER DUST TEST 65

APPENDIX B. ELECTROSTATIC FORCES BASED ON HUMIDITIY 67

APPENDIX C. PARTICLE SIZE DISTRIBUTION 70

APPENDIX D. SCANNING THRESHOLD IMAGES 72

APPENDIX E. TABLE OF ANOVA AND CORRELATIONS 75

APPENDIX F. ADDITIONAL MICROSCOPE IMAGES 82

APPENDIX G. INSTRUCTIONS FOR SCANNING PARTICLES 85

Appendix H. RAW DATA 89

Appendix I. IMAGEJ PROGRAM FOR A SINGLE IMAGE 109

BIOGRAPHY OF THE AUTHOR 153

LIST OF TABLES

Table 2.1 Tests to determine optimal parameter conditions. 25

Table 2.2 Basic Statistics of sample B performed 10 times on the Paper Dust Tester. Particle count number is in units of particles per sheet and surface area number is in units of squared millimeters per sheet. 28

Table 2.3 Basic Statistics of sample B performed on the Tape Test. The surface area number has units of square millimeters per sheet. 31

Table 2.4 Summary of Parameters for each test method. 32

Table 3.1 Names and ID's of the Commercial Paper Grades. 34

Table 3.2 Testing Parameters for Study 1. Test for paper dusting caused by bending and stressing the paper. 35

Table 3.3 Testing parameters for study 2, paper dusting caused by edge effects when the paper is bent and stressed..... 35

Table 3.4 Testing parameters for study 3, paper dusting caused by abrading the paper over a rod. 36

Table 3.5 Testing Parameters for study 4, removal of surface contamination from the tape test. 37

Table 3.6 Properties of the three handsheets formed tested under standard Tappi conditions. 39

Table 3.7 Properties of the six commercial grade papers tested under the standard Tappi conditions. 39

Table 3.8 Fiber properties of the size commercial grades of paper. 40

Table A.1 Slitter dust correlation to paper properties as stated from adapted simple slitter dust test. 66

Table B.1 Testing materials and negative generator place placement for each test. 67

Table E.1 ANOVA of the study of parameters for the Paper Dust Tester. 75

Table E.2 ANOVA of using various number of iterations for the paper safe tape (PST). 75

Table E.3 ANOVA results from Study 1, Bending and Stressing test vs the controlled handsheets and the commercial grades of paper..... 76

Table E.4 ANOVA results from Study 2, Edge effects test using the factory cut edges vs commercial grades of paper. 77

Table E.5 ANOVA results for Study 2, Edge effects using benchtop paper cutter cut edges vs both the controlled handsheets and the commercial grades. 77

Table E.6 ANOVA results for Study 3, Abrasive test vs the controlled handsheets and the commercial grades of paper. 78

Table E.7 ANOVA performed on the tape test against the 6 commercial grades of paper. 79

Table E.8 ANOVA performed on the electrical tape of the tape test against the 6 commercial grades of paper. 79

Table E.9 Correlation of the relationship of the ash value, the tensile index and the surface roughness. 80

Table E.10 Correlation of the ash value, the surface roughness and the results from studies 1 – 3. 80

Table E.11 Correlation of the laser printer test, the industrial tester and the results from studies 1-3. 80

Table E.12 Correlations of the laser printer test, the industrial tester and study 4, tape test results. 81

Table E.13 Correlation of the laser printer test, the industrial tester and the paper properties. 81

Table H.1 Data table for laser printer test 90

Table H.2 Data tables for test method 1, configuration 1: parameter determination 91

Table H.3 Data table for capture method: electrical tape 92

Table H.4 Data table for capture method: paper safe tape 93

Table H.5 Data table for capture method data: membranes 94

Table H.6 Data table for study 1 96

Table H.7 Data table for study 2 99

Table H.8 Data table for study 3 104

Table H.9 Data table for study 4. 107

LIST OF FIGURES

Figure 2.1 Flow diagram for the program built in ImageJ. 14

Figure 2.2 Average particle area vs threshold and the total surface area of particles for the filter membrane using capture method. 16

Figure 2.3 False positive particle size distribution of the filter membrane background. 17

Figure 2.4 Examples of microscope images of the filter membrane. 17

Figure 2.5 Examples of scanner images of the filter membrane before and after the threshold using 2.8σ. 18

Figure 2.6 Examples of the scanned images of the electrical tape before and after the thresholding using 3.1σ. 19

Figure 2.7 Examples of the scanner images of the paper safe tape before and after the thresholding using 3.1σ. 19

Figure 2.8 Schematic of the Paper Dust Tester front (left) and side view (right). 22

Figure 2.9 First configuration of the Paper Dust Tester called the bending test. 23

Figure 2.10 The second configuration of the Paper Dust Tester call the abrasion test. 24

Figure 2.11 Paper Dust Tester parameter tests with scenario 1) max 2) 160N/m of tension 3) 10 iterations 4) 3.2mm radius rod. 26

Figure 3.1 The back compartment of the HP Color Laser Jet Printer, cleaning locations. 38

Figure 3.2 ANOVA results for compiled dusting results from the Hp Color Laserjet Printer analyzed after 1000 sheets. 41

Figure 3.3 Particle Size Distribution of the dust collected from the laser printer (Left) and the average feret length to width ratio distribution (Right). 42

Figure 3.4 Example of images taken from sample B of the laser jet printer test. 42

Figure 3.5 SEM images of sample grade E from the laser printer test after drying from a colloidal dispersion. 43

Figure 3.6 SEM images of sample grade E from the laser printer test taking directly from the back plate of the printer. 400x magnification (left) and 2500x magnification (right). 43

Figure 3.7 Example image of the back plate of the laser printer after 500 sheets were tested. 44

Figure 3.8 Image of particles under a black light on the back panel of the scanner and the brightness intensity distribution of particles from the center of the panel to the side. 44

Figure 3.9 Dusting Results from the industrial tester and the laser printer test. The test is normalized to sample A to show a reduction of dusting between sample A and B-F. 45

Figure 3.10 Dusting values for the bending test using handsheets. 46

Figure 3.11 Dusting values for the bending test using commercial grades of paper. 46

Figure 3.12 Dusting values of the handsheets using bending test but collecting dust from edges. 47

Figure 3.13 Dusting values of the commercial grades caused by factory edge effects from the bending test by collecting dust near the edge. 49

Figure 3.14 Dusting values of the commercial grades caused by the benchtop paper cutters effects on the edges using bending test and collecting edge dust. 49

Figure 3.15 Dusting values of the handsheets using Testing Method 1, Configuration 2. 51

Figure 3.16 Dusting values of the handsheets using Testing Method 1, Configuration 2. 51

Figure 3.17 The particle count and surface area of the surface contamination collected, using electrical tape pull. 52

Figure 3.18 The particle count and surface area of the surface contamination collected from test method 2, paper safe tape. 53

Figure 4.1 Example image of the second model of the Paper Dust Tester. 60

Figure A.1 Slitter dust collect as stated from the adapted simple slitter dust test from Roix 2010..... 66

Figure B.1 Particle size distribution for test 1 (Left) and 2(Right) exposed to an electric field after 10 seconds. 68

Figure B.2 Particle size distribution for test 3 (Left) and 4 (Right) for blotter paper fibers exposed to an electric field after 10 seconds. 68

Figure C.1 The particle size distribution of Study 1. Handsheets (Left), Commercial Grades (Right). The results is the moving average of 3 points. 70

Figure C.2 The particle size distribution of Study 2. Handsheets (Left), Commercial Grades (Right). The results are the moving average of 3 points. 70

Figure C.3 The particle size distribution of Study 3. Handsheets (Left), Commercial Grades (Right) The results are the moving average of 3 points. 71

Figure D.1 The background noise of using a microscope vs a tested sample to determine the acceptable cutoff range of using a microscope. 72

Figure D.2 Average particle area vs threshold (Left) and total surface area of particles vs threshold (Right) for the electrical tape using capture method. 73

Figure D.3 False positive particles distribution of electrical tape used on sample B (Left). The difference between a tested sample of B and the blank sample (Right). 73

Figure D.4 Average particle area vs threshold (Left)_ and the total surface area of particles vs threshold (Right) for the paper safe tape using capture method. 74

Figure D.5 Particle size distribution of the false positive particle caused by the background of the paper safe tape (Left) and the particle size distribution for the paper safe tape tested on the sample B with 1, 5, and 10 different iterations per note (Right). 74

Figure F.1 Optical microscope image montage of the Hp Color Laser Jet printer test. 82

Figure F.2 Additional SEM Images of the fibers and filters of sample E after drying from the colloidal solution. 83

Figure F.3 Additional SEM images of the fibers and fillers for sample C after drying from the colloidal solution. 83

Figure F.4 Handsheet X-0(Left) and Z-33(Right) scanner samples from Study 3. 84

Figure F.5 Handsheet x-0(Left) and Z033(Right). Microscope sample montage for Study 3. 84

1. INTRODUCTION

1.1. Motivation

Paper dust can be problematic in various printing and converting processes that range in severity. Dust in the printing process can cause quality issues, cause downtime on the press, and can cause health issues with the operators. The causes of the paper dust spawns from several factors that include the fiber and filler used to produce paper and other paper additives. Dust may also be a result of slitting operations. In general, well bonded paper is not expected to have a dusting issue.

While a number of studies have tried to understand dusting, currently there is not a device or a standard method to measure the dusting tendency for a paper sample. Some current methods can measure dusting while the paper is being made, but it is not clear if this predicts the dusting tendency when the paper is being printed or converted. Some companies have various ways to test for the dusting tendency, but these methods are not published. Other methods involve sending a large number of sheets through a printer and measuring the collected dust. There is a need for a laboratory based test to measure the propensity of a paper sample to dust in a printing operation.

1.2. Dust and Linting

On any printing machine, contamination from the paper can become a serious issue with the quality, printability, runnability or cost effectiveness of a printing process. Dusting and linting are common issues that relate to the release of surface contamination. Linting is a term that is used when fibers or fillers on the paper's surface are removed when the paper comes in contact with a printing plate or blanket. The particles will build up over time and eventually cause printing quality losses if not cleaned; the buildup of particles on the printing blanket is referred

to as piling (Glassman, 1985). Paper dusting is more commonly understood when loose particles on the surface become airborne and are dispersed in a gaseous medium (Bernhardt, 1994). For uncoated grades, the same dust particles may be pre-emptively picked up by the felt and are acting as linting; for this case, dusting is one of several factors of linting that causes contamination buildup on the printing web but for other cases, dusting can cause additional issues not related to linting (Murata, 2015). For coated grades, dust particles may be mixed in a similar fashion with picking in which picking is the delamination of the coated layer of paper.

1.3. Paper Making Process

The process to make paper includes many steps from the harvesting of wood to the final product of paper. The primary steps of paper making include wood harvesting, pulping, stock preparation, paper formation and drying. The key aspects of dusting relate to how well the fiber and filler system are bonded together. This attribute is linked to the stock preparation and the forming operations.

The stock prep system is where all the components of the paper are mixed and furnished to form the final paper slurry. The general, components placed into the blending chest are the fibrous stock and non-fibrous additives such as pigments and starch. The less general fibrous furnish components includes the wood fibers that can be from mechanical or chemical treatment of the wood, and the non-fibrous additives include starch, pigment, dyes, coagulants, retention aids and pH controllers (Smook, 1992). These fibers and additives are the general components of paper but other components may be included in the paper slurry to increase the properties of the paper. The rate at which each of the components are added to the slurry depends on the furnish of the paper as well as the rate of production of the machine. All of the

flow rates should be automated so that if any changes occur to a single flow rate, the system will adapt to the given change (Smook, 1992).

Most of the mixing occurs in the blend chest. Once after the components are blended, the stock is moved to a machine chest which stores the paper slurry until it is placed onto the machine (Smook, 1992).

On the machine, there are several methods of forming the paper sheet. A typical method includes spreading the stock into a thin layer as it flows through the head box. This layer is drained on wires either in one direction or in two directions with twin wire machines or top formers. The layer is sent through a press section to press water from the pulp mat. Finally, the layer goes through the drier section where thermal energy is used to remove the water. All of these steps may have some influence on the dusting tendency of paper.

1.4. Particle Properties

Paper dust can be formed from any material component that was used to form the paper. The complexity of understanding the characteristics of the dust particles increase due to a large variety of cationic and anionic particle bonding within the stock solution; because of minor particle flocking, the investigation of paper dust is not limited to the pure fine filler particles but the filler aggregates and flocs of as well.

The dust particle size is critical component of understanding the behavior of paper dust formation and collection. The size of the dust particle is largely dependent on dust composition which may range between different machines. The major components of the paper stock are wood fibers and pigments; the minor components are starch and resins. Pigments are generally used in the paper industry to increase the weight of the paper as well as alter the papers brightness and opacity (Smook, 1992). The size of the pigment differs based on the kind of

pigment used; kaolin, calcium carbonate and talc are three typical pigments used in the paper industry (Smook, 1992).

Wood fibers are the largest component of paper where the length of the fiber can range from 1.7mm to 6.1mm, depending on the species of the fiber. The diameter of the fibers average 28μm to 57μm in diameter but may also depend on the species of wood (Smook, 1992).

Pigments are often used as a filling component in the papermaking process to improve opacity, brightness and printing capabilities. Several types of pigments include calcium carbonate, talc and kaolins. Calcium carbonate can be used in its precipitated form (PCC) or is ground form (GCC). Fewer impurities can be found in PCC then in GCC but impurities can be found in both types which effects the particle-particle interaction of the molecules (Modgi, 2007). Talc has many advantages in comparison with calcium carbonate but is more difficult to obtain due to its geographic dependence. Talc is also often used to increase paper weight and particle retention of paper. Lastly, kaolins are also used to increase paper weight, particle retention and other paper properties. The size ranges of each particle can be typically custom made or selected depending on the user's specifications. Particle ranges of PCC and GCC and typically be found under 1.75μm and over half of the particles under 0.64μm (Gess, 1998).

1.5. Printing Process

Offset lithography printing is the most common printing process. Offset printing utilizes a blanket as the printing plate that comes in contact with the paper. The blanket will also come in contact with the imprinted metal plate as well as the paper; the use of a blanket can be advantageous where the wear and tear of the metal imprint plate is reduced (Glassman, 1985). One of the disadvantages to this type of printing is the effects of linting on the blanket. Because all inks have some level of tackiness, the inks will cause loose dust to be pulled from the paper

surface as well as lightly adhered fibers (Libby, 1962). A buildup of particles on the blanket surface is called piling and will cause quality problems if not cleaned (Glassman, 1985).

Another type of lithography printing uses an electrophotographic plate with laser printers and common copy machines. In this case, a plate is charged using a corona wire and an imager is used to create a specific pattern on the plate (Glassman, 1985). The charged regions of the plate can attract the toner and later be imprinted on the paper. Because paper is made from several material components that are susceptible to electric fields, the use of electrical forces can cause paper dust to lift off the paper surface and re-adhered to other surfaces.

1.6. Paper Parameters Linked With Dusting

Paper dusting has been linked to increase with increasing filler loading (Shen et al., 2009). Filler loading is a term for increasing the filler content of the paper while keeping the base sheet a constant weight. Increasing the filler content of paper has many advantages but the side effect of strength reduction is what often limits the amount of filler used in a specific paper grade (Libby, 1962). As filler is added, the hydrogen bonding of the cellulose fibers becomes limited; resulting is some filler that is not bonded in the sample. The dust particles may be composed of either filler of fibers and may be present in both the air or non-adhered to the paper surface. The airborne particles will eventually settle onto the surfaces in the surrounding environment and machinery.

The effects of each component of paper on dusting are not fully understood but filler loading has been linked to cause an increase in paper dusting (Shen et al., 2009). Fillers which are poorly attached to the fibers have the tendency to be released to cause dust (Libby, 1962). Extreme increases in filler can cause large amounts of dusting. At high concentrations of filler, the paper has the tendency to have “two-sidedness” which is when the filler loading on the top side of the

paper is different than the wire side (Libby, 1962). As a result, the effects of filler loading can be different for both sides of the paper.

The paper dusting tendency may not be affected just by the tendency of loose filler particles but also by the adverse effects of the filler on the paper characteristics. Rosin which is responsible for the sizing of the paper can be affected by an increase of the filler. More importantly the physical strength of the paper can be greatly affected due to a reduction of the fiber-fiber bonds (Libby, 1962). It has been reported that increasing the loading of either ground calcium carbonate or precipitated calcium carbonate will decrease the tensile, tear and burst strength of the paper (Fortuna et al. , 2013) (Fan et al. , 2014) (Huiming Fan D. W., 2012). The effects of PCC loading on tensile, tear and burst reduced the strength by 32%, 38%, 40% respectively across the filler increase from 0% to 18% (Huiming Fan D. W., 2012). It can also be noted that increasing the PCC to starch ratio to 1:0.15 allowed for an unchanging tensile, tear and burst properties as loading increased. Starch can be used as a component to reduce the negative effects of filler loading on paper strength. One important aspect of loading that is often underestimated is the effects of filler size on the paper strength. Particle size does have an effect where small particles have been reported to cause greater negative effects on paper strength (Fan et al. , 2014).

Dust is a critical problem with the runability of any machinery. The use of grease is often required to reduce friction, wear and tear and downtime on machines. Certain machines can have high exposure to dust and contamination which becomes problematic to the ball and joints of the machinery (Seal protets ball scrw from dust while retaining grease, 2011). Paper dust particles can penetrate the seal of shafts and contaminate the grease; contaminated grease must be replace otherwise it will cause premature failure of the parts (New grease concquers

dust, 2005). A study from Koulocheris et al (2014) showed particle contamination in grease reduced the life of the bearings used. Increasing particle size increased the damage to the bearing but large particles over 100μm had the tendency to be crushed and reduced in size (Koulocheris et al. , 2014). Printing toner can be an additional contaminant specifically in the printing industry (Lubricated nylon solves printer problems, 1998).Dust contamination in grease is problematic for many industries other than paper.

1.7.1. Current Linting and Dust Testing Equipment

There have been many advancements in the designs of dusting and linting tests. The current section will describe the most recent testing equipment for dusting and linting tests. This excludes the tests that are kept as trade secrets among the private companies.

The standard IGT pick test has been a useful method of determining the picking tendency of paper at different speeds and forces. In respect to linting, the IGT pick test was adapted to test for the lint propensity of the paper by examining the printed strips for the unprinted paper reflection. The results in Gerli and Eigenbrood (2012) showed excellent correlation in the first study with the coldset CMYK series and the IGT linting with an R squared of 0.998. Their second study showed that the correlation between the upper cyan unit running 45000 sheets and the IGT Pick test with an R squared of 0.991. Because of the IGT's relation to the printing press, this method is highly useful in determining the linting tendency of the paper (Gerli et al., 2012).

LintView's original design was developed at the University of Quebec in Trois-Rivières (UQTR) and was later simplified to become portable. The device uses a light adhesive tape placed on the surface of the paper to remove surface particles. To measure the initial accuracy of the test, the device was correlated with the linting propensity of an offset press. The coefficient of determination was 0.71 (R^2). The additional tests that were performed were the Prüfbau

laboratory press, the MB Lint Tester (MacMillan Bloedel Lint and Dust Tester) and the IGT Pick Test. The results between the Prüfbau laboratory press and LintView showed an R squared value of 0.74. The results between MB Lint Tester and LintView showed an R squared value of 0.84. Lastly, the LintView Test was correlated against the IGT Pick Test for determining particle fluff. The coefficient of determination between the IGT and the LintView was 0.80. Additional environmental tests were performed to determine that temperature did not have a major impact on the LintView test but humidity did impact the test dramatically over a RH range of 30% to 65% and values from 1 to 4.5 on the topside of the paper and 0.7 to 3.0 on the bottom side of the paper. The overall results showed that this test method correlated with the results from an active printing press as well as several other linting test methods (Gratton et al. , 2006). However, it is not clear that this test should correlate with electrographic printing where the paper does not see a water or ink layer that generates a z directional force.

The Dust Propensity Analyzer (DPA) was designed from ACA Systems' for the intention of measuring the dust propensity on the paper machine. DPA's main form of causing dust includes a steel bar in which paper must run over followed by a vacuum supported by several pressurized air ports to blow dust off of the paper. The results of the DPA are calculated from the pressure difference of the filter used in the vacuum. One advantage of this device is that it is built into the paper machine and will give live dusting results. DPA was compared with two other dusting method, the Emerson's Black Felt Method (Emerson, 1997) and the MacMillan Bloede's Lint & Dust Tester. The coefficient of correlations between DPA and Emerson's Dusting Gauge was 0.79 (R) and the MacMillan Bloedel's Test correlation was 0.75 (R). The article from Komulainen states that the dust propensity of paper is a variable of all raw materials used and that unlike many other paper qualities, a single factor, not the sum of all paper properties, can cause poor dusting of the paper (Komulainen et al., 2011).

The Emerson Dusting Gauge, also linked to the black felt method, has been a well-known method of determining the dusting tendency of paper on the paper machine. The dusting gauge forces a black felt on the surface of the moving jumbo roll and collects surface debris for a set distance of the paper shown in Figure 1. The patented use does not determine how to quantify the dusting capability but simple methods can be performed to index the surface contamination in a quantifiable amount. In the report from Komulainen et al. (2011), the results showed that the correlation between the black felt method and the DPA was 0.79 (R^2) (Komulainen et al., 2011). The Emerson dusting gauge is a useful tool due to its simple and quick nature of obtaining results (Emerson, 1997).

One unpublished industrial dust tester is a device used to measure the surface contamination of grades of paper. Sheets of paper are fed into a rolling nip where one of the two rolls is wetted and cleaned with water. After several hundred sheets, the water is then drained through a filter and the filter is measured for the surface contamination. This test should be performed once for each side and the number of sheets used should represent the full population size of the sample. An index value is given with a higher number representing a large dusting propensity. This test is not widely used in the industry but may give some insight as to the amount of loose material on a large sample of paper.

All of the linting and dusting tests have some draw backs. For the linting tests described, a strong z-directional force is applied to the surface to simulate the printing process using offset inks, but this does not represent the situation in which paper dust is formed when paper is moves through the machines. The dusting test involves the testing of large rolls on machine and has not been correlated to the real dusting issues on many machines. The tests that involve tape or a water film also are tests that are applying a z-directional force or use a significant

amount of paper sample. There is a clear need for a simple lab scale test to estimate dusting that may occur in electrostatic type printing methods that does not require a large amount of paper.

1.8. Thesis Summary

The main objective of this thesis is to develop a new testing device that should result in a laboratory based method to test for dusting propensity of paper sample. The initial goal of the testing method was to incorporate a quick, quantitative, qualitative, mobile and inexpensive test. The second chapter will explain the designing of the equipment and the test methods that were developed.

The secondary objective was to gain additional knowledge of what causes paper to dust. In chapter 3, an investigation of filler loading was performed along with six commercial grades of paper. Handsheets with varying filler content were formed as controls to the test methods and insight into the effects of paper loading were analyzed.

Lastly, chapter 3 also contains the comparisons of the handsheets and commercial grades with an industrial tester and the laser printer dust formation. This thesis was designed to form a quick and reliable test method and to understand the possibility of filler content and paper strength as factors of paper dusting.

2. DUST TEST EQUIPMENT DESIGN

2.1. Introduction

In this chapter, the steps and procedure for a quick and inexpensive paper dust test are presented. The steps of designing the dust test were split into several separate investigations that involve measuring and analyzing the dust particles, collection of the particles and the removal of particles from the paper. This chapter will begin by explaining the methods of taking a visual observation of the dust particles and turning the observation into a computerized measurement. This process will include using a flatbed scanner and traditional microscopes to image the particles and then process the images through imaging software. Determining reliable methods of physically capturing the particles is important to understand and an investigation into using gravity, electrostatic fields and air filtration was performed.

The designing of the dust testers itself was split into several topics and many of which were not successful. Two testing methods were finalized; the first used a structure to bend, stress and abrade paper to create dust; the second used tape to pull particles from the surface of the paper. The first test was designed in conjunction with the three collection methods and the use of the imaging equipment. An analysis of the optimal parameters was performed to determine the best testing conditions and the standard deviation of the results. The second test was also performed to understand the best testing conditions when using electrical tape and a paper safe tape to pull particles from the paper surface.

2.2. Image Capture Methods

Two imaging equipment are used. The first is an optical microscope (Nikon SMZ-2T, Nikon from Japan) with a fiber optic light source (Series 180, Fiber-Lite) for particle illumination and a microscope camera (AmScope M500, AmScope). The second imaging equipment is the flatbed

scanner (Epson Perfection V370 Photo Scanner, Epson) with a max scanning resolution of 4800 dots per inch and a pixel width of 5.3μm per pixel.

Often dust is collected on a film or tape that is not transparent or able to be imaged using traditional microscope techniques. The primary mediums used are a 5μm filter membrane (AA-GWR Test Filter, KALTEC SCIENTIFIC INC), black electrical tape (53723 7mil Utilitech) and a paper safe tape (Black Post-it Notes 654-5SSSC, 3M).

When using the microscope, light will not penetrate the materials easily so instead, a light source at a low angle was used. The incident ray should be positioned at a 5° angle from the x-y plane of the imaged sample. When capturing the imaged, the background substrate should be barely visible or borderline black to ensure the particles to background exposure difference is maximized. Setting the exposure of the camera so the images are too dark will only diminish the visibility of the particles; setting the exposure of the camera to be too high will cause the software to have difficulty reducing the background from the particles; each image should use an exposure that barely exposes the background or barely blacks out the background. When selecting the imaging sites, the selected sites should be evenly spread across the entire imaging section.

When using the scanner to image the samples, two additional items are needed. First, a low tack adhesive tape is required to be placed on the scanner surface prior to imaging; removing the tape will remove most particles that are within scanning resolution; other methods of removing dust may cause streaks, static electric attraction or damage to the scanner surface. The second item required is a black construction paper to act as an overlaying and contrasting background. Each dusting sample is placed face down on the scanner surface after removing the tape. The Epson program should also be “reset” before each run to normalize the scan.

2.3. Particle Analysis

The primary method of separating the background from the particles is a threshold method, also known as binarization, that turns the multi bit image into a binary image that contains only false pixels that are not particles and true pixels that are particles (Mittal, 2013) (Gélinas et al. , 2010). Being that most images are at least 8-bit, multiple intensity values can be listed for each pixel. The correct threshold should be determined by selecting the brightness value that reduces the background noise and selects only the particles. Unfortunately, situations do arises when the brightness of the background noise and the particles overlap. In this case selecting an improper threshold value can reduces the background noise as well as reject or erode known particles (Gélinas et al. , 2010). If the background noise and particle brightness curves overlap, a capture method can be used to analyze the image and determine the best fit threshold value (Mittal, 2013). For simple cases, ImageJ has a built in threshold program that will determine the best threshold value for each image.

After capturing an image, difficulties arise when transforming the image into a numeric count. To do this, two macros were formed within ImageJ to do the analyses of the image. The designs of the macros are to count the number of particles within an image, the effective diameter of each particle and the total surface area. A core program was designed which includes the basic image manipulation, binarization and data acquisition of the particles. Three sub programs were designed be used with the core. The first sub program runs a capture method to output the particle count and total surface area at different thresholds values on the same image. The second program runs the average of multiple images within a file. The third program runs an adaptive control for the threshold by determining the threshold at the minimum background particle size. **Figure 2.1** shows the general flow of the programs.

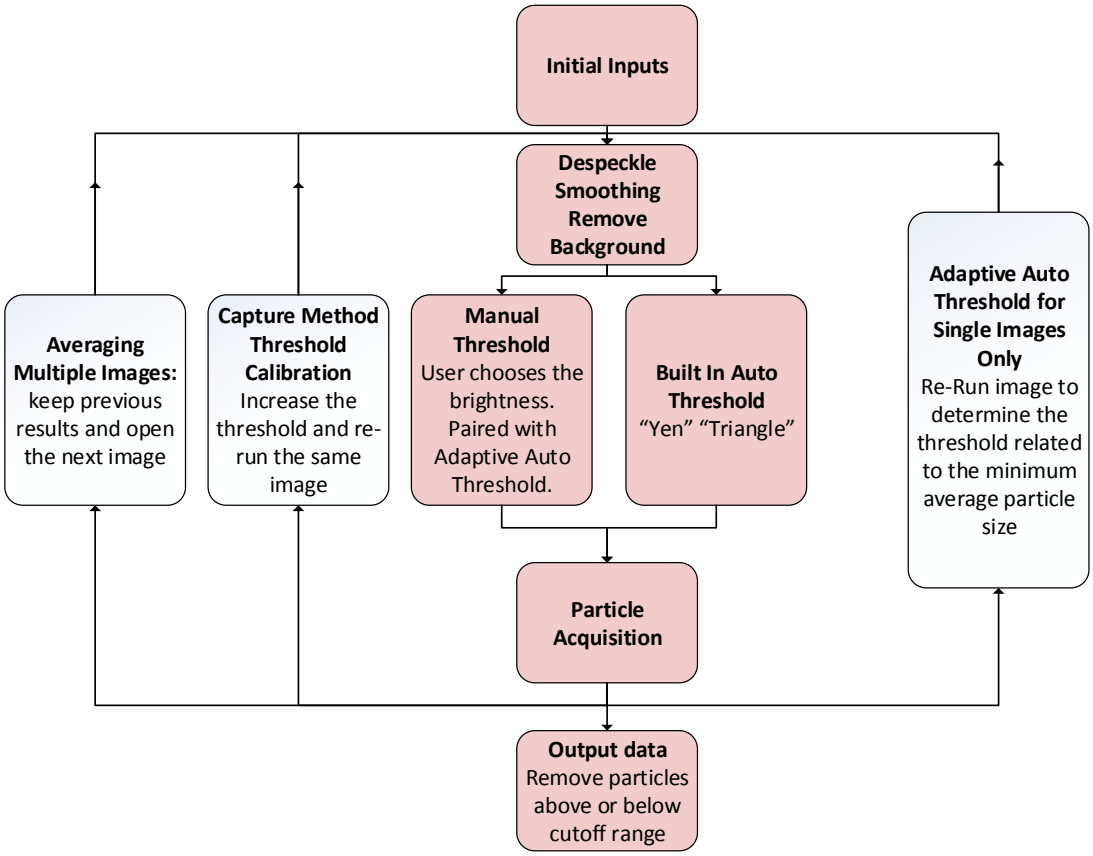

Figure 2.1: Flow diagram for the program built in ImageJ.

A method was used to determine the primary thresholding values of any background. This method calculates the average surface area per particle as well as the total surface area of the true and false positive particles in the image at various threshold values. The results should indicate the threshold value at which a minimum surface area to particle exists. This point represents the minimum size false particles of the background noise. Ten random samples using the filter membrane was selected in this thesis to be investigated using capture method. The types of images that ImageJ requires are 8-bit which gives a brightness value between 0 and 255. Instead of using a direct numeric value for a threshold, the programs will determine the threshold in terms of standard deviations from the mean brightness value.

Threshold values between 1.5 and 6 standard deviations from the mean brightness were used when performing capture method. After acquiring a reliable threshold value, three blank filter

membranes were used to inspect the background noise of the imaged surface for false particles. Analyzing the electrical tape and paper safe tape, 40 samples tested using paper grade B were used. 40 blank samples of the electrical tape and the paper safe tape were also analyzed for the background noise. Threshold values between 1.5 and 6 standard deviations from the mean brightness were used. The average surface area per particle and the total area of the particles will determine the appropriate threshold values to be used for each collection medium. Similar to the filter membrane, a background analysis was performed on the tape sample to determine the false positive particle distribution and size of the respective medium and desired threshold.

Although a more simple method of determining the particle count can be performed, there are a few reasons why someone should be careful when performing thresholds. First, if the threshold value is too high, the program may erode the known particles and cause a single particle to be cut into several. A low threshold will cause the background to be counted as positive particles. Also, the variability of the brightness range of each image may vary enough to cause problems when selecting a constant threshold; the threshold value chosen will be in reference to the number of standard deviations (σ) greater than the mean brightness. The analysis for the correct threshold value was performed as well as the background false positive particle distribution. The programs used in this thesis are not required to perform the analysis but when performing the thresholds; caution should be used to ensure repeatable results.

After analyzing 10 images of the filter membrane, one significant point occurred at 2.8σ which is the minimum speckle size of the background. At 3.4σ, there was a noticeable erosion of particles both visually and numerically. Both of these points can be seen in **Figure 2.2**. After inspecting this range, the minimum and maximum limits are 0.2σ and 0.5σ above the minimum speckle size or a constant 3.0σ and 3.3σ.

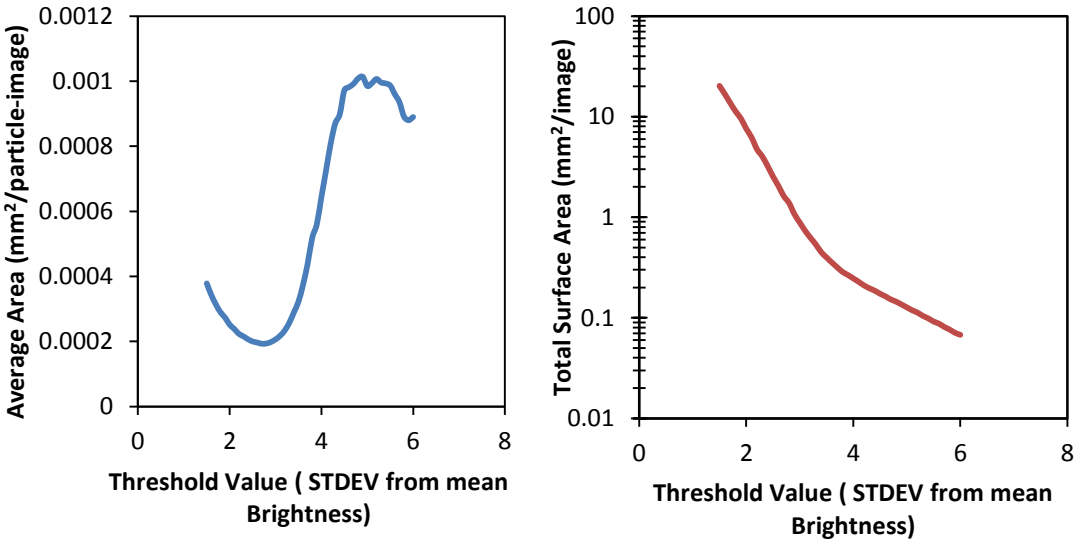

Figure 2.2: Average particle area vs threshold and the total surface area of particles for the filter membranes using capture method.

Using these values, background analyses of the images were performed. The analysis shown in **Figure 2.3** showed that the background noise was reduced to a minimal quantity after 40μm; to reduce the effects of background noise; particles under 40μm should not be counted using the scanner. Instead, using the microscope is requested for particles under 40μm.

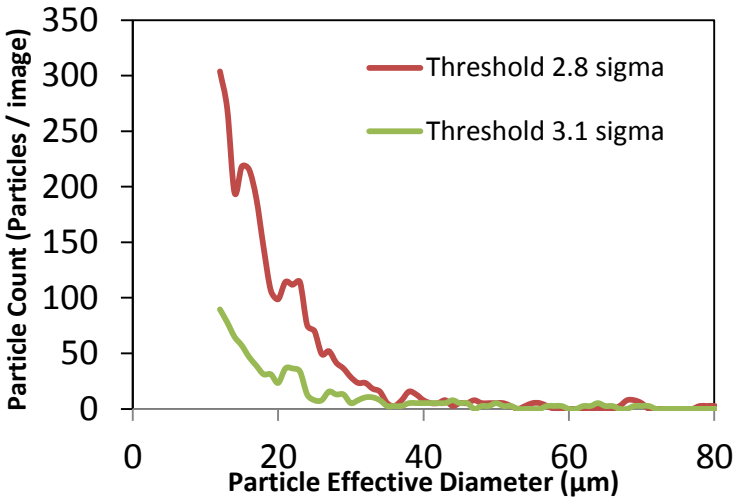

Figure 2.3: False positive particle size distribution of the filter membrane background.

Performing a threshold analysis on the images of the microscope, it was found that particles under 8µm in size are inconsistent and that particles between 8 and 40µm can be counted using the microscope. The graphical information for each of the backgrounds can be found in **Appendix D**. Examples of images taken from the microscope are shown in **Figure 2.4** and an image taken from the scanner are in **Figure 2.5.**

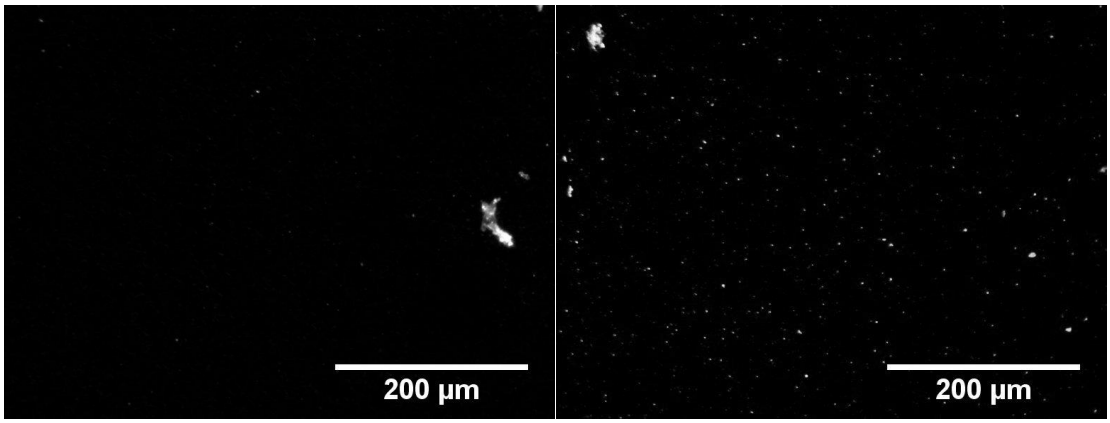

Figure 2.4: Examples of microscope images of the filter membrane. The images are taken from study 3 from chapter 3 in which the left image is from X-0 and the right is from sample Z-33.

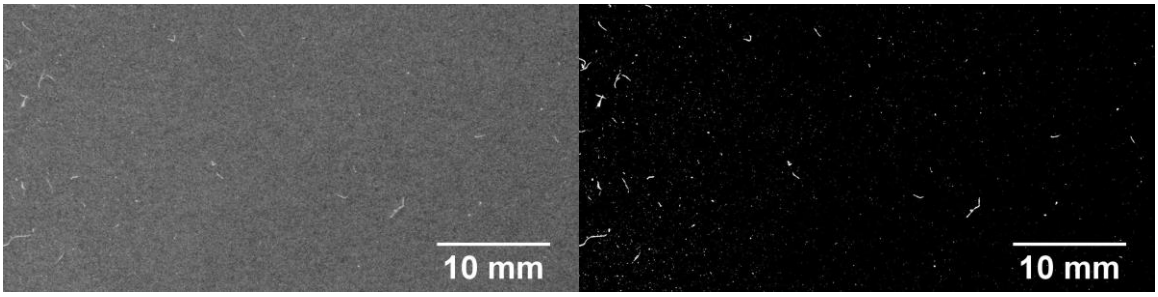

Figure 2.5: Examples of scanner images of the filter membrane before and after the threshold using 2.8σ.

The same analysis was performed on particles collected with electrical tape with 40 tested samples. The tape was place on the paper sample, a 306N/m rolling pin was placed over the tape and then removed at a 180° angle; after removing, the tape was imaged on the scanner and then analyzed. The minimum average speckle size was located to be 2.3σ. The lower and upper threshold values to be used are 0.4σ and 0.8σ above the minimum and since the adaptive step cannot be used for this specific case, a constant threshold of 3.1σ and 3.5σ will be used to image all electrical tape samples. An analysis on the background noise was also performed using the two threshold values. The false positive particle count decreases as the effective diameter increases and the particle count diminishes after 80μm for both threshold values. Although a significant number of particles may exist under 80μm in diameter, the false positive background noise of the tape exists at the same diameter size. Only particles above 80μm in diameter should be used without using other analytical methods of calculating the particles. Examples of the electrical tape are shown in **Figure 2.6.**

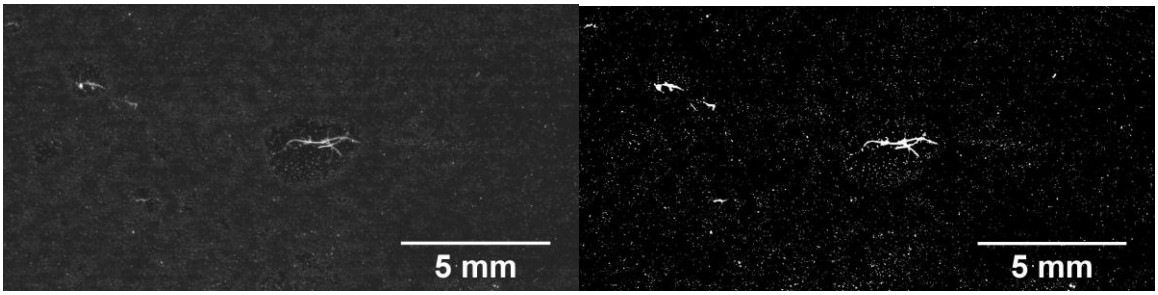

Figure 2.6: Examples of the scanned images of the electrical tape before and after the thresholding using 3.1σ.

The paper safe tape was analyzed after 40 tests were performed. The tape was placed on the paper sample, a 306N/m rolling pin was applied to the tape and then removed normally; the tape is re-applied 4 more times to create 5 iterations; after removing the tape for the last time, the sample was imaged on the scanner and then analyzed. The minimum speckle size was determined as 2.7σ. The lower and upper limit was determined to be 0.4σ and .8σ can be used when performing the adaptive threshold or a constant 3.1σ and 3.5σ as a minimum and maximum threshold can be used if performing a constant threshold. The background analysis was also performed and false positive particle smaller than 60μm existed. Counting only particles above 60μm was determined. Examples of the paper safe tape before and after using the threshold are shown in **Figure 2.7** below.

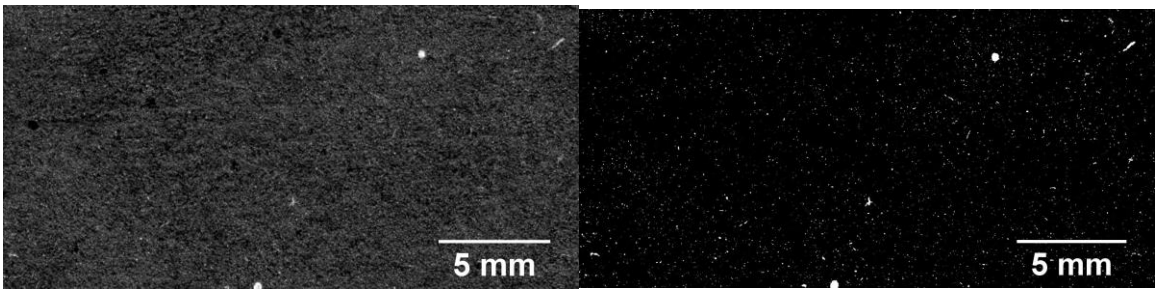

Figure 2.7: Examples of the scanner images of the paper safe tape before and after the thresholding using 3.1σ.

Because of these results, the adaptive threshold program was installed into the macros to determine threshold value from the minimum speckle size for each image. The membrane used

the adaptive step program and a threshold of 0.2σ and 0.5σ above the minimum particle area. The paper safe tape also is capable of using the adaptive threshold program and a threshold of 0.4σ and 0.8σ above the minimum speckle value was chosen. The electrical tape could not use the adaptive threshold due to the unevenness of the average particle area curve to threshold value. The electrical tape must use a constant lower and upper threshold of 3.1σ and 3.5σ.

2.4. Particle Collection Methods

Three methods of collecting particles were investigated and tested when using the Paper Dust Tester. The three methods include settling particles onto a plate using gravity, attracting particles using electrostatic forces and using air filtration to pull particles onto a membrane.

Particles that are suspended in a liquid or a gas are subjected to the natural gravitational force of the earth and these forces can be used to settle particles from air. In a simple situation, particles will settle relatively fast but in realistic turbulent air, the settling times may vary as expressed in Yang and Shy's model of stokes factor against particle movement (Yang et al. , 2005).

Electrical fields play an important role in the use of laser printers when applying toner to the paper. Paper has the natural tendency to build charges and because of this, electrical fields may form due to the abrasion of paper against the printer. The magnitude of the electrical force required to move a particle is linearly dependent on the charge of the particle which can be offset by increasing an electrical field. There are many other factors that should be understood when working with electrical fields; Paper components are composed of many types of particles, some of which are hydrophilic insolated particles. These insolated particles reduce the electron movement and restrict the tendency to reverse the charge in the presence of a polarized plate. Additionally, the hydrophilic nature of paper particles allows for water double layers to form;

this double layer causes inconsistencies with the charge of a particle when exposed to different environmental humidity's (Sow et al. , 2013) (Gao et al. , 2012) (Wang et al., 2013).

The use of air filtration has been used to collect dust in many industrial applications (Jung et al., 2013). There are many designs of filters used to remove particles from air; four core types of filters are generally used, granular, fabric, fiber and membrane (Brown, 1993) and each of the filters were investigated for their use to collect dust.

Fabric filters can be reused and easily cleaned but due to their high porosity, the retention of particles is low (Brown, 1993). Fibrous filters are better used for disposable situations but they have high retention rates but an inability to hold particles on the surface (Brown, 1993). Membrane filters will retain the particles on the surface but the volumetric flow rate of the particles are low (Warkiani et al., 2015) (Allen, 1990).

After an investigation, the chosen method is the membrane filter due to its ability to retain particles on the surface of the substrate. Data collected in Soo et al. gave the relative efficiencies, pressure drops and flow rates of commercially used filter membranes. The Polycarbonate filter membrane from Millipore that had a 5μm pore size was tested at 0.404 L/min and gave a collection efficiency range for aerosol particles between 65% and 94%. The particle collection efficiency is much greater for those close to or above the pore size. The initial pressure drop across the system for the same filter was 1.2kPa (0.174psi) which are relatively close to the values used in the design of the collection method (Soo et al., 2016).

2.5. Testing Method 1: Paper Dust Tester

The idea of the first method is to bend and stress paper in order to increase the amount of dust that is produced from a single sheet of paper; the hope is that the dusting tendency can be estimated from a few samples instead of a large number of sheets. A structure was designed to vary five variables. The variables are the tension on the paper, the total angle of deflection, the radius of the rod used to deflect the paper, the gap distance between the collection plate and the collection method used to collect the dust. The structure of the equipment is shown in **Figure 2.8**.

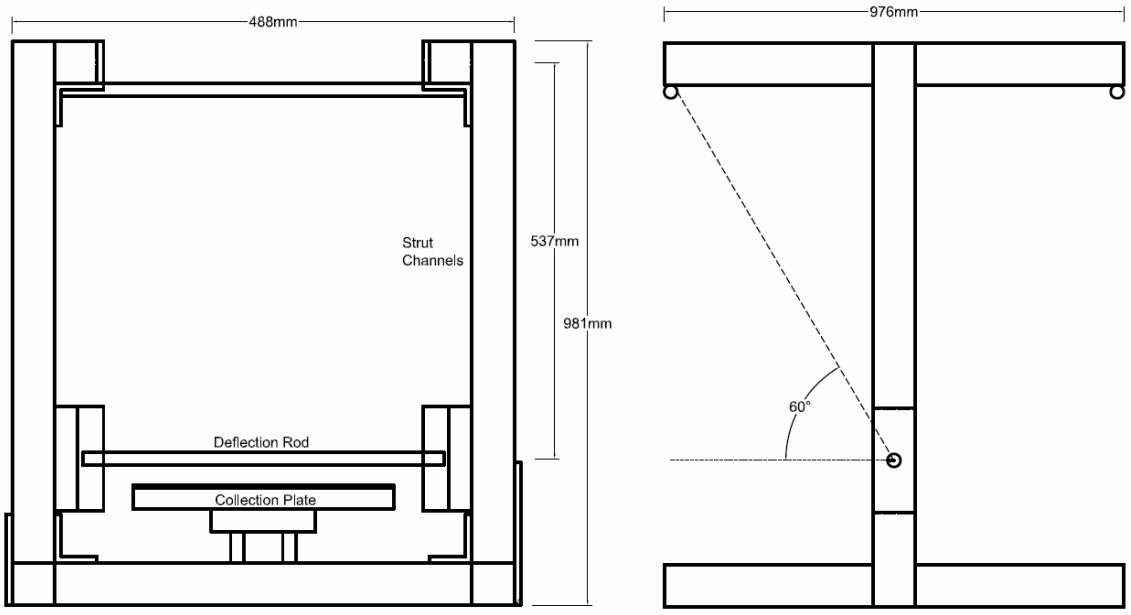

Figure 2.8: Schematic of the Paper Dust Tester front (left) and side view (right).

The tension on the paper will be varied by the weights used and measured by the width of the paper sample. The total angle of deflection can be changed based on the difference in height of the deflection rod and width the upper shafts. The radius of the rod can be changed by detaching the center rod and replacing it with other attachments. Only a 3.2mm radius rod and a blade with a measured 75 μm curvature radius were used.

Two different configurations are used for this structure. The first configuration tests the bending and stressing of the paper by placing the paper between the collection plate and the rod as shown in **Figure 2.9**. The intention for this test is to form dust from bending and stressing the paper and collect only the dust that falls from the surface of each sample. The location of the collection plate can make a difference in the type of dust collected and should be noted when performing the tests. This method of bending the paper under tension should be similar to what occurs in a laser jet printer.

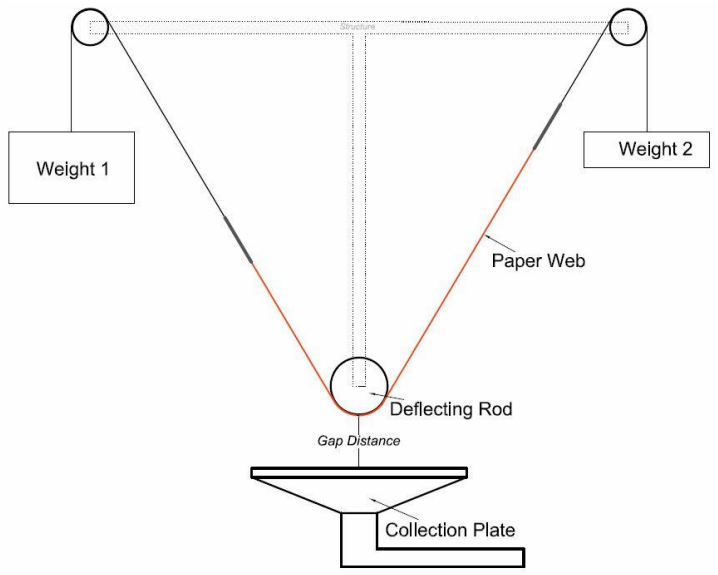

Figure 2.9: First configuration of the Paper Dust Tester called the bending test.

The second configuration uses the abrasion or rubbing of the paper over a rod to increase the dust collected. Shown in **Figure 2.10**, the collection plate is on the same side as the rod, but now the paper sample is wrapped on top of the rod, and when it moves, it rubs against the rod with a known tension.

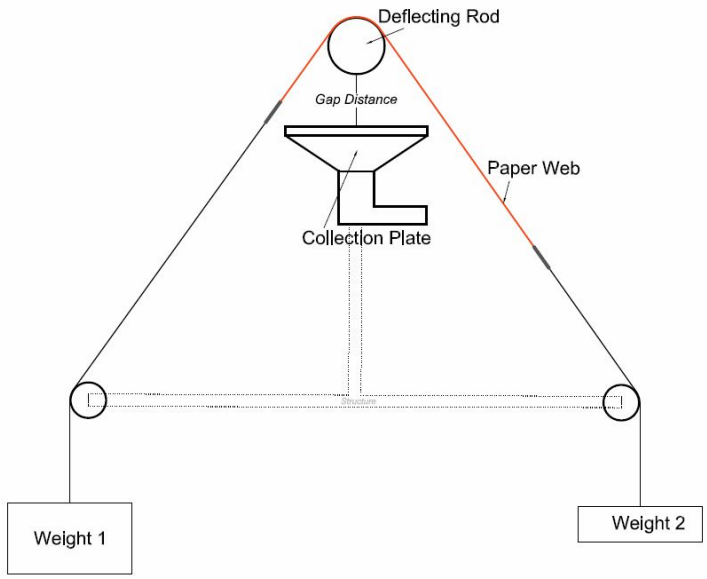

Figure 2.10: The second configuration of the Paper Dust Tester call the abrasion test.

Three collection methods were investigated using configuration 1: 1) particle settling using gravity onto a collection plate, 2) air filtration and 3) electrostatic attraction. The method using sedimentation required only gravity and that a 15.24cm by 12.7cm collection plate is placed under the deflecting rod. Black construction paper was placed as the collection plate and as the contrasting background for imaging. The collection method using air filtration required a suction vessel with a 5µm filter membrane to collect any dust particles. The collection method using electrical fields required that the deflection rod was charged with a -9.5kV and a metal collection plate below the rod was grounded. The black construction paper was placed onto the surface of the grounded plate to collect particles.

The variables for any individual test included the number of sheets, the number of iteration of a single sheet and the tension placed on the paper. A test was performed to investigate the UM Paper Dust Tester's performance with varying the parameters of the method. The total deflection of the paper was kept constant at 120° and the gap distance between the rod and the collection plate was also kept constant at 6mm. For each of the following sets, 3 tests were

performed and imaged only on the scanner. The paper sample that was used for these tests is sample B.

The three collection methods were tested along with four other scenarios shown in **Table 2.1**. The four scenarios included the maximum conditions of using 3 sheets with 20 iterations per sheet, a tension of 320N/m and the use of a blade as the deflection rod. This condition generates dust that can be seen. Sets 2 through 4 include reducing the tension to 160N/m, reducing the iterations to 10 and using a 3.175mm rod respectively while keeping the other parameters constant.

Table 2.1: Tests to determine optimal parameter conditions.

	Number of Sheets	Number of Iterations	Tension (N/m)	Rod Type
1 - Max	3	20	320	Blade
2 - Tension	3	20	160	Blade
3 - Iteration	3	10	320	Blade
4 - Rod	3	20	320	3.175mm Rod

The data collected from the four sets are shown in **Figure 2.11**. Both methods of using gravity and electrostatic attraction have side effects with the collection of the dust. When using only gravity, dust from the topside and the edges of the paper were observed settling onto the collection plate under the rod. Although this increased the dusting value, it also included the dusting of other mechanisms which may complicate the results. Using electrical fields was also problematic when the charge reversal of particles became apparent. Because particles may lift-off the collection plate, the observed particles collected may not fully represent the emitted dust but only that of particles with a distinct polarity. Humidity may also influence the charge of each particle; performing these tests in a changing humidity environment may cause different results. The filter membrane created the best results with the least side effects.

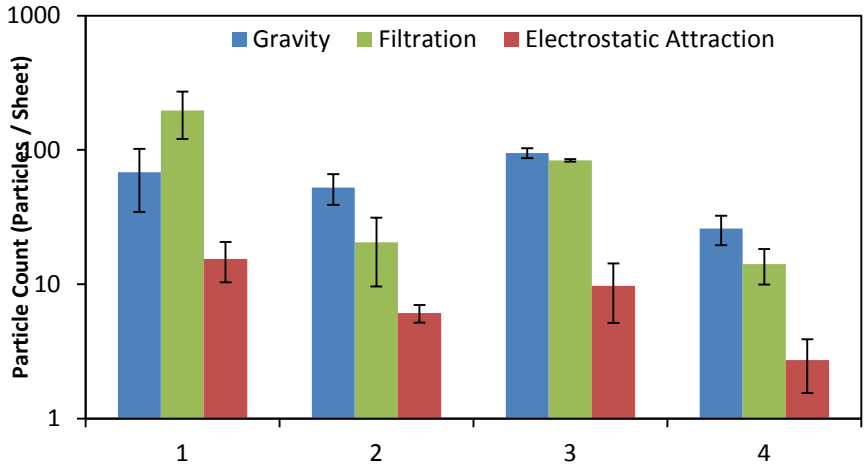

Figure 2.11: Paper Dust Tester parameter tests with scenario 1) max 2) 160N/m of tension 3) 10 iterations 4) 3.2mm radius rod.

An Analysis of Variance (ANOVA) was performed through the program MiniTab on the different scenarios. The result shows that reducing the tension on the paper from 320N/m to 160N/m reduces the dusting effect of the paper. Reducing the iterations performed on the paper from 20 to 10 also partially reduced the dusting effect but not significantly. Changing out the blade for the use of the 3.2mm radius rod also showed a reduced dusting count. The ANOVA Table can be found in **Appendix E**.

To understand the variability of the test, each test will undergo 10 separate samples of tests. The three tests that were performed are the configuration 1 or the bending test to test for dust falling from the surface of the paper; the bending test collecting dust on the edges to quantify the dust accumulating from the cut edges of the paper and configuration 2 or the abrasion test that quantifies the dust accumulating from abrading the paper over a rod.

The parameters chosen for configuration 1 testing for both bending and edge related dusting include using 320N/m of tension, 120° of deflection, a gap distance of 6mm, 3 sheets and 20

iterations of the same sheet. The collection method used is air filtration with membrane filter as the collection medium. When testing edge effects, two tests accounts for one sheet of paper due to a single sheet of paper having two edges. When testing for dust caused by bending and stressing the paper, the filter should be placed no closer than 2.54cm from either side of the paper edge. When testing for edge effects, the filter should be placed directly under the edge of the paper.

The parameters for configuration 2 testing for abrasive effects was chosen to be 220N/m of tension, 80° of deflection, a gap distance of 20 mm, 1 sheet and 30 iterations of the same sheet. The location of the filter should be placed no closer than 2.54 cm to either edge of the paper.

The paper sample was performed ten times on each of the three testing configurations, bending, edge and abrasion. The accumulated data is presented in **Table 2.2** with the mean, standard deviation and the relative standard deviation (RStDev) in respect to the mean. Buildup of debris on the deflection rod may account for added friction between cleanings. Additional information taken from the tests performed in chapter 3 shows a decrease in the pooled standard deviation of the edge effect test when three sheets were used instead of one sheet for a single sample. The data showed that when using a single sheet, the pooled relative standard deviation was 73% in comparison with the 54.5% given from 3 sheets. This shows that increasing the number of sheets tested will decrease the overall standard deviation of the sample but a time restriction is placed on how many sheets can be used. Other causes of variance include the number of microscope images taken for each sample may determine the confidence error of the sample set versus the bulk distribution. Lastly, contamination from the air can vary. The time that the membrane is exposed to open air is minimized during the test. The variability of the measured surface area is more than the particle count. Surface area has the added error that

small increase in the size of a large particle affects the surface area but not the probability of obtaining the particle.

Table 2.2: Basic Statistics of sample B performed 10 times on the Paper Dust Tester. Particle count number is in units of particles per sheet and surface area number is in units of squared milimeters per sheet.

Variable		Total Count	Mean	StDev	RStDev*
Particle Count	C1-Bending and Stressing	10	295.4	102.2	34.59
Surface Area	C1-Bending and Stressing	10	0.0751	0.0363	48.33
Particle Count	C1-Edge Effect	10	418.5	137.8	32.927
Surface Area	C1-Edge Effects	10	0.1498	0.0817	54.539
Partice Count	C2-Abrasive	10	463.6	189.3	40.832
Surface Area	C2-Abrasive	10	0.1111	0.0514	46.264

* Relative Standard Deviation - Calculated data outside of Minitab

This test was to determine the parameters and restrictions of the Paper Dust tester's limitation. The limitations are as followed.

- Reducing the tension on the paper will reduce the dusting tendency but the paper has a maximum tension based on the structural capability of the sheets. The maximum tension should be restricted to extreme circumstances due to unnecessary damaging of the paper.
- The choice parameters for configuration 1 include using the filter membrane as the collection method, using the 3.2mm diameter rod as the deflection beam. Using the blade caused additional unwanted damage to the paper.
- The number of sheets used has a general maximum of 3 sheets per test due to the time requirement.
- The maximum iterations allowed to be performed are 30 due to the damaging of the paper.

- Because of the scanners compatibility with the background of the membrane, only particles over 40μm should be counted to avoid counting background noise.
- For each test in this thesis, the parameter sets must be kept constant for the entirety of the test.
- For each test, the humidity and temperature should be monitored and kept constant

2.6. Testing Method 2: Tape Tests

The tape tests are similar to other tape linting tests but the focus of this tape test is to reduce the z-directional force and collect loose particles on the paper surface. The tape used is electrical tape and the paper safe tape as described in section 2.2.

The electrical tape test is performed by placing the tape on the paper surface, applying a set amount of pressure and removing the tape at an extreme angle to reduce the z-directional force. The variables of the test include the pressure placed on the tape, the angle that the tape is removed, and the total area of the tape per sample. The pressure placed on the tape will be kept constant by using a 306N/m rolling pin and move the roller twice over the tape. The black electrical tape will be removed at a 180° angle to the resting position once after. The tape is then placed face own on the scanner surface. The paper safe tape tests are performed by placing the tape on the paper surface and then rolling the 306N/m rolling pin over the tape twice. The tape is removed in a natural form once after. Once removed, the tape can be re adhered to another paper's surface or placed face down on the scanner to be analyzed.

Using paper sample B, the electrical tape test was performed 40 times as well as 40 additional blank tape samples with a scanned area of 1.25cm^2 each. To measure the standard deviation, two analysis were performed. The first calculated the deviation of the results from each of the 40 samples and the second calculated the standard deviation by forming 13 sets of 3 samples.

The paper safe tape test also use sample B and was tested being adhered five times on different sheets for the same sample. 40 samples for each of the iterative tests will be performed along with 40 blank samples. The area of the scanned surface is 6.45cm^2.

Using the paper safe tape, three tests were performed. The first test included a single tape pull, one with five tape pulls per single tape and the last with ten pulls per single tape sample. To inspect if each individual test has a significantly different collection then the other, an Analysis of Variance was performed. The results shows that there is a significant increase of collected particles until five pulls of a single tape sample but a similar amount of dust was formed after 10 iterations of the same tape. The use of five iterations of a single paper safe tape was the optimal use.

The standard deviation of the tape tests are shown in **Table 2.3**. The data shows that the relative standard deviation of each test ranges between 33% on the electrical tape to 48% on paper safe tape. Averaging three samples of electrical tape reduced the relative standard deviation of the results by up to 10%. The testing errors that may cause the deviation are the variability in paper sample, small sample set error, picking, remaining scanner noise and non-paper related surface contamination. Paper sheets can vary slightly in their properties and testing a small area of an inch or inches can cause added variance to the results.

Table 2.3: Basic Statistics of sample B performed on the Tape Test. The surface area number has units of square millimeters per sheet.

Variable	Total Count	Mean	StDev	%StDev**
ETape PC av-1	40	5394	2484.6	46.05
ETape SA av-1	40	70.41	29.75	42.25
ETape PC1 av-3	13	5361	1900	35.44
ETape SA1 av-3	13	67.63	22.07	32.63
PST PC1	40	759.2	254.4	33.51
PST SA1	40	5.936	2.866	48.28

**Relative Standard Deviation
Note : PC = Particle Count
Note : Surface Area
Note : Electrical Tape Samples that are averaged with 3 individual samples has one less image then the individually tested samples.

The preferred testing parameters for the tape test is that the electrical tape should be removed using a 180° angle of removal and three samples of 161.3mm^2 area. A 306N/m rolling pin should be rolled over the tape twice. The sample set of tape should average 3 individually placed samples of tape to reduce the deviation of the results. The preferred testing parameters for paper safe tape is to remove the tape naturally and use a single tape applied five separate times with a scanned area of 6.45cm^2 total.

2.7. Summary

Table 2.4: Summary of Parameters for each test method.

Summary of Parameters									
Testing Method	Threshold Min/Max		Size Cutoff	Sheets	Iteration	Rod Type (mm)	Tension (N/m)	Collection Type	% StDev
Test Method 1 Configuration 1 Bending	0.2σ	0.5σ	40μm	3	20	3.2	320	Membrane	48.3
Test Method 1 Configuration 1 Edge	0.2σ	0.5σ	40μm	3	20	3.2	320	Membrane	54.5
Test Method 1 Configuration 2 Abrasive	0.2σ	0.5σ	40μm	1	30	3.2	220	Membrane	46.3
Testing Method	Threshold Min/Max		Size Cutoff	Iteration	Angle of Removal	Pressure	%StDev		
Test Method 2 Electrical Tape	3.1σ*	3.5σ*	80μm	1	180	306N/m	32.6		
Test Method 2 Paper Safe Tape	0.4σ	0.8σ	60μm	5	Normal	306N/m	48.3		

The best conditions for each test were generally similar between each test using the Paper Dust Tester and separately, the two tape tests. The paper dust tester should not use more than three separate paper samples due to the time requirement but may re-test the same sheet up to 30 iterations before causing damage to the paper. A deflection rod was used instead of a blade to reduce the damage on the paper and a membrane was used to collect particles that are can be imaged from the surface. Due to the background noise, particles between 8 and 40μm can be counted using the microscope and the scanner can be used to image particles above 40μm in diameter. The tape test included using both electrical tape and a paper safe tape in which the electrical tape can be adhered only once and the paper safe tape was recommended to be re-adhered up to five times. The electrical tape required a removal of 180° to reduce the chance of picking; the paper safe tape can be removed normally without the effects of picking. For the electrical tape and paper safe tape, the minimum size requirement to count the particles are 80μm and 60μm respectively.

3. DUSTING RESULTS FROM FILLER LOADING PARAMETERS

3.1. Introduction

This chapter will investigate five different studies using the bending test with both center and edge dust collection, the abrasion test with center dust collection and the tape tests using two tapes. Two additional tests were performed to compare the results of the testing methods. Using a standard commercial laser printer, paper dust was collected from the printer after processing 1000 sheets. This test was compared with the five studies as well with an industrial dust test. The key objective is to look for correlations of the tests or paper properties with the laser printer results.

3.2. Experimental

The dusting tests described in chapter 2 are performed on a set of handsheets and six commercial grades of paper. The commercial grades are identified with a code and listed in **Table 3.1**. These were selected to give a range of quality, but their actual dusting tendency was not known. The initial plan was to have paper samples from paper companies that had a range of dusting characteristics, but these samples were difficult to obtain.

Three sets of handsheets were formed under the guidelines of TAPPI Standard T-205. The furnish of the handsheets used a mixture of chemical pulps with 50% softwood and 50% hardwood, which were mixed previous to adding any of the other filler components. Precipitated Calcium Carbonate (Specialty Minerals) is used as the only pigment component. Anionic Poly-Acrylamide (PERCOL 155, BASF) is used at 0.1% weight on the dry weight of paper slurry. The target basis weight of the handsheet was 60 g/m^2.

Each grade of paper was tested for its ash value, tabor stiffness, tensile, caliper, permeability and Sheffield roughness as stated from the Tappi standards T211, T404, T494, T460, T538, T410, T411 and the conditioning of the paper in method T402.

Each sample was labeled A through F for their specific identifications as well as the rounded ash value associated with the grade as shown in **Table 3.1**. For example A-13 shows that paper A has an ash level of 13% by weight.

Table 3.1: Names and ID's of the Commercial Paper Grades.

Thesis ID	Purchased/trade Names
A-13	HP Ultra White Multipurpose Paper
B-16	Staple's Multiuse
C-16	Hammermill Copy Paper
D-21	Hammermill Premium Inkjet & Laser
E-21	HP Premium Laser Paper
F-23	Staple's Mulipurpose 50% Recycled

3.2.1 Study 1—3 3: Dusting Tests From Test Method 1

This study tests the effects of bending paper to produce dust and were tested using the commercial grades as well as the handsheets. The parameters of the structure for the this study are listed in **Table 3.2.** The paper width of the handsheet is kept unchanged with a 17 cm round handsheet to reduce the effects of edges during the test and the average tension is used.

Table 3.2: Testing Parameters for Study 1. Test for paper dusting caused by bending and stressing the paper.

Testing Parameters for the Bending and Stressing test using Test Method 1, Configuration 1						
Handsheet Parameters				Commercial Grade Parameters		
Parameter	Value	Units		Parameter	Value	Units
Deflection Angle	120	Deg		Deflection Angle	120	
Gap Distance	6	mm		Gap Distance	6	mm
Tension		N/m		Tension	320	N/m
Number of Sheets	1			Number of Sheets	3	
Length of Testing	152	mm		Length of Testing	203	mm
Paper Width	170	mm-diameter		Paper Width	107	mm
Number of Iterations per sheet	30			Number of Iterations per sheet	20	
Number of microscope images	20			Number of microscope images	20	

The second study tests the papers dust tendency when the paper is exposed to bending under tension and the dust is collected specifically from the edges. The three handsheets and the six commercial grades were tested under conditions for the bending test. The handsheets were cut using a standard benchtop paper cutter. For the commercial grades, two tests were performed. One tested the edges of the paper cut by the factory and the second test measured the dust after being cut from a benchtop paper cutter. The parameters of the structure when testing both the handsheets and the commercial grades are listed in **Table 3.3**. The paper width of the handsheet is cut to a 50.8mm width. A single sheet of paper counts as two sides of the sheet.

Table 3.3: Testing parameters for study 2, paper dusting caused by edge effects when the paper is bent and stressed.

Testing Parameters for the edge effects using Test Method 1, Configuration 1						
Handsheet Parameters				Commercial Grade Parameters		
Parameter	Value	Units		Parameter	Value	Units
Deflection Angle	120	Deg		Deflection Angle	120	
Gap Distance	6	mm		Gap Distance	6	mm
Tension		N/m		Tension	320	N/m
Number of Sides Tested	3			Number of Sides tested	6	
Length of Testing	102	mm		Length of Testing	203	mm
Paper Width	50.8	mm		Paper Width	50.8	mm
Number of Iterations per sheet	30			Number of Iterations per sheet	20	
Number of microscope images	20			Number of microscope images	20	

The third study tests the dusting tendency of the papers when rubbed against a rod. The parameters of the structure when testing both the handsheets and the commercial grades are listed in **Table 3.4**. In comparison with the previous tests, the testing length is only 4 inches for the commercial grades due to the lack of distance able to be performed.

Table 3.4: Testing parameters for study 3, paper dusting caused by abrading the paper over a rod.

Testing Parameters for the abrasive test using Test Method 1, Configuration 2						
Handsheet Parameters				Commercial Grade Parameters		
Parameter	Value	Units		Parameter	Value	Units
Deflection Angle	80	Deg		Deflection Angle	80	
Gap Distance	1.5	cm Diameter		Gap Distance	1.5	cm
Tension		N/m		Tension	320	N/m
Number of Sheets	1			Number of Sheets	3	
Length of Testing	102	mm		Length of Testing	152	mm
Paper Width	170	mm Diameter		Paper Width	107	mm
Number of Iterations per sheet	30			Number of Iterations per sheet	20	
Number of microscope images	20			Number of microscope images	20	

3.2.2. Study 4: Tape Tests

The fourth study tests the surface contamination of the paper samples using tape. The tests will include the use of electrical tape and the paper safe tape on each of the six commercial grades of paper. The method will not be tested on the handsheets because the z-directional strength of the handsheets is too low. Both tests will follow the guidelines of the second test method from chapter two. The testing parameters for the tape tests are shown in **Table 3.5.** The angle of removing the electrical tape is held at an extreme angle to the original position. Removing the paper safe tape should be performed naturally.

Table 3.5: Testing Parameters for study 4, removal of surface contamination from the tape test.

Electrical Tape		
Parameters	Value	Units
Number of tape samples per total sample	3	
Number of total samples per set	9	
Rolling pin weight	306	N/m
Angle of removal	175	deg

Paper Safe Tape		
Parameters	Value	Units
Number of tape samples per total sample	1	
Number of total samples per set	6	
Rolling pin weight	306	N/m
Angle of removal	Normally	deg

3.2.3. Comparison Tests

Two tests are used to compare the results from the four studies; the tests include the industrial tester as described in chapter 1 of this thesis and dust collected from within laser jet printer.

The six grades of commercial paper were shipped to an external company to be tested. The general procedure of the test includes testing several hundred sheets of paper through a rolling nip that has a water film on it. The rolling nip is constantly being cleaned with water and at the end of the test, the water sample is filtered and tested for contaminants. After receiving the results, the data was normalized based on the sample A.

The key test performed used a laser printer (Color Laser Jet Pro MFP M4700 fdw, HP) and the six commercial grades of paper. The test also used a Bousch and Lomb Microscope, microscope slides and a flat fine tip paint brush used to clean the printer. The test procedure included running 1000 total sheets of paper through the laser printer in two increments of 500 sheets. 1mL of filtered water was prepared in a 2.5mL vial previous to performing the test. After 500 sheets are run through the printer, the back compartment door, as shown in **Figure 3.1**, is opened. Specific sites in the back compartment are cleaned by using the paint brush and rinsing

the tip of the brush in the vial of water. The cleaning locations are specifically the thin metal plates of the in the lower guide rail. The same is performed after the second 500 sheets are run.

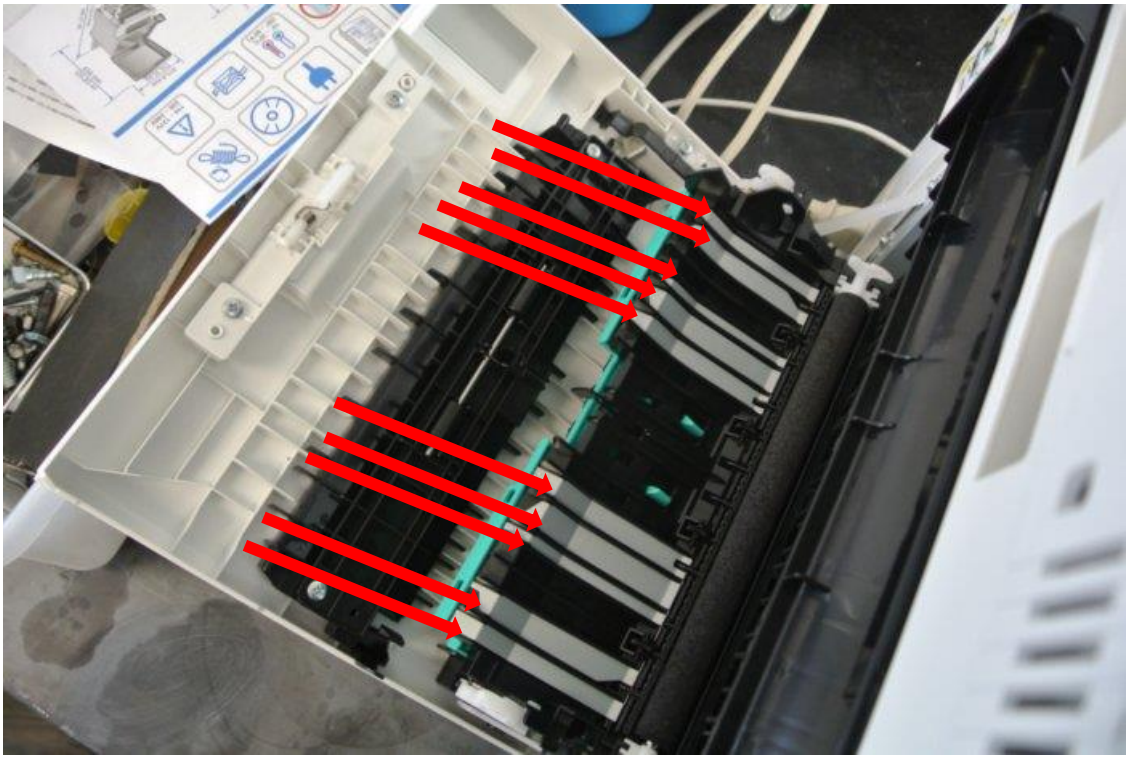

Figure 3.1: The back compartment of the HP Color Laser Jet Printer, cleaning locations.

After all 1000 sheets are run through the printer, the contaminated water sample is then analyzed under a microscope. This is performed by forming a water well on a microscope slide with electrical tape and a hole punch and placing 5µL of the sample into the well and taking multiple images of the well at different magnifications. This is performed multiple times for each sample.

It was noticed that the dust collected from the laser printer was not equal at the center compared to the edges. A second analysis was performed by running an additional 500 sheets of

paper grades B and C separately. Once all 500 sheets passed through the printer, a Nikon J1 camera with an exposure of 15 seconds and a black light (F15T8/BLB Bulb Fluorescent Light, Can You Imagine) was used to image the back compartment. The analysis performed was intended to investigate the uneven dusting from the center of the back plate to the outer edges.

3.3. Results and Discussion

The different handsheets are labeled X through Z with the relative tested ash value and the specific tested properties for the handsheets are shown in **Table 3.6**. The property data for the commercial grades are shown in **Table 3.7**. The six grades of paper were disintegrated to 0.15% solid using a standard disintegrator (Model 500, NORMEC) and diluted to 0.015% solids. The fibers were processed through a fiber size analyzer (MORFI compact, Techpap) and the results are shown in **Table 3.8**.

Table 3.6: Properties of the three handsheets formed tested under standard Tappi conditions.

	Ash (%)	Tabor Stiffness (mN-m)	Elastic Modulus (Mpa)	Tensile Index (N-m/gm)	Air Resistance (s)	Sheffield Surface Roughness (SU)	Basis Weight (gm/m^2) Target	Caliper (mil)
X0	0.2%	1.332	484.22	5.54	1.66	251	60	4.71
Y16	15.9%	0.646	257.74	2.94	1.98	227	60	4.72
Z33	33.1%	0.428	173.25	1.50	2.96	175	60	4.79

Table 3.7: Properties of the six commercial grade papers tested under the standard Tappi conditions.

	Ash (%)	Tabor Stiffness (mN-m)	Elastic Modulus (GPa)	Tensile Index (N-m/gm)	Air Resistance (s)	Sheffield Surface Roughness (SU)	Basis Weight (gm/m2)	Caliper (mil)
A-13	12.96	2.12	1.22	54.90	8.50	118.87	78.21	4.216
B-16	15.50	1.88	1.01	59.06	11.37	163.29	76.87	4.006
C-16	15.58	2.11	1.04	56.18	7.65	126.67	76.54	4.192
D-21	21.20	3.20	1.08	59.51	20.87	132.64	92.29	4.826
E-21	21.40	4.17	0.96	48.44	30.96	57.36	121.35	5.516
F-23	22.81	2.41	0.95	52.18	19.80	118.33	89.85	4.549

Table 3.8: Fiber properties of the six commercial grades of paper.

	Fibers (million/gm)	Length unweighted (mm)	Width (μm)	Coarsenss (mg/m)	Rate in Length of Macrofibrills (%)	Broken ends (%)	Fines Elements	Percentage of fines elements (% area)
A	11.076	0.792	27.4	0.1136	0.779	44.94	44.1	10.27
B	14.077	0.771	26.8	0.0922	0.791	45.74	43.6	9.79
C	11.276	0.766	28.6	0.1144	0.901	46.25	49.3	10.34
D	14.99	0.792	28.6	0.083	0.927	47.95	49.9	11.01
E	21.752	0.575	23.6	0.0767	0.84	38.85	46.8	12.25
F	11.3	0.681	26.4	0.1273	0.817	41.15	44.3	11.12

For specific data sets, three statistical methods will be performed. The first is the Analysis of Variance (ANOVA) which measures the difference of three or more sample sets. A t-test may be performed which measures the difference between two similar samples. Lastly, a measurement of the Pearson Coefficient may be performed to understand the correlation of two trends; a value between -1 and 1 will be given in relevance to how strong of a correlation exists; a P-Value will be given which determines the confidence of the correlation. All three statistical analyses are performed through the statistical software, MiniTab.

3.3.1 Results for Comparison Tests

The results of the six grades of paper tested using the laser printer are shown in **Figure 3.2**. The data from laser printer test was compiled using two separate ANOVA tests for the larger and smaller particles size ranges; the mean values and confidence intervals were combined to form the data. The test was performed once for each of the samples except for sample C which was performed twice to show a definite minimum. Three distinct groups were formed, samples A and E, samples B, D and F and sample C. Sample C was shown to have the lowest definite dusting number. The dusting range had a minimum of 0.093 mm^2 per sheet for sample C and a maximum of 0.221 mm^2 per sheet for sample A.

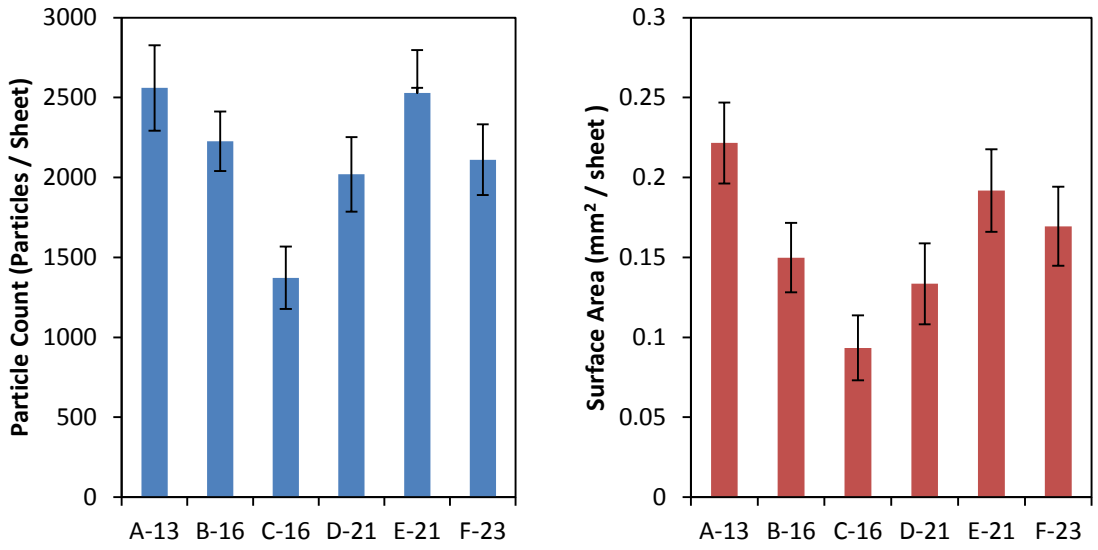

Figure 3.2: ANOVA results for compiled dusting results from the Hp Color Laserjet Printer analyzed after 1000 sheets.

The particle size distribution shown in **Figure 3.3** indicates that there are few particles above 100μm in effective diameter. Particles that are too large may indicate picking or ripping of the sheets. Unlike dust that accumulates in the air, the particles collected from the printer were dispersed in water which may result in the particles breaking down into their finest forms. The ratio of the longest length to width also shows that most of the particles has a ratio below four. These particles are elongated but do not exhibit the same lengths as standard long fibers. Examples are shown in **Figure 3.4**, **Figure 3.5**Figure and **Figure 3.6**. Additional images can be found in the **Appendix F**.

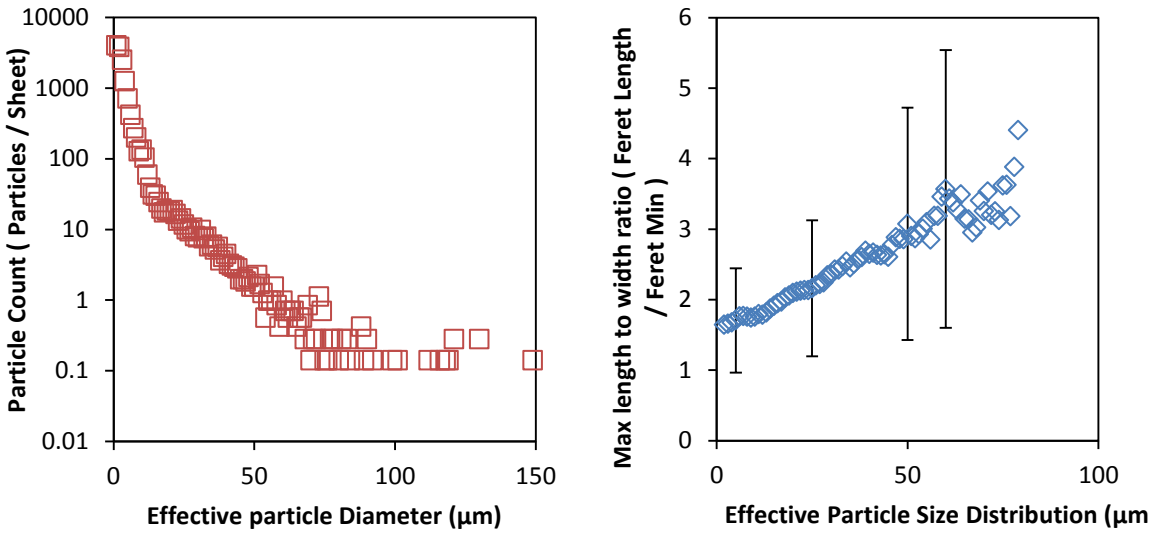

Figure 3.3: Particle Size Distribution of the dust collected from the laser printer (Left) and the average feret length to width ratio distribution (Right).

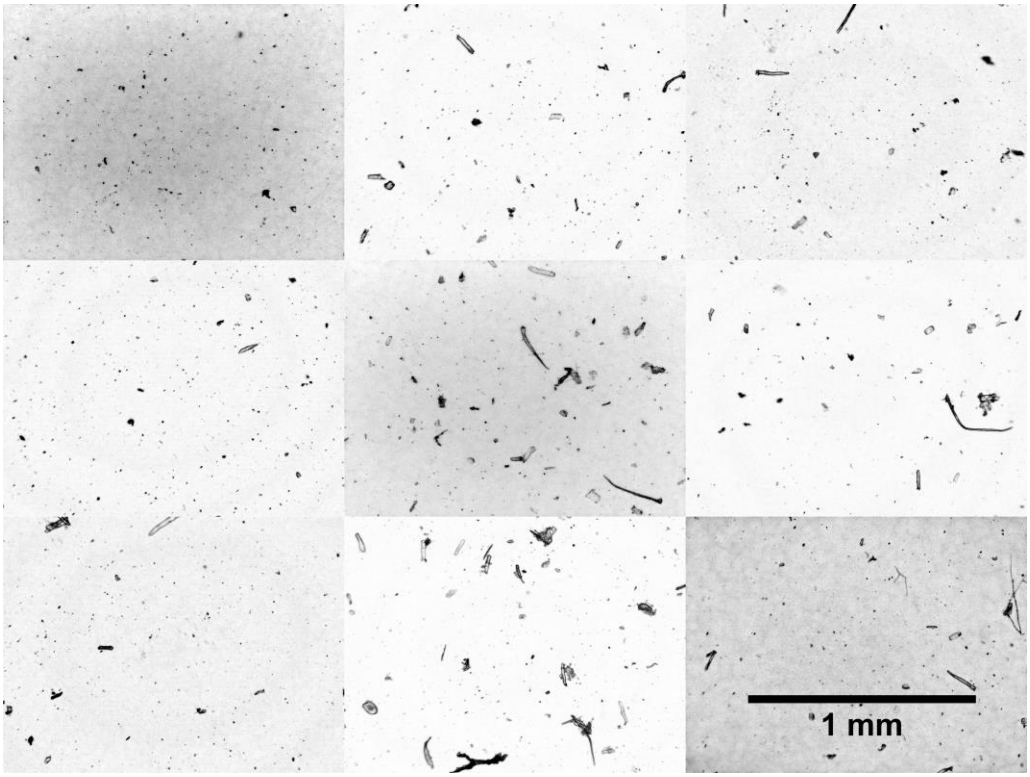

Figure 3.4: Example of images taken from sample B of the laser jet printer test.

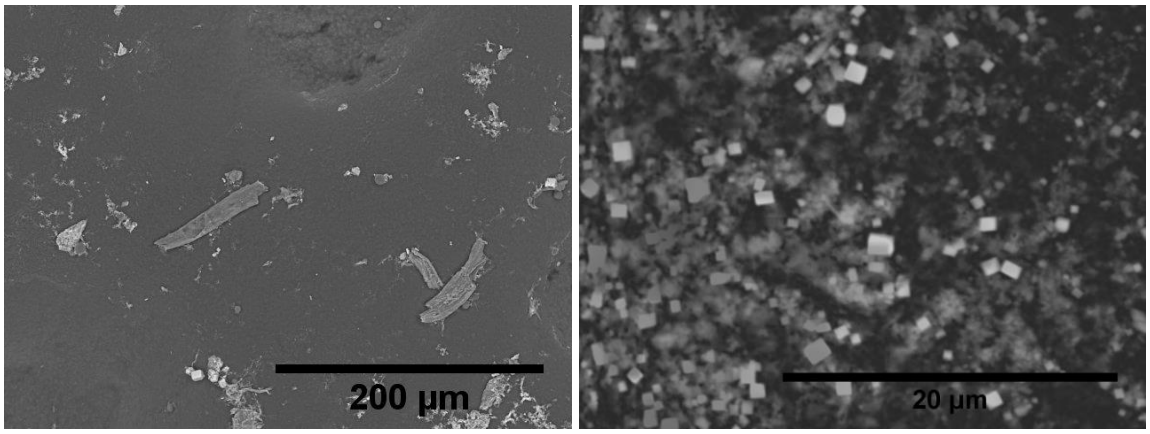

Figure 3.5: SEM images of the dust from the laser printer test and sample grade E after drying from a colloidal dispersion.

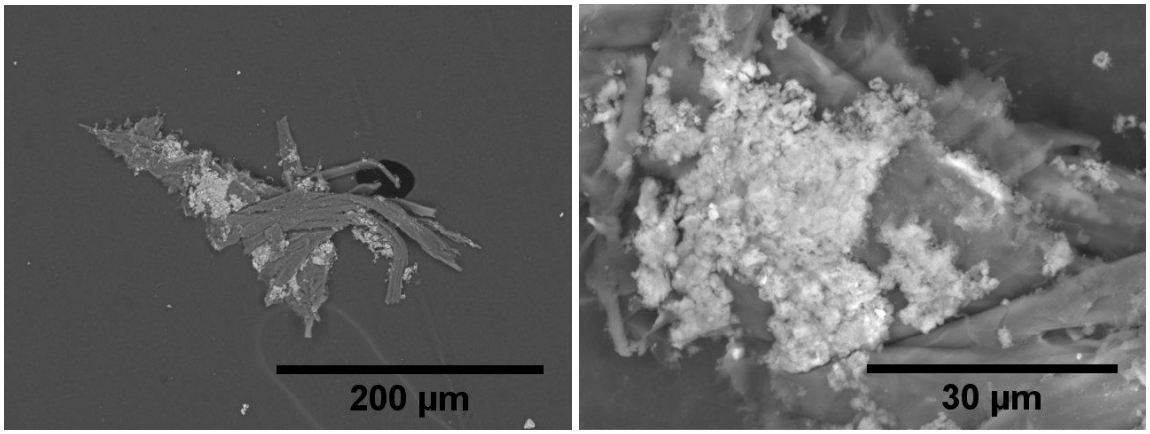

Figure 3.6: SEM images of dust collected from sample grade E from the laser printer test taking directly from the back plate of the printer. 400x magnification (Left) and 2500x magnification of the same particle (Right).

During the cleaning of the laser printer, it was observed that a larger quantity of the visible dust appeared at the outer edges of the back panel. Because of this observation, an additional test was performed to measure the dusting quantity at the outside edge.

The analysis on the particle distribution from the center of the laser printer to the outside edge was performed. An image of the back panel is shown in **Figure 3.7** and the true particle pixel distribution is shown in **Figure 3.8**; the data indicates greater dusting at the edges then at the point of 4 cm from the center with a ratio of 4.3 : 1 for sample B and 3.8 : 1 for sample C.

Possible causes includes dust being released from the paper edge and particles migrating from the center outward.

Figure 3.7: Example image of the back plate of the laser printer after 500 sheets were tested.

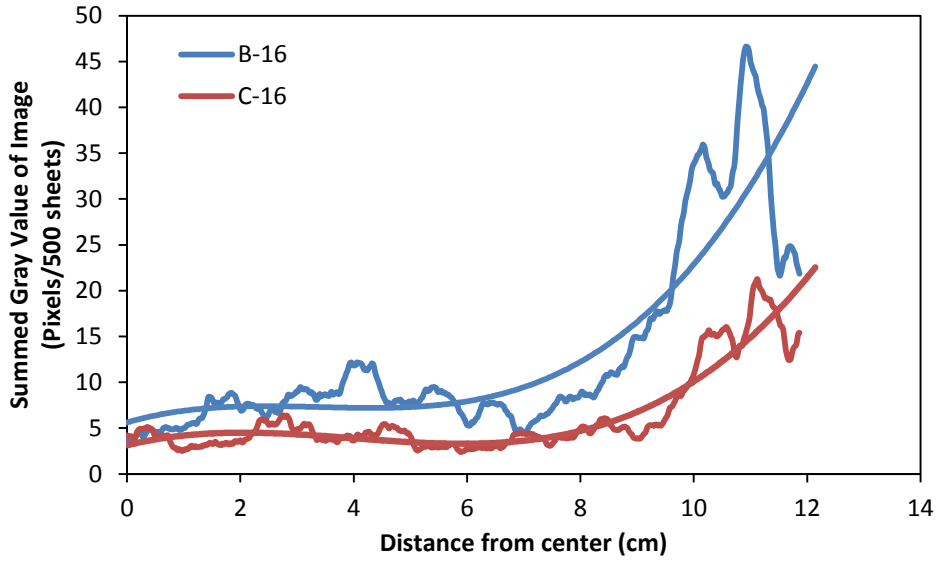

Figure 3.8: Image of particles under a black light on the back panel of the scanner and the brightness intensity distribution of particles from the center of the panel to the side.

Figure 3.9 shows the results of the industrial test compared against the laser printer test. The results from the industrial test shows that the latter of the six grades dusted less than the first. Although the data is observed do not correlate with filler loading, the unknown additives of the paper may cause the higher loaded grades to dust less. Although a variety of grades were

chosen to represents standard paper versus high quality printing paper, all six grades were considered to be low dusting paper as disclosed by the tester operators. As is clear, the test did not correlate with the laser printer results.

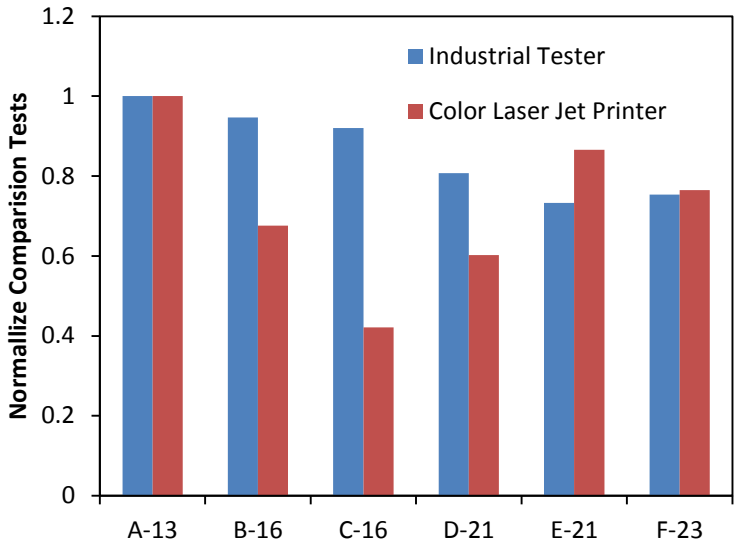

Figure 3.9: Dusting Results from the industrial tester and the laser printer test. The test is normalized to sample A to show a reduction of dusting between sample A and B-F.

3.3.2. Results From Bending Test

The results for the handsheet and commercial grade papers are shown in **Figure 3.10 and 3.11,** respectively. The error bars used in the following graphs are a single standard deviation of 48.3%. The dusting values for the results of the handsheets tests show an increase of dusting between 16% filler loading and 33% filler loading. In comparison with particles diameter under 40μm, the particle count of particles over 40μm was insignificant with an average contribution of 3.7% of the total particle accumulation. When comparing the total surface area of both size ranges, particles with a diameter over and under 40μm were significant in the results. The results from the commercial grade tests show no significant difference between the results but

by visual inspection, a common decrease in the dusting values occurred as the ash values increased. Similar to the handsheets, the particle count of particles over 40µm in diameter was insignificant with an average of 1.9% of the total particle accumulation.

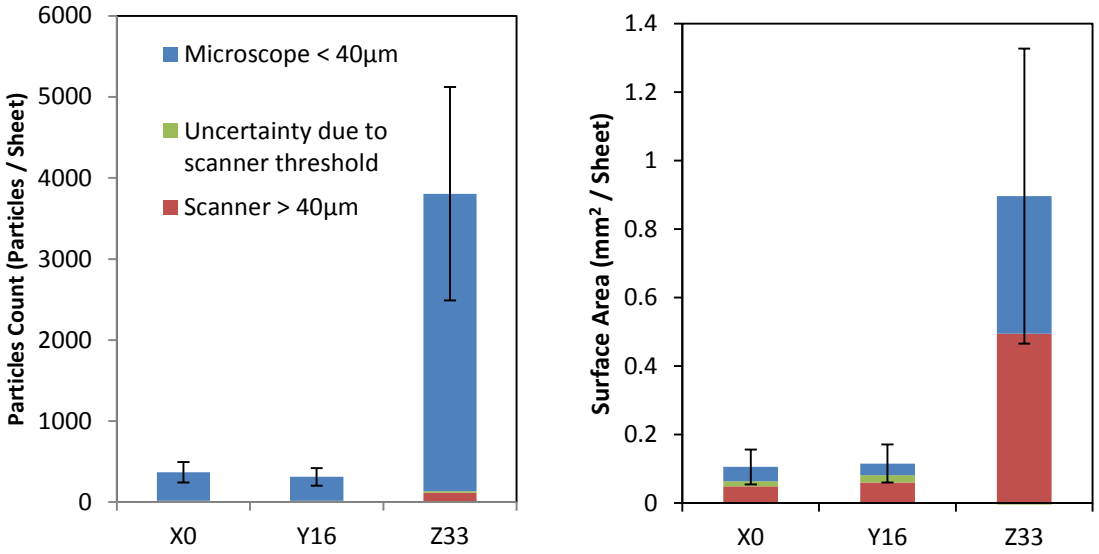

Figure 3.10: Dusting values for the bending test using handsheets.

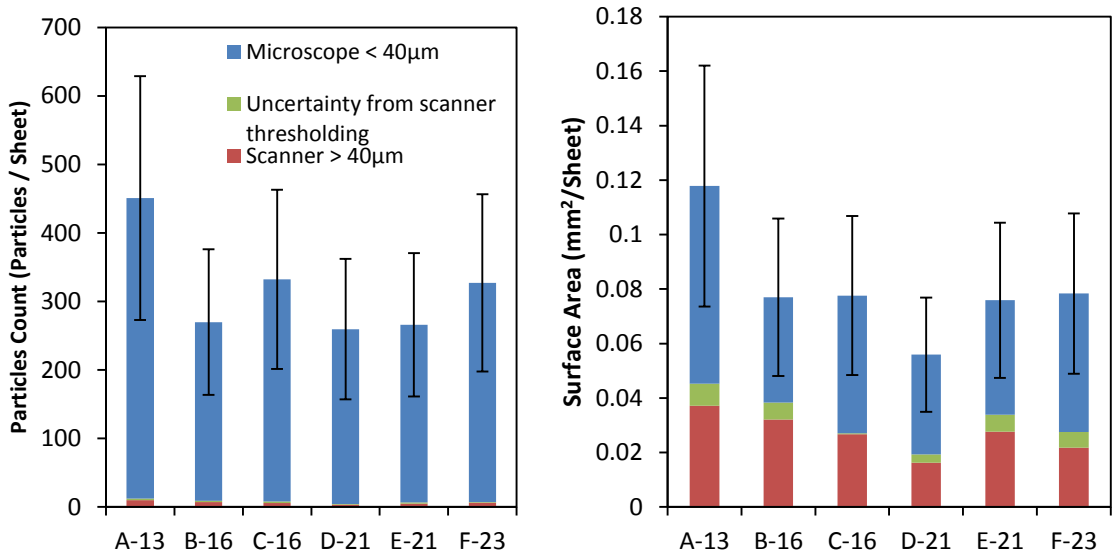

Figure 3.11: Dusting values for the bending test using commercial grades of paper.

The ANOVA was performed on surface area results for both the handsheets and the commercial grades and the results states that there is a significant difference between handsheet Z-33 and the samples X-0 – Y-16 with a P-Value of 0.006 and a F-Value of 13.6. No difference was found for the commercial grades of paper. The direct filler loading of the paper contributed to the overall increase of paper dusting using this test method; the data does not state if the increase of dusting is directly caused by the increase of released filler particles or if the dusting is caused by a reduction in strength

The overall test was capable of determining an increase of dusting between two handsheets at different loading values but was not able to determine a significant difference between the commercial papers.

3.3.3. Results from Edge Effect Test

Using the same configuration, the dusting tendencies of the paper edges were tested on both the handsheet samples as well as the commercial grades. The results for each test are showed in **Figure 3.12** through **Figure 3.14**. The result from the factory cut and laboratory cut commercial samples are in Figures 3.13 and 3.14, respectively. The error bars shown in the figures is a single standard deviation as 54.5%.

The results for the handsheets tested for edge effects showed that the sheet with 0% filler content has a particle count of 21 particles per sheet where the handsheets with 16% filler content had 226 particles per sheet. Unlike the previous study, the contribution of particles over 40μm is on average 5.4% of the total accumulation. A surprising result was that the 15% ash content had similar dusting level as the 33% ash content sample, measured either as a count or by area. This result may be due to the cutting action that causes a significant amount of loose material for both of these samples, while the case where the dust is collected from the center,

the ash content becomes important. The results from the commercial grades shown in **Figure 3.13** and **Figure 3.14 .** The results for both tests did not visually show any trends or difference but a t-test was performed on the data between similar grades to show if there is a difference between the factory cut edges and a benchtop paper cutter.

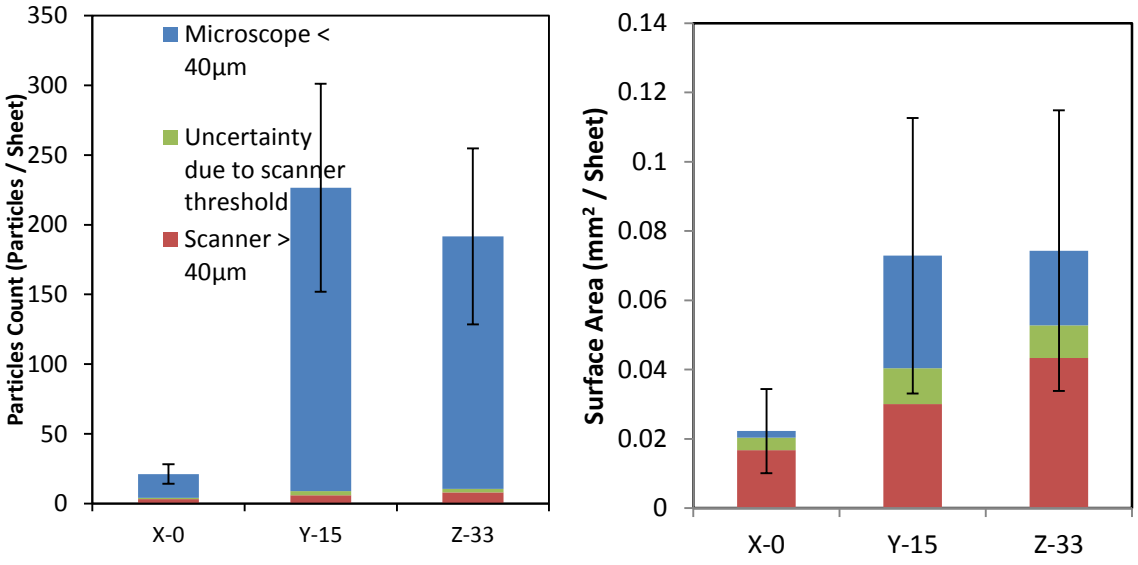

Figure 3.12: Dusting values of the handsheets using bending test but collecting dust from edges.

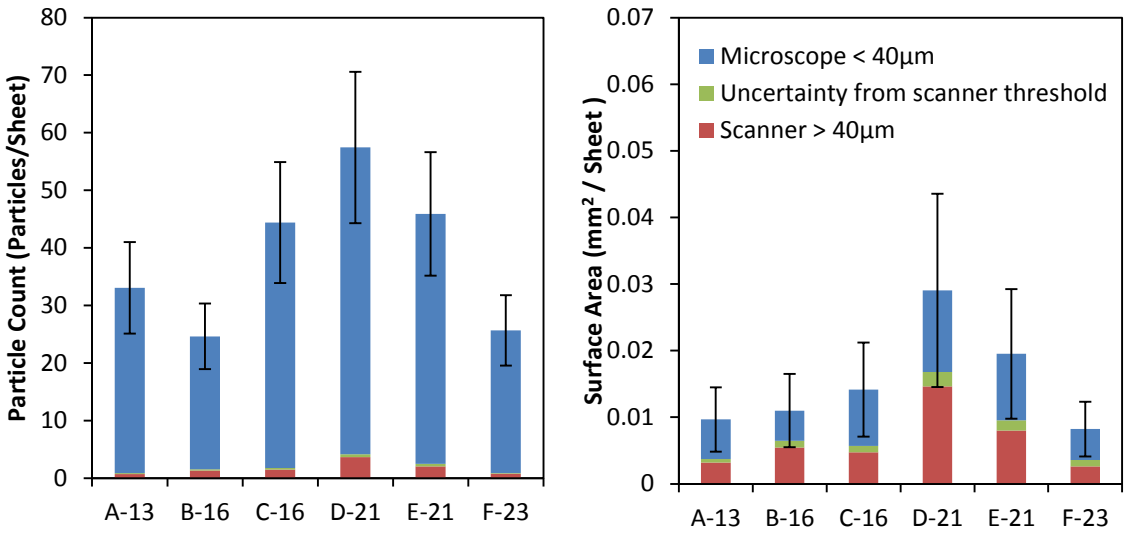

Figure 3.13: Dusting values of the commercial grades caused by factory edge effects from the bending test by collecting dust near the edge.

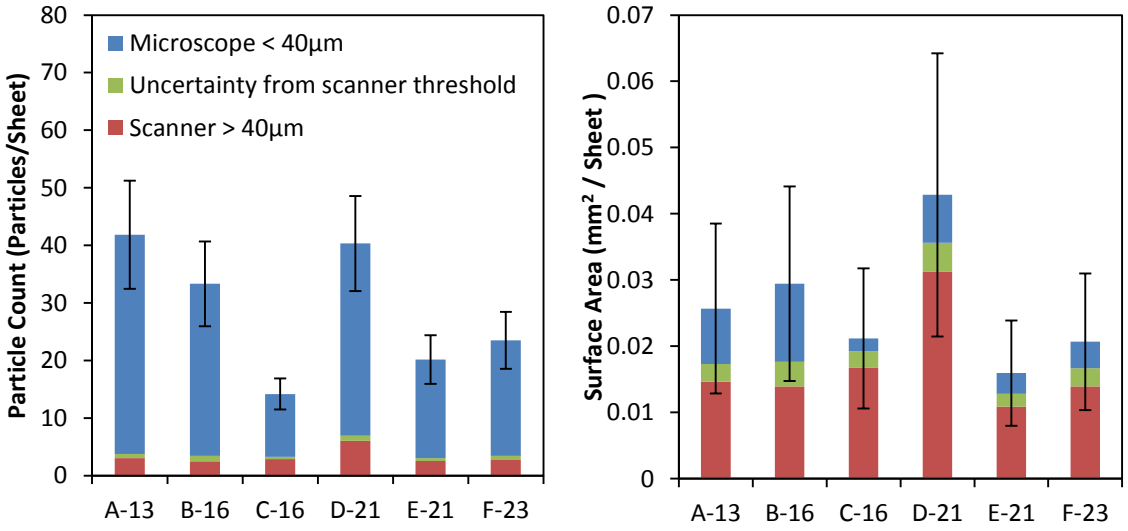

Figure 3.14: Dusting values of the commercial grades caused by the benchtop paper cutters effects on the edges using bending test and collecting edge dust.

Greater dusting values for the benchtop cutter was shown for samples A and F with a t-value greater than 3.7 and a P-Value less than 0.05 of the results from the scanned surface area, the total particle count and the total surface area. This increase may be a result of the high quality of cut that can be obtained for the commercial sheets. The correlation of dust with the laser

printer results is still not clear in either case. For the lab cut case, sample C was the lowest dusting situation that also relates to the lowest dusting sample with the laser printer. However, this result is not satisfying because the laser printer test used the factory cut samples.

The overall results indicate that edge effects cause a significant difference in the dusting value of two grades of paper based on the method of paper cutting. Not all of the grades showed an increase of dusting when compared between the factory cut edge and the benchtop. The normalized tests using both the factory slitter and the benchtop cutter showed a difference between paper grade samples C-F and D.

3.3.4. Results From Abrasive Test

The results of dusting for the case where the paper rubs against the rod are shown in **Figure 3.15** through **Figure 3.16**. The error bars on the following figures are shown as a single standard deviation of 46.3%. Similar to the bending test, the dusting tendency of the handsheet grades increased with increasing filler content. Particles with a diameter larger than 40μm contributed to 7.9 % of the total accumulated particle count. The particle count of the commercial tests is composed primarily of particles under an effective diameter of 40μm with a contribution of particle above 40μm of 3.1%; all particles are significant for the measurement of the surface area. The results do not correlate with the laser printer results.

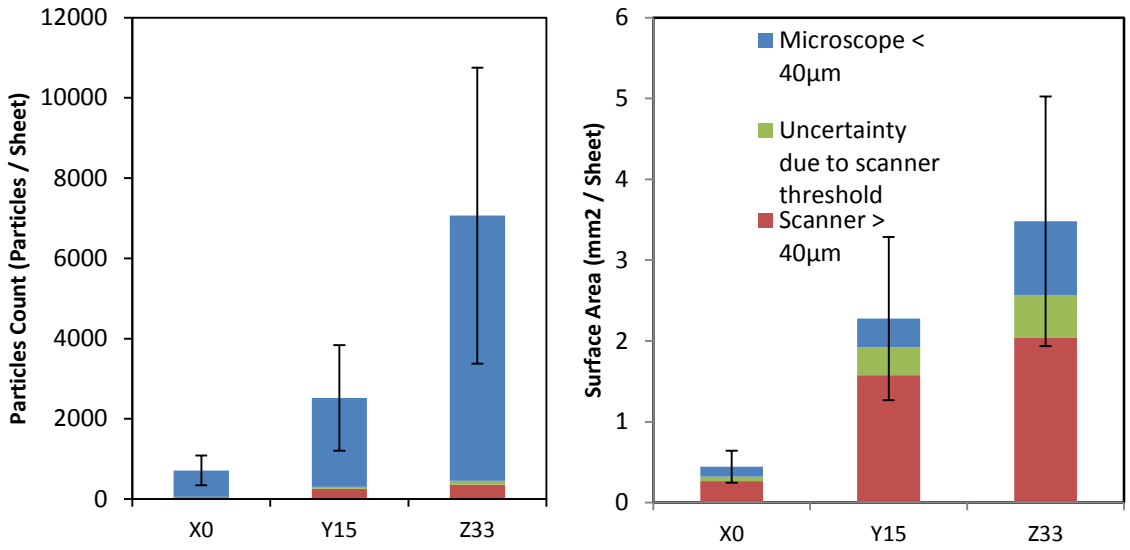

Figure 3.15: Dusting values of the handsheets using Testing Method 1, Configuration 2.

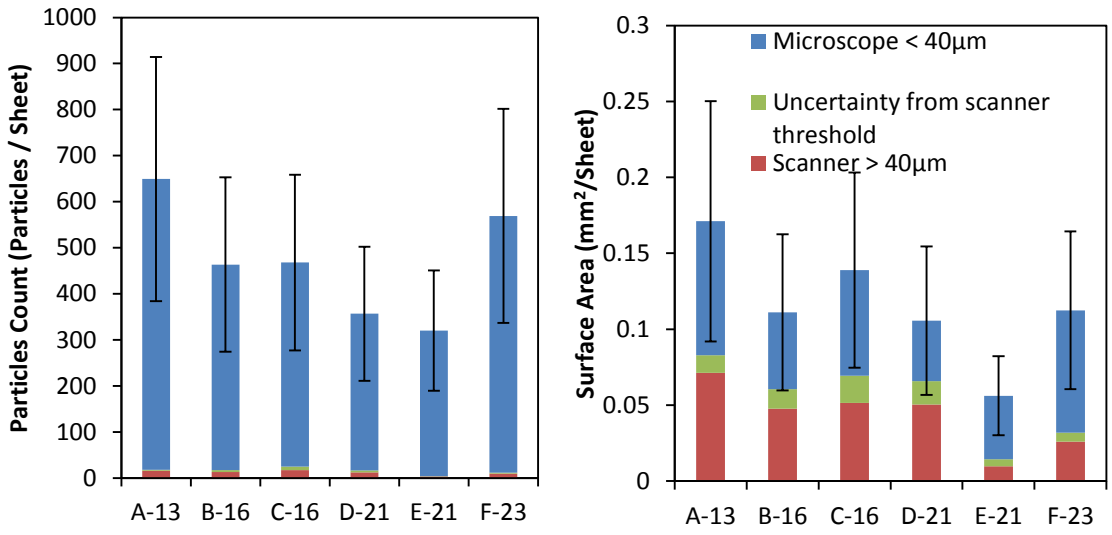

Figure 3.16: Dusting values of the handsheets using Testing Method 1, Configuration 2.

The ANOVA test is performed for both the handsheets and the commercial grades. The ANOVA showed that there were no significant difference between the commercial grade samples but a closer investigation into the sample sizing may show that a single sheet per test may not be sufficient in providing enough dust.

The overall results states that the abrasive test has the capability to determine poor dusting paper but the large variance of the test requires that large differences in the dusting tendencies are needed to signify a difference in the results. No significant difference was found between the commercial grades when grouped together but a significant data set was found between samples A and E as well as B and E. A significant difference was found between the handsheet grades X-0 and Z-33 with an ANOVA P-Value of 0.024 and an F-Value of 7.4.

3.3.5. Results From Tape Pull Tests

The tape test which includes the use of electrical tape and paper safe tapes was performed on the commercial grades of paper. Unlike the previous studies, the background of the electrical tape and the paper safe tape is more difficult to remove using thresholding and results in a more significant uncertainty range. Because of this and the data collected, the electrical tape did not show any significant difference in the results but visually showed similarities with the laser printer test as shown in **Figure 3.17.**

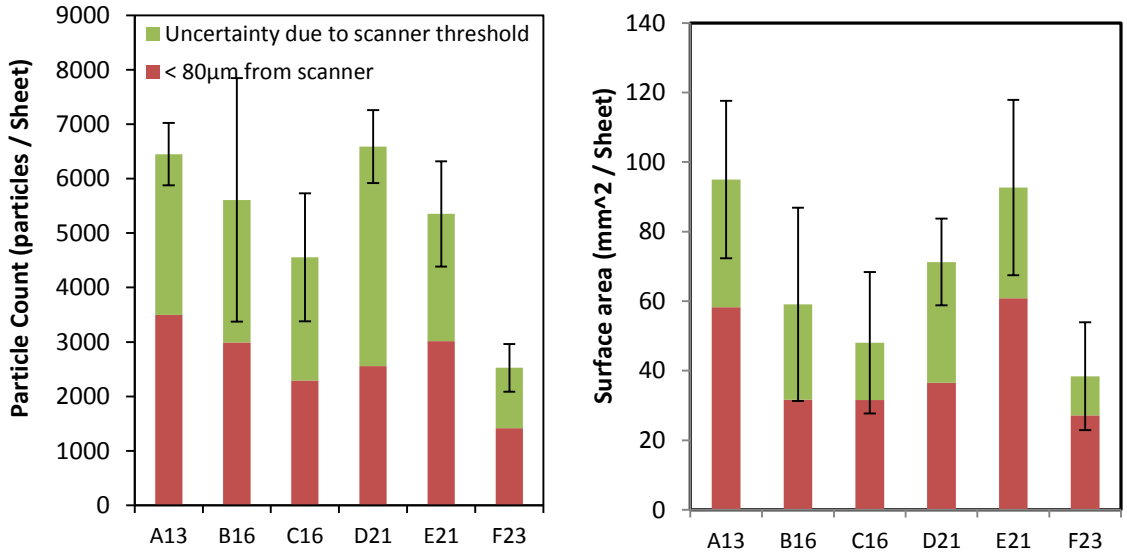

Figure 3.17: The particle count and surface area of the surface contamination collected, using electrical tape pull.

For the paper safe tape, particle count significantly increased between sample set C and D as shown in **Figure 3.18**. The surface area of the collected particles also showed the same increase in comparison with the particle count.

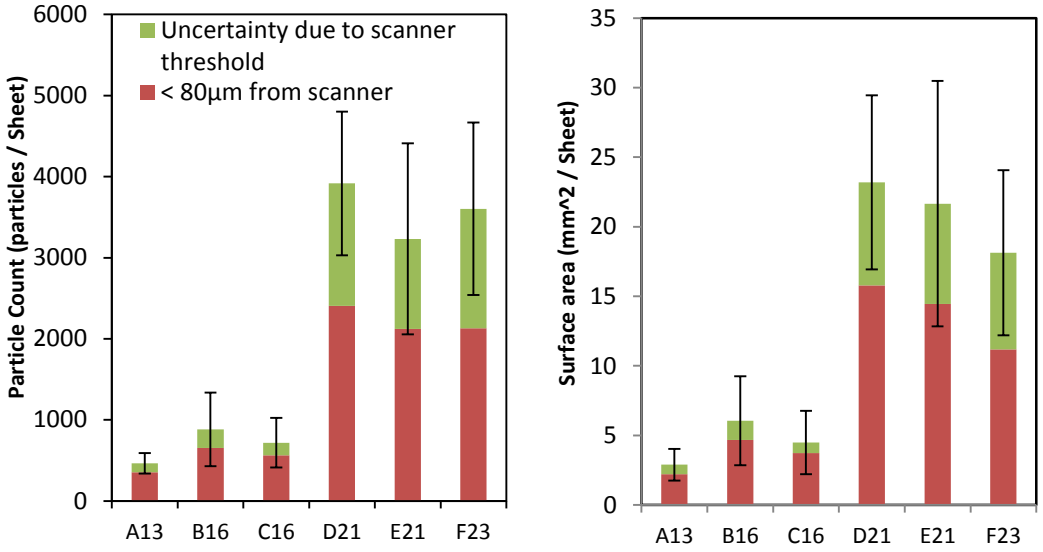

Figure 3.18: The particle count and surface area of the surface contamination collected from test method 2, paper safe tape.

An ANOVA was performed on both the data collected from the electrical tape and the paper safe tapes. The uncertainty of the threshold used for the electrical tape test is much larger than any of the other tests. Performing an ANOVA could result in a difference between A and F but with a large uncertainty, the difference would remain inconclusive. The uncertainty is much smaller and after an ANOVA was performed, the data does show that there is a difference between group A-B-C and D-E-F.

The overall amount of particles pulled from the surface is significantly greater than that of normal dusting quantities but the observation of the quantity of particles pulled from the electrical tape closely resembles that of the laser printer test. The trends of the paper safe tape did not correlate with either of the comparison tests or any of the tests from the first method.

The effects of the tape test may be more closely related to linting then to dusting but this thesis does not include the comparison tests for a traditional linting experiment.

3.3.6. Correlations

The purpose of the handsheets is to create a known poor dusting paper as well as to investigate the dusting correlation to filler loading. The complex furnish of the paper grades may greatly affect the dusting properties of the paper and with an unknown quantity of strength additives and retention aids, it may be difficult to relate the properties of unknown grades. Because of this, handsheets will generally be used to correlate the ash content and the commercial grades will be compared with the industrial tester and the laser printer test. The full correlation tables can be found in **Appendix E.**

Using the handsheets, the data was able to be correlated with the ash value; the relation between the ash value, surface roughness and tensile strength were similar and because of this, only the ash value is reported. The bending test showed that the increase in dusting partially correlated with the ash content with an R^2 of 0.8 and a P-Value of 0.01. The edge effect test did not correlate with the ash content, test method 1, 2 and or the comparison tests. The edge effect test did correlate with basis weight with a R^2 of 0.552 and a P-Value of 0.009. The abrasive test correlated well with the ash value with a R^2 of 0.834 and a P-Value of 0.005. These tests showed that when bending, stressing and or abrading paper against a rod, the effects of direct filler loading causes an increase in dusting.

Using the commercial grades, the data was compared with the laser printer test as well as the industrial tester. The laser printer test did not correlate with any of the paper properties nor the industrial tester dust results. None of the tests correlated with the laser printer. The electrical tape test from test method 2 visually correlated with the laser printer test but failed to achieve a

specific confidence with an R^2 of 0.31 and a P-Value of 0.085. The industrial tester was able to correlate with specific results given from only the scanner. The bending and abrasive test correlated with the industrial tester with an R^2 of 0.448 and 0.428 respectively. Since the poor correlation may be from the variability of the test, a Pearson's Correlation of the average values for each grade was taken. Achieving a P-Value of 0.037, the abrasive test correlated with the industrial tester with an R^2 of 0.839.

These results showed that filler loading did cause an increase in paper dusting using both the bending test and the abrasion test but the tests were not conclusive with relating the results to the laser printer test. Observing all of the results, there seems to be a difference in the relationship between the laser printer test and the industrial tester.

3.4. Discussion

Inspecting each test individually, the results are conclusive that there are no relationship between either of the two test methods and the laser printer test. By bending, stressing and abrading the paper over a rod and to repeat the action multiple times, the test was designed to increase the dusting effects of the paper and to collect a measurable amount. The test was also designed to minimize the possibility of causing additional dusting problems. The results between both test methods and the laser printer test shows that unrelated dusting may be occurring due to the bending, stressing, abrading or repetition of the design. Reducing the harshness of the test would require more extensive measures to collect dust; the measured dust is already at a minimum.

Considering all of the data between the handsheets, the commercial grades and the laser printer test, the behavior of the dusting is related but not restricted to only filler loading. If dusting was restricted to only filler loading, an increase of dusting would have been seen in the

commercial grades as well as the handsheets. Another properties that may contribute to dusting is the strength characteristics of the paper, which was not controlled when forming the handsheet. When determining the characteristics of the handsheets, it was decided that no binders would be included because the binder may also adhere the filler particles as well; it would be difficult to determine if a reduction in dusting would be from strength characteristics or from the binder directly.

The mechanisms of dusting are not fully known and when examining all of the data in this chapter, it is more clear that multiple mechanisms exist, not all of which may apply to the laser printer. Bending, stressing, abrading and re-iterating these actions were not the right combination of mimicking the laser printer. Also, the results from the commercial paper were more closely related to the industrial tester, of which is a surface test. For each case that dust is produced in the industry, it is possible that a unique combination of mechanisms may contribute to the production and that each case may not be the same.

3.5. Conclusions

Dusting tests were conducted on handsheets and commercial papers using the range of tests described in Chapter 2 and compared to an industrial dusting test and the results using a laser printer test. The results are compared and correlated with paper properties and more specifically the ash value.

The test performed on the laser printer showed that paper grade C had the lowest dusting value and grade A had the highest. The dusting accumulation across the printer showed an increase of dust at the outer edges of the printer; this suggests that the slitting of the sheets likely generates a significant amount of the dust that can influence the printer. The largest frequent particle size is an effective diameter of 50μm for a minimum count of one particle per sheet. The

ratio of the ferret length to the ferret width of the same particles reached an average maximum of 4 : 1. The particles captured from the laser printer test are mostly short fibers. The industrial test showed a consistent decrease of dusting between commercial grade A through commercial grade F and when compared to the three test methods, the bending test and the abrasive test for particles over 40μm partially correlated with the results.

The results for the handsheets have an increase of dusting with filler loading: both the bending test and abrasive test agreed with this expected result. Edge effects did not show the same increase when analyzing the handsheet tests but after completing a separate test, the use of a benchtop paper cutter versus the factory cut edges showed an increase of dusting for two grades of commercial paper. The edge effects also showed a partial correlation to the basis weight of the commercial paper.

When performing the tape tests, neither result correlated well with the industrial test, the laser printer test nor the three testing configurations. The electrical tape results showed a visual relationship with the laser printer results.

Overall, the tests that were performed gave good insight into the possible behavior of paper dusting but the accuracy and repeatability of the test is relatively poor with high deviation values. The behavior of the dusting tendency for each test was different in which the edge effects performed much differently than the other two. The test that performed the best is the abrasive test which correlated with the industrial test. The result from the edge effect test shows that dusting from the edges may fall under a different category of dusting other than dust produced from surface contamination. The laser printer showed an increase of dust accumulating from the edges; this does not confirm that the particles are being released from edges but it may be caused by slitter dust resting close to the paper edge.

4. CONCLUSIONS AND FUTURE WORK

4.1. Concluding Remarks

The work performed in this thesis included the design of test methods that could be used in a paper testing laboratory using limited number of samples. A considerable portion of this thesis was determining an accurate method of collecting and measuring dust particles. The restrictions of collecting dust often require an opaque or a solid background where accurate particle detection becomes difficult. Optical microscope imaging gave the resolution needed to count the fine particles, but several images need to be analyzed to obtain reasonable statistics. A photo scanner can be used to image the full collection area but due to background noise from various collection surfaces, the smallest particle that can be counted is 40μm: this cut off misses most of the dust that is generated in the various tests.

For the bending and abrasion type tests, the best method to collect dust was using a vacuum with a filter to collect. Optimum conditions for these tests were determined. Control tests were performed to measure the deviation of the results; the standard deviation of each result showed to be as high as 54% of the average. This variation likely comes from the variation of the paper samples: improvement to the method would be to measure more samples.

The bending and abrasion test confirm the expected result for the handsheets in that dusting increased with filler content. When testing the edges of the handsheets, the results were not statistically conclusive on the increase of dusting based on filler loading.

The tests with the laser printer did show some difference in dusting between the commercial grades, but no other test or paper property was able to correlate with the laser printer test. The bending and abrasion tests did not show statistical differences between the commercial grades. Only when the edge effect test was compared against the factory cut edges of the paper and a

benchtop cut edges, the results showed a difference in two grades that relate back to the laser printer test. The increase in dust collection near the sides of the printer and the edge effect results indicate that the dusting propensity of the commercial grades likely relates to the cut quality as well as combined paper properties. The industrial dust test did not correlate with the laser printer and in fact had opposite trends: this likely is caused by the different mechanism of dust release and collection between the printer and this test.

While a clear method to test paper for dusting did not emerge from this work, a few key points were found.

- A measurable portion of the dust collected from the commercial samples likely came from the slitting event.
- Bending or abrasion of the paper surface does generate measureable amount of dust with three sheets, but the amount of dust does not seem to correlate with the amount of dust obtained in the laser printer.
- Tests that involve pulling material from the sheet of the paper such as the industrial test or the tape tests also generate a measurable amount of dust, but these results do not correlate to the printer, likely because of the different physical situation.

4.2. Future Work

Additional tests may be desired to complete the results and to form better conclusion. One of the problems encountered in this thesis is the lack of a set of samples that had clear differences in dusting tendency. The commercial samples were likely all reasonable good in terms of dusting propensity. Having a known sample set that went from low to high dusting would help clarify which test methods gave the best results. The bending and abrasion tests were intended

to create a significant amount of dust with just a few sheets, but it seems like tests that involve a large number of sheets may be needed.

The work here was to help design a lab based dust tester. A more compact, reliable version of the test can be formed by using a design with the rod and collection plate moving instead of the paper. A data acquisition method may also be required to analyze particles in the lower size range. Although scanning can efficiently detect large particles, small particles are more difficult. Methods may include laser light scattering or removing the background noise of a solid material. An example image of the next version is shown in **Figure 4.1**.

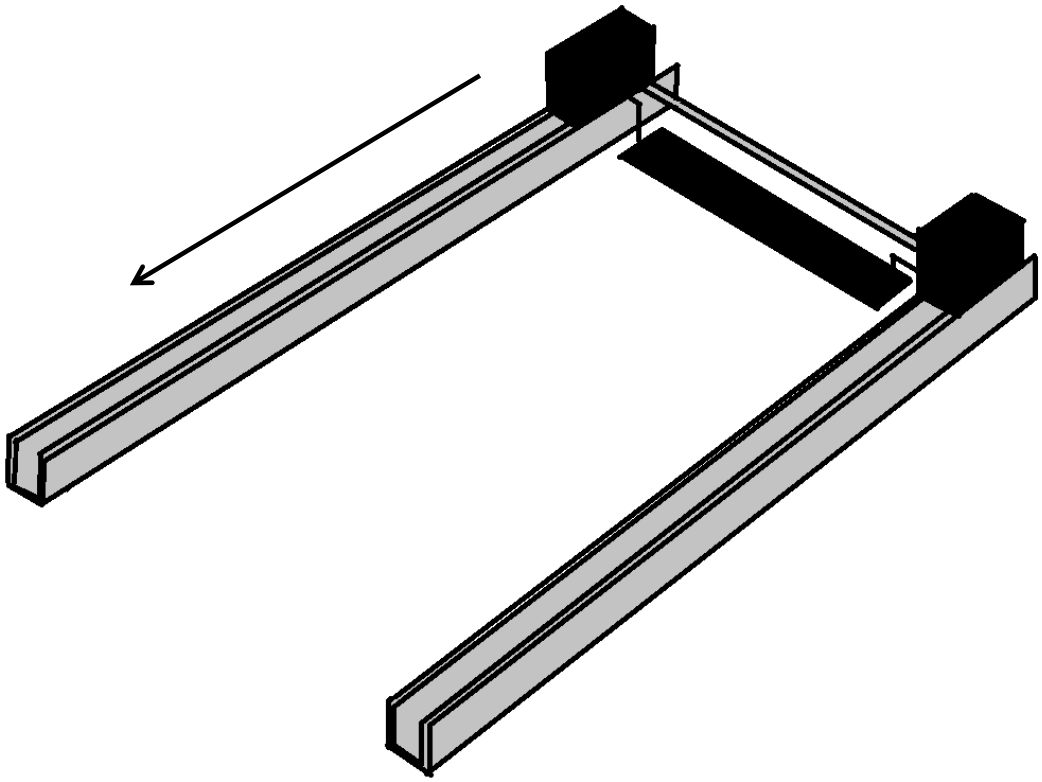

Figure 4.1: Example image of the second model of the Paper Dust Tester.

Investigating better equipment to measure dust from a scanner could increase the efficiency of the work. Observing a software used in industry, dirt and hole detection uses similar techniques of data acquisition and may be beneficial if the program can be used to measure dust. Additionally, better scanning resolution would be preferred to give more accurate particle perimeter information. The model used in this thesis included only a 4800 dots per inch resolution but scanning resolutions can increase up to 6400 or 9600 dots per inch. This would not increase the ability to detect particles due to the limiting background haze but the scanners can decrease the error given by significant size pixels. Investigating additional collection materials may be beneficial for increasing the flow rate of air that passes through the filter; keeping in mind that the material must collect the particles on the surface of the filter and the retention of the filter should be high.

The dusting tendency caused by a reduction in paper strength may also be included as an additional study. During the testing of the 0% filler handsheet, a noticeable amount of dust was measured which concludes that the paper dust tester was able to produce dust without the effects of filler. Loading the handsheet with filler components increased the dusting tendency from the test but the mechanisms are not certain whether additional filler particles are being released or if the fibers are being released due to the reduced fiber-fiber bonds.

The effects of filler loading can be studied to understand the mechanism but one critical problem that was not solved in this thesis and remains a current problem in industry is the quantification of filler particles versus fibrous particles. There are several tools that can depict the difference between fibers and fillers but many of them require a specific quantity of a sample. An ash test or the use of a thermogravimetric analysis may be performed to distinguish

the difference between filler and fibrous particles but the minimum requirement of the tests requires 5mg of dust. This amount of dust is hard to collect with current methods.

Testing the effects of humidity on the charge of the particle may change the results. Electrostatic charges are always difficult to control and the particle-particle interaction has been known to vary with varying humidity. All of the tests performed in this thesis were tested in a relative humidity range of 37% ± 3% unless stated otherwise. The effects of humidity are known to cause differences in linting and it is possible that humidity will cause a difference in dusting as well. Primary data on the effects of electrostatic attraction and its relationship to particle liftoff can be found in **Appendix B**.

The behavior of dust caused by coated grades may be different than that of uncoated. An investigation of the dusting tendency of coated grades would be useful. Testing the dusting tendency of cracking the coating may prove to be useful as well.

REFERENCES

Allen, Terence (1990). *Particle Size Measurement* (4th ed.). New York; London Chapman and Hall . 806.

Bernhardt, I. C. (2012). *Particle size analysis: Classification and sedimentation methods* (Vol. 5). Springer Science & Business Media.

Brown, R. C. (1993). *Air filtration: an integrated approach to the theory and applications of fibrous filters*. Pergamon.

Emerson, R. A. (1997). *U.S. Patent No. 5,628,228*. Washington, DC: U.S. Patent and Trademark Office.

Fan, H., Wang, S., & Liu, J. (2014). The influence of particle size of starch-sodium stearate complex modified GCC filler on paper physical strength. *BioResources*, *9*(4), 5883-5892.

Fortuna, M. E., Harja, M., Bucur, D., & Cimpeanu, S. M. (2013). Obtaining and Utilizing Cellulose Fibers with in-Situ Loading as an Additive for Printing Paper. *Materials*, *6*(10), 4532-4544.

Gao, J., & Xie, G. (2012). Characteristics of electric charges carried by dust particles and their effects on connector contact failure. *Chinese Journal of Electronics*, *21*(3), 559-565.

Gerli, A., & Eigenbrood, L. C. (2012). A novel method for the determination of linting propensity of paper. *TAPPI JOURNAL*, *11*(10), 9-17.

Gélinas, V., & Vidal, D. (2010). Determination of particle shape distribution of clay using an automated AFM image analysis method. *Powder Technology*, *203*(2), 254-264.

Gess, J. M. (Ed.). (1998). *Retention of fines and fillers during papermaking*. TAPPI press. 357.

Glassman, A. (Ed.). (1985). *Printing fundamentals*. Atlanta, Ga; Tappi Press. 388

Gratton, M. F., & Frigon, P. (2006). Predicting lint propensity of paper at the mill: a test that works. In *ANNUAL MEETING-PULP AND PAPER TECHNICAL ASSOCIATION OF CANADA* (Vol. 92, No. A, p. 175). Pulp and Paper Technical Association of Canada; 1999.

Jung, C. H., Park, H. S., & Kim, Y. P. (2013). Theoretical study for the most penetrating particle size of dust-loaded fiber filters. *Separation and Purification Technology*, *116*, 248-252.

Komulainen, P., Mustalahti, H., Karinen, K., & Launonen, U. (2012). New dusting propensity analyser. *Appita Journal: Journal of the Technical Association of the Australian and New Zealand Pulp and Paper Industry*, *65*(2), 142.

Koulocheris, D., Stathis, A., Costopoulos, T., & Tsantiotis, D. (2014). Experimental study of the impact of grease particle contaminants on wear and fatigue life of ball bearings. *Engineering Failure Analysis*, *39*, 164-180.

Libby, C. E. (Ed.). (1962). *Pulp and Paper Science and Technology: Paper* (Vol. 2). McGraw-Hill.

Lubricated nylon solves printer problem. (1998). *Reinforced Plastics, 42*(9), 29-29. doi:10.1016/S0034-3617(98)92009-4

Mittal, K. L. (Ed.). (2013). *Particles on Surfaces 3: Detection, Adhesion, and Removal*. Springer Science & Business Media. 328.

Murata, K. (2016). *U.S. Patent Application No. 15/209,629*.

Modgi, S. (2007). *Interaction of fibres and additives in mechanical pulp suspensions* (Doctoral dissertation, University of British Columbia).

New grease concquers dust (2005) Arlington Heights. Reed Business Information Inc. (US)

Rioux Jr, R. A. (2008). *Mechanical testing of coated paper systems*. The University of Maine.

Seal protects ball screw from dust while retaining grease. (2011). *Sealing Technology 2011(3).* 4-4. Doi 10 1016/S1350-4789(11)70056-3

Shen, J., Song, Z., Qian, X., & Liu, W. (2009). Modification of papermaking grade fillers: A brief review. *BioResources*, *4*(3), 1190-1209.

Smook, G. A. (1992). *Handbook for pulp & paper technologists*. Tappi. 419

Soo, J. C., Monaghan, K., Lee, T., Kashon, M., & Harper, M. (2016). Air sampling filtration media: Collection efficiency for respirable size-selective sampling. *Aerosol Science and Technology*, *50*(1), 76-87.

Sow, M., Widenor, R., Akande, A. R., Robinson, K. S., Sankaran, R. M., & Lacks, D. J. (2013). The role of humidity on the lift-off of particles in electric fields. *Journal of the Brazilian Chemical Society*, *24*(2), 273-279.

Wang, X., & You, C. (2013). Effect of humidity on negative corona discharge of electrostatic precipitators. *IEEE Transactions on Dielectrics and Electrical Insulation*, *20*(5), 1720-1726.

Warkiani, M. E., Wicaksana, F., Fane, A. G., & Gong, H. Q. (2015). Investigation of membrane fouling at the microscale using isopore filters. *Microfluidics and Nanofluidics*, *19*(2), 307-315.

Yang, T. S., & Shy, S. S. (2005). Two-way interaction between solid particles and homogeneous air turbulence: particle settling rate and turbulence modification measurements. *Journal of fluid mechanics*, *526*, 171-216.

Appendix A. SLITTER DUST TEST

The simple Slitter Dust Test was designed by Robert Rioux (Rioux, 2008) in his thesis to quantify the dusting tendency of slitter dust produced as a lab scale method. The method was performed by taking a utility blade and cutting paper on a benchtop. The paper is laid flat on a benchtop and the utility blade is held at a 45° angle to the paper. (20) six inch cuts are made into the paper at a 45° angle moving at 1 inch per second. The dust is collected using a vacuum and a 5μm filter membrane and weighed using a scale. Due to the time requirement of the test, only one test was performed per sheet. The limitation to the test was that the base paper formed less dust than the coated paper for Rioux's Tests.

The test was performed with Rioux's procedure and the quantity of dust collected was too small to be measured. An adaptation to the procedure was made by stringing the paper over two beams, clamping one side down and applying light tension to the other side. A razor blade is used to cut the paper twenty times at six inches per cut. A vacuum with a 5μm GWR-420 filter membrane was used to collect the dust immediately falling from the slit. The dust particles were scanned onto the scanner and analyzed as stated from chapter 2 of this thesis.

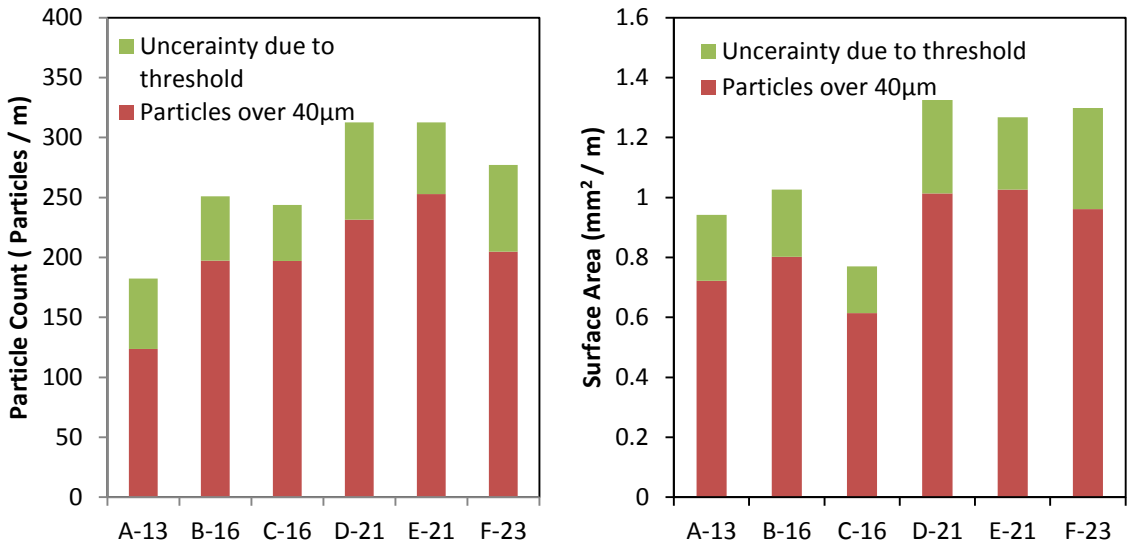

Figure A.1: Slitter dust collect as stated from the adapted simple slitter dust test form Roix 2010.

Table A.1: Slitter dust correlation to paper properties as stated from adapted simple slitter dust test.

	Slitter PC	Slitter SA
Slitter SA	0.756	
	0.082	
Ash	0.879	0.874
	0.021	0.023
Tensile Index	-0.198	-0.274
	0.707	0.599
Basis Weight	0.717	0.669
	0.109	0.147

The data shows an increasing dusting count as well as total surface area as the ash content increases. The slitter dust collected correlates with the ash value with an R^2 of .879 and .874 for the particle count and total surface area.

Appendix B. ELECTROSTATIC FORCES BASED ON HUMIDITY

A test was performed to understand the effects of particle lift off as well as the particles tendency to stay attached to a plate in an electrical field. As stated in chapter 2, the charge of hydrophilic insolated particles can change due to the humidity; a water double layer forms on the surface of specific particles changes the particle properties. The test is to measure the particles behavior in an electrical field at varying humidity and different electrical fields.

Using the Paper Dust Tester's structure, two plates were placed at gap distances of 0.5cm and 1.9cm and an electric generator of 9.5kV to create an electrical field of 1900kV/m and 500kV/m. The particles used is Hydrocarb 60 ground calcium carbonate and shredded fibers from standard blotter paper. One half gram of the particles is placed on the lower plate and the field is activated. After 10 seconds, the field is deactivated and the upper plate is measured under the Donsanto SMZ-2T microscope. Four tests were performed and shown in **Table B.1**. Each set included 3 images of 3 sets of data. The results will be the particle size distribution that will settle on the upper plate.

Table B.1: Testing materials and negative generator plate placement for each test.

Test	Material	Placement of electrical field
1	GCC	Lower
2	GCC	Upper
3	Fiber	Lower
4	Fiber	Upper

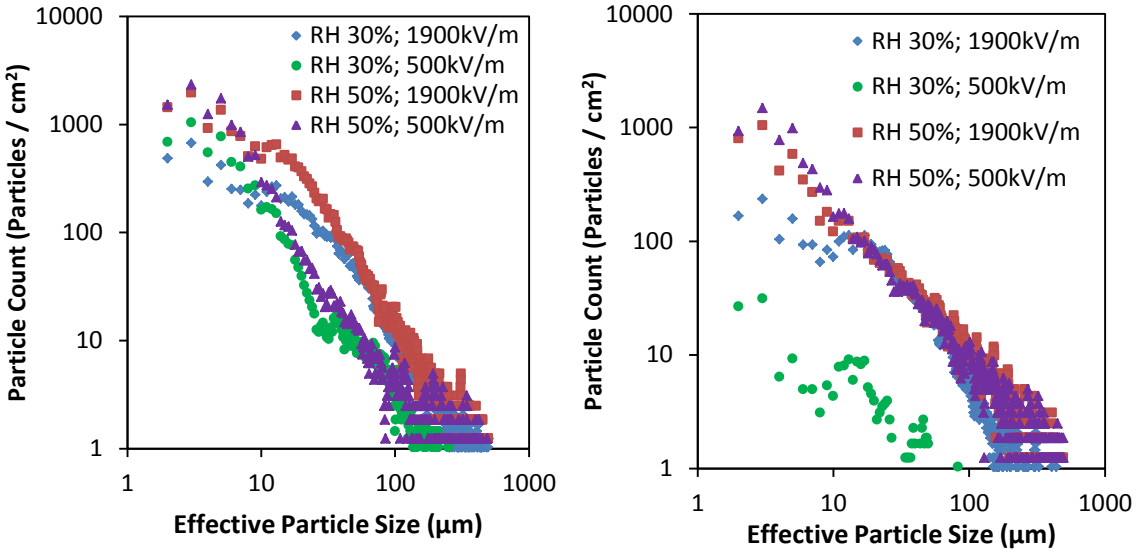

Figure B.1: Particle size distribution for tests 1 (Left) and 2(Right) exposed to an electrical field after 10 seconds.

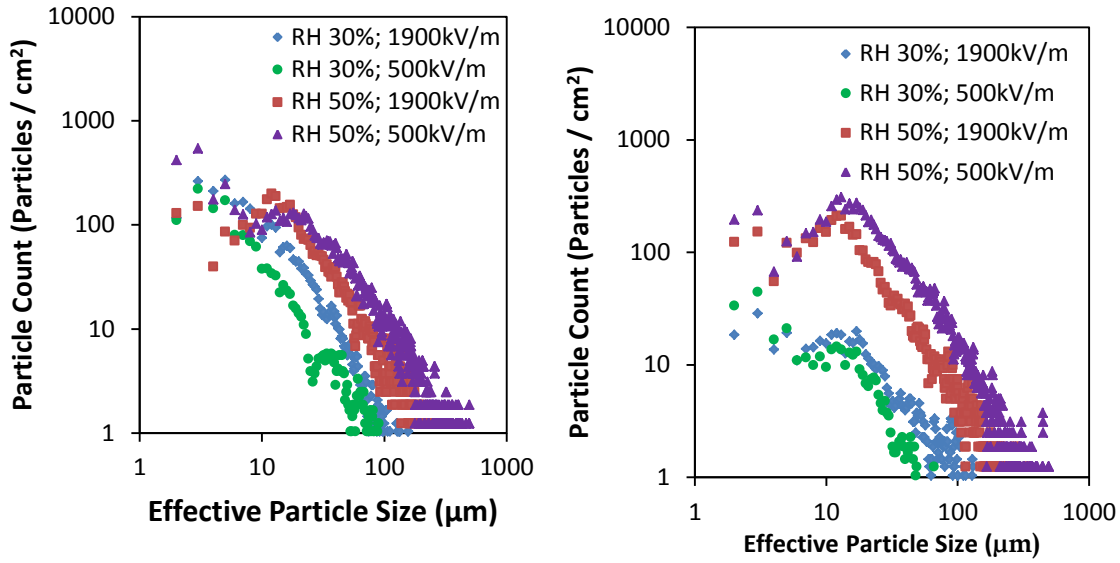

Figure B.2: Particle size distribution for tests 3 (Left) and 4 (Right) for blotter paper fibers exposed to an electrical field after 10 seconds.

Figure B.1 and **Figure B2** shows the particle size distribution of GCC and Fibers collected on the upper plate after 10 seconds. The behavior of GCC was more affected by the electrical field then that of the humidity for both placements of the negative charge generator. In **Figure B.1**, the particle collection at 500kV/m was noticeably lower than that of 1900kV/m. The fibers particle counts were largely affected by the humidity in the air. In **Figure B.2**, the particle count of particles exposed to lower humidity were noticeably lower than that of the 50% controlled humidity. From these results, the effects of using electrostatic attraction with the Paper Dust Tester may affect the behavior of different types of particles.

Appendix C. PARTICLE SIZE DISTRIBUTION

For each study concluded in chapter 3, particle size distributions were able to be made. The following graphs are the particle size distribution for both the handsheets and the commercial grades for studies 1-3.

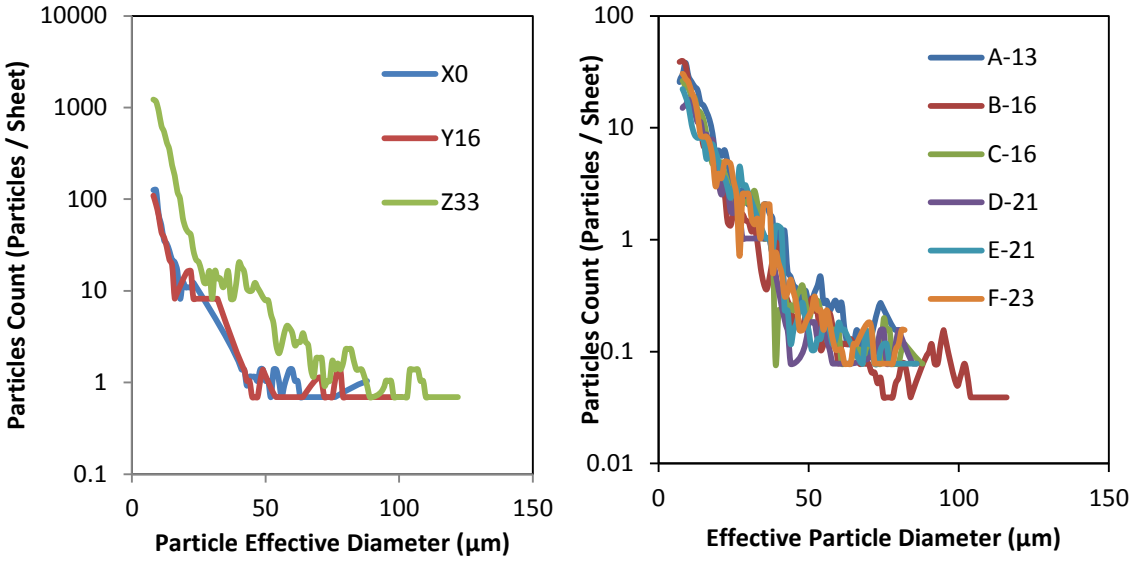

Figure C.1: The particle size distribution of Study 1. Handsheets (Left), Commercial Grades (Right). The result is the moving average of 3 points.

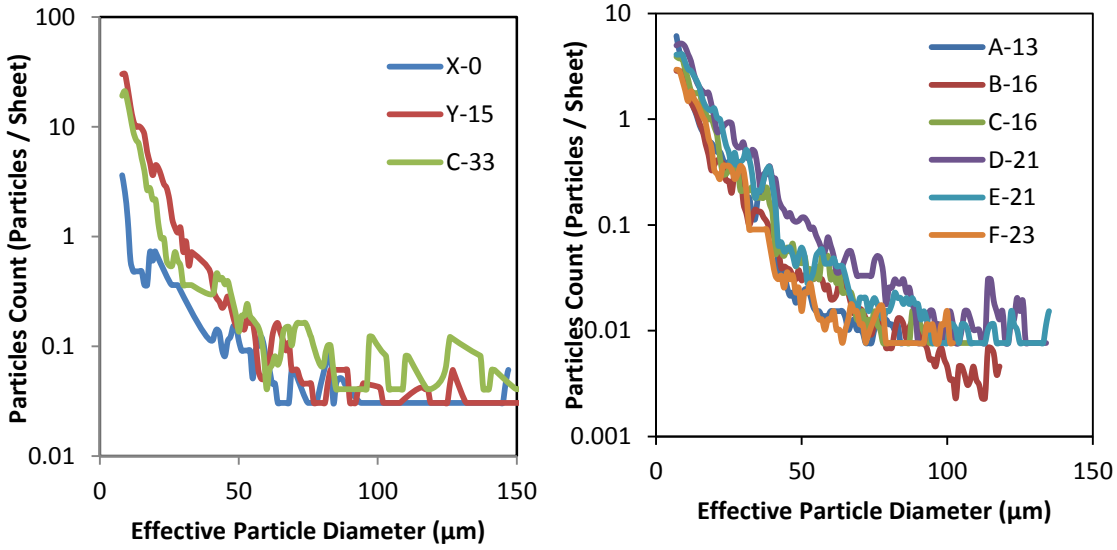

Figure C.2: The particle size distribution of Study 2. Handsheets (Left), Commercial Grades (Right). The results are the moving average of 3 points.

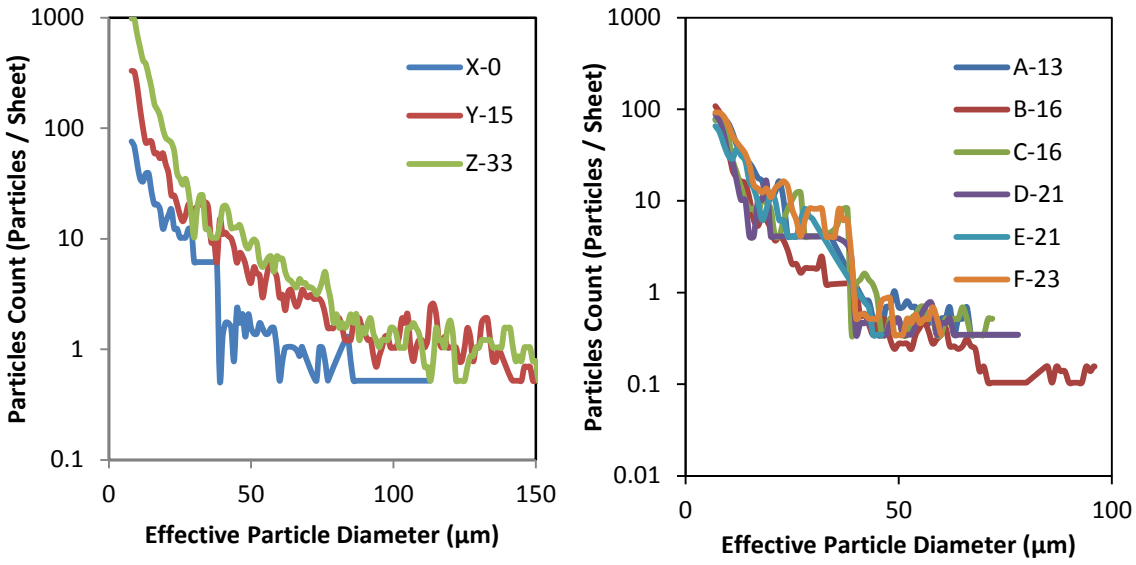

Figure C.3: The particle size distribution of Study 3. Handsheets (Left), Commercial Grades (Right). The results are the moving average of 3 points.

Appendix D. SCANNING THRESHOLD IMAGES

The following graphs are the graphical interpretation of the capture method performed in chapter 2. The concept is to depict a point where the background noise is minimized and the foreground particles is being measured.

Capture method has been used to determine the correct threshold to detect particles or objects. For the purpose of this work, the threshold determined based off of the number of standard deviations away from the mean brightness of a specific image. The tests ranges from 1.5σ to 6σ. Two graphs are formed. The first is an average area per particle in which the minimum on the graph shows the threshold at the smallest particle size. The second is the cumulative area of all the particles.

Specific tests for the background noise of the membrane observed under a microscope, electrical tape imaged on the scanner and the paper safe tape imaged on the scanner are also shown.

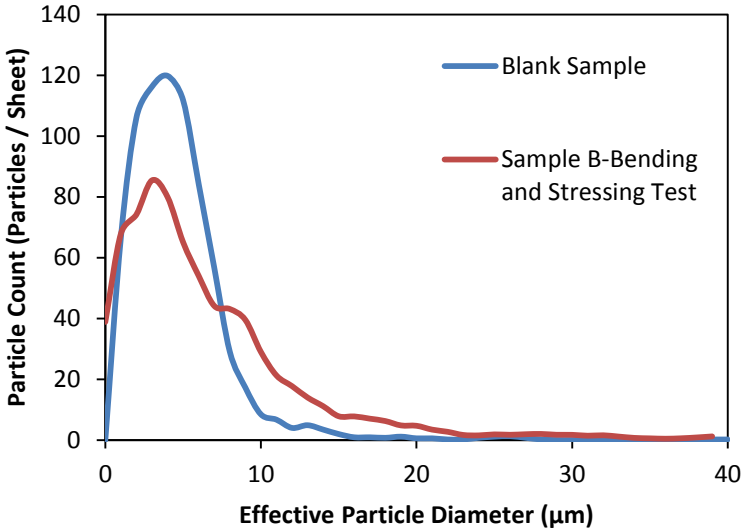

Figure D.1: The background noise of using a microscope vs a tested sample to determine the acceptable cutoff range of using a microscope.

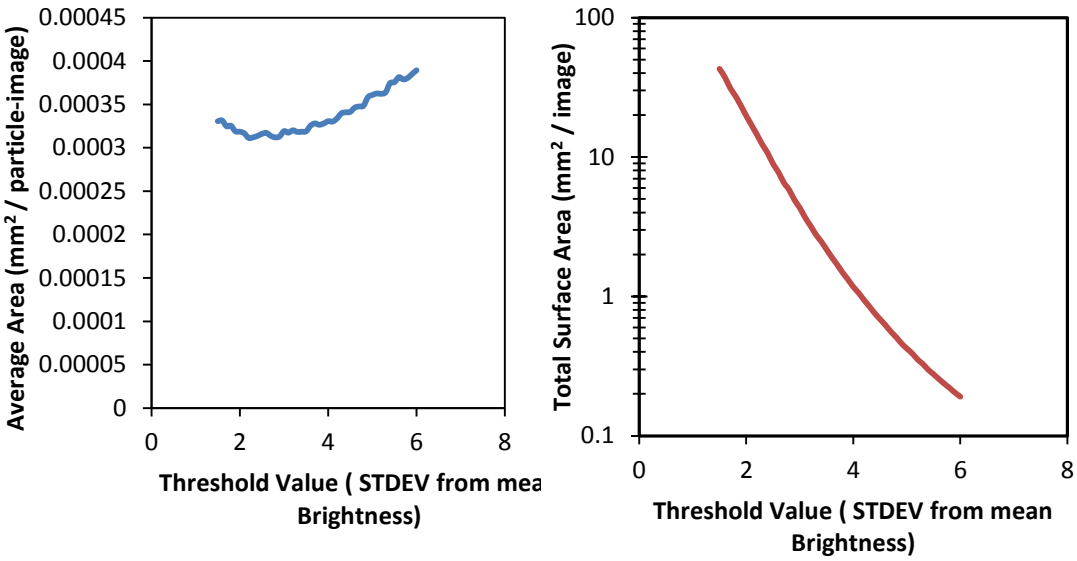

Figure D.2: Average particle area vs threshold (Left) and total surface area of particles vs Threshold (Right) for the electrical tape using capture method.

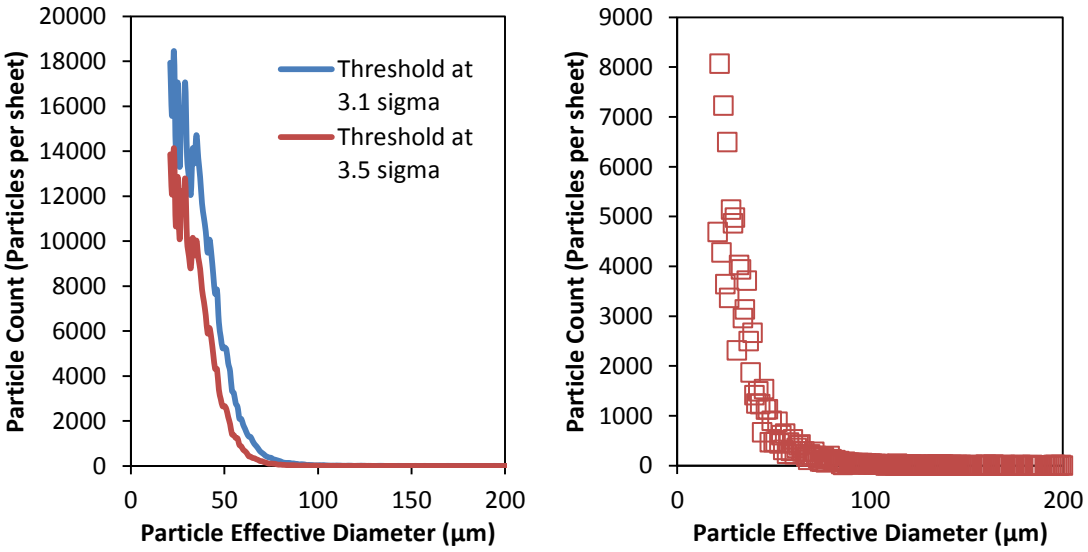

Figure D.3: False positive particle distribution of electrical tape used on sample B (Left). The difference between a tested sample of B and the blank sample (Right).

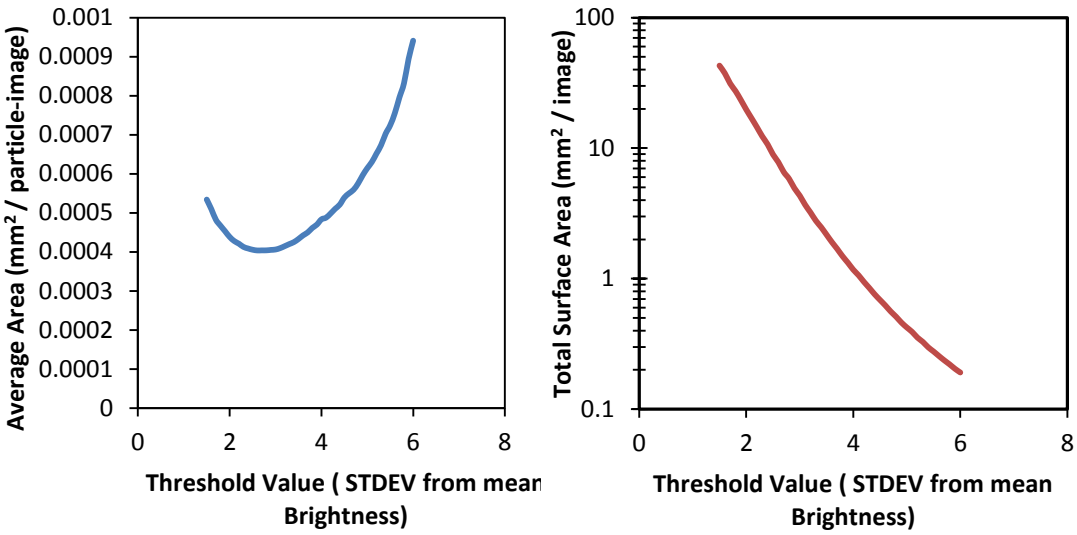

Figure D.4: Average particle area vs threshold (Left) and the total surface area of particles vs threshold (Right) for the paper safe tape using capture method.

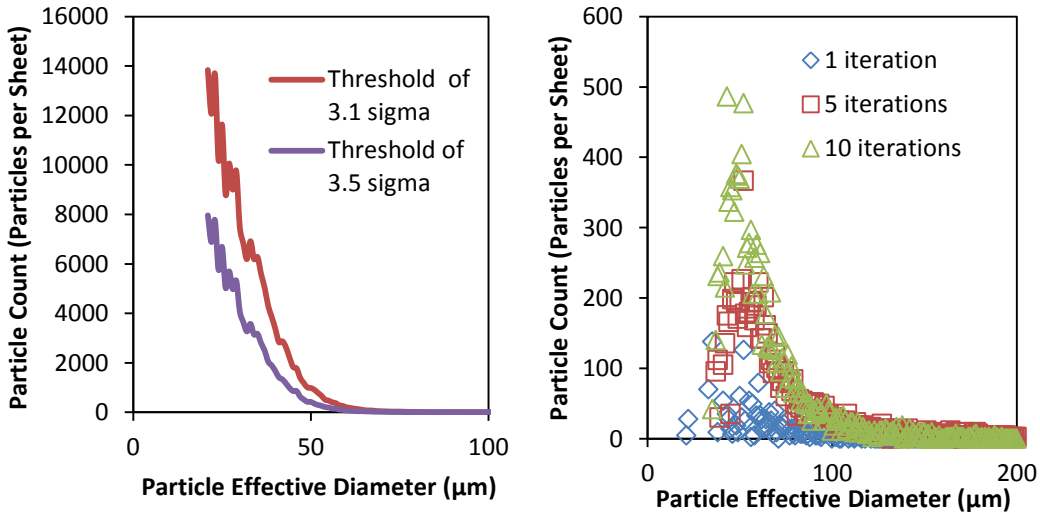

Figure D.5: Particle size distribution of the false positive particles cause by the background of the paper safe tape (Left) and the particle size distribution for the paper safe tape tested on sample B with 1, 5 and 10 different iterations per note (Right).

Appendix E. TABLE OF ANOVA AND CORRELATIONS

Tables E.1 through E.8 are the ANOVA calculations performed through Minitab for the studies performed in this thesis. Each table includes an F-Value for the given data as well as a P-Value for the null Hypothesis. A table including the tabulated confidence interval of the data is also given. For specific cases, each table may be listed with its respective paper type (Handsheets or Commercial Grades). If a label does not appear, the table is defaulted to commercial grades.

Tables E.9 through E.13 includes the correlation calculations. The data is formatted with the Pearsons Correlation Number (R) and the P-Value associated with the number.

Table E.1: ANOVA of the study of parameters for the Paper Dust Tester.

```
Analysis of Variance
Source  DF  Adj SS  Adj MS  F-Value  P-Value
Factor   3   64319   21440    12.72    0.003
Error    7   11802    1686
Total   10   76121

Model Summary
      S    R-sq  R-sq(adj)  R-sq(pred)
41.0605  84.50%     77.85%      65.10%

Means
Factor                   N   Mean     StDev       95% CI
1-Max                    3  196.5     75.5  ( 140.4,  252.5)
2-Tension                3  20.52    13.32  (-35.54,  76.57)
3-Iterations             2  83.76     2.75  ( 15.11, 152.42)
4-Rod                    3  14.15     5.14  (-41.90,  70.21)
```

Table E.2: ANOVA of using various number of iterations for the paper safe tape (PST).

```
Analysis of Variance
Source   DF     Adj SS     Adj MS  F-Value  P-Value
Factor    3  606994743  202331581   344.16    0.000
Error   156   91711885     587897
Total   159  698706628

Model Summary
      S    R-sq  R-sq(adj)  R-sq(pred)
766.744  86.87%     86.62%      86.19%

Means
Factor                   N    Mean    StDev       95% CI
Blank PST-P              40   514.3   347.9  (274.8,  753.7)
PST    1-P               40  1171.1   447.2  (931.6, 1410.6)
PST    5-P               40    4495    1038  ( 4256,   4734)
PST    10-P              40    4904     976  ( 4665,   5144)
```

Table E.3: ANOVA results for Study 1, Bending and Stressing test vs the controlled handsheets and the commercial grades of paper.

Handsheets:

Analysis of Variance

Source	DF	Adj SS	Adj MS	F-Value	P-Value
Factor	2	1.7801	0.89007	13.61	0.006
Error	6	0.3925	0.06541		
Total	8	2.1726			

Model Summary

S	R-sq	R-sq(adj)	R-sq(pred)
0.255753	81.94%	75.91%	59.36%

Means

Factor	N	Mean	StDev	95% CI
X-Bending SA	3	0.1055	0.0372	(-0.2558, 0.4668)
Y-Bending SA	3	0.1154	0.0837	(-0.2459, 0.4767)
Z-Bending SA	3	1.054	0.433	(0.693, 1.415)

Commercial Grades

Analysis of Variance

Source	DF	Adj SS	Adj MS	F-Value	P-Value
Factor	5	0.004378	0.000876	1.30	0.304
Error	19	0.012750	0.000671		
Total	24	0.017128			

Model Summary

S	R-sq	R-sq(adj)	R-sq(pred)
0.0259048	25.56%	5.97%	0.00%

Means

Factor	N	Mean	StDev	95% CI
A-Bending SA	3	0.1033	0.0272	(0.0720, 0.1346)
B-Bending SA	10	0.06946	0.02610	(0.05231, 0.08661)
C-Bending SA	3	0.0822	0.0285	(0.0509, 0.1135)
D-Bending SA	3	0.05581	0.00562	(0.02451, 0.08712)
E-Bending SA	3	0.0862	0.0345	(0.0549, 0.1175)
F-Bending SA	3	0.0813	0.0233	(0.0500, 0.1126)

Pooled StDev = 0.0259048

Table E.4: ANOVA results for Study 2, Edge effects test using the factory cut edges vs commercial grades of paper.

```
Analysis of Variance
Source  DF   Adj SS    Adj MS  F-Value  P-Value
Factor   5  0.34244  0.068489    14.69    0.000
Error   19  0.08856  0.004661
Total   24  0.43100

Model Summary
        S    R-sq  R-sq(adj)  R-sq(pred)
0.0682712  79.45%     74.05%      67.91%

Means
Factor                     N    Mean    StDev        95% CI
A-Edge-Factory SA          3  0.1645  0.0315  (0.0820, 0.2470)
B-Edge-Factory SA         10  0.1498  0.0817  (0.1046, 0.1949)
C-Edge-Factory SA          3  0.1926  0.0659  (0.1101, 0.2751)
D-Edge-Factory SA          3  0.4939  0.0788  (0.4114, 0.5764)
E-Edge-Factory SA          3  0.3317  0.0359  (0.2492, 0.4142)
F-Edge-Factory SA          3  0.1400  0.0377  (0.0575, 0.2225)
```

Table E.5: ANOVA results for Study 2, Edge effects using benchtop paper cutter cut edges vs both the controlled handsheets and the commercial grades.

Handsheets:

```
Analysis of Variance
Source  DF    Adj SS    Adj MS  F-Value  P-Value
Factor   2  0.005276  0.002638     2.15    0.198
Error    6  0.007360  0.001227
Total    8  0.012637

Model Summary
        S    R-sq  R-sq(adj)  R-sq(pred)
0.0350241  41.76%     22.34%       0.00%

Means
Factor                   N     Mean    StDev         95% CI
X0-Edge-Bench SA         3  0.02224  0.00344 (-0.02724, 0.07172)
Y15-Edge-Bench SA        3   0.0729   0.0474  (  0.0234,  0.1223)
Z33-Edge-Bench SA        3   0.0743   0.0377  (  0.0248,  0.1238)
```

Commercial Grades:

```
Analysis of Variance
Source  DF    Adj SS    Adj MS  F-Value  P-Value
Factor   5  0.002121  0.000424     3.75    0.017
Error   18  0.002036  0.000113
Total   23  0.004157

Model Summary
        S    R-sq  R-sq(adj)  R-sq(pred)
0.0106363  51.01%     37.41%      12.91%

Means
Factor                   N     Mean     StDev        95% CI
A-Edge-Bench SA          4  0.02569   0.00664  (0.01452, 0.03686)
B-Edge-Bench SA          4  0.02576   0.01429  (0.01459, 0.03694)
C-Edge-Bench SA          4  0.02331   0.00919  (0.01214, 0.03448)
D-Edge-Bench SA          4  0.04860   0.01361  (0.03742, 0.05977)
E-Edge-Bench SA          4  0.02020   0.01115  (0.00903, 0.03137)
F-Edge-Bench SA          4  0.02442   0.00604  (0.01325, 0.03559)
```

Table E.6: ANOVA results for Study 3, Abrasive test vs the controlled handsheets and the commercial grades of paper.

Handsheets:

Analysis of Variance

Source	DF	Adj SS	Adj MS	F-Value	P-Value
Factor	2	13.954	6.9768	7.40	0.024
Error	6	5.657	0.9429		
Total	8	19.611			

Model Summary

S	R-sq	R-sq(adj)	R-sq(pred)
0.971026	71.15%	61.54%	35.09%

Means:

Factor	N	Mean	StDev	95% CI
X0-Abrasive SA	3	0.451	0.267	(-0.921, 1.822)
Y16-Abrasive SA	3	2.277	1.014	(0.906, 3.649)
Z33-Abrasive SA	3	3.479	1.315	(2.107, 4.851)

Commercial Grades:

Analysis of Variance

Source	DF	Adj SS	Adj MS	F-Value	P-Value
Factor	5	0.02085	0.004170	2.12	0.107
Error	19	0.03733	0.001965		
Total	24	0.05818			

Model Summary

S	R-sq	R-sq(adj)	R-sq(pred)
0.0443234	35.84%	18.95%	0.00%

Means

Factor	N	Mean	StDev	95% CI
A-Abrasive SA	3	0.1711	0.0483	(0.1175, 0.2247)
B-Abrasive SA	10	0.1111	0.0514	(0.0817, 0.1404)
C-Abrasive SA	3	0.1389	0.0324	(0.0853, 0.1924)
D-Abrasive SA	3	0.1056	0.0327	(0.0521, 0.1592)
E-Abrasive SA	3	0.0755	0.0175	(0.0219, 0.1290)
F-Abrasive SA	3	0.1598	0.0451	(0.1062, 0.2133)

Table E.7: ANOVA performed on the tape test against the 6 commercial grades of paper.

```
Analysis of Variance
Source  DF  Adj SS  Adj MS  F-Value  P-Value
Factor   5    3779  755.78     9.88    0.000
Error   48    3672   76.50
Total   53    7451

Model Summary
      S    R-sq  R-sq(adj)  R-sq(pred)
8.74644  50.72%     45.58%      37.63%

Means
Factor                   N   Mean  StDev       95% CI
A-PST  SA                9  2.885  1.496  (-2.977, 8.747)
B-PST  SA                9   6.05   4.13  (  0.18, 11.91)
C-PST  SA                9   4.98   3.65  ( -0.88, 10.84)
D-PST  SA                9  23.19   9.52  ( 17.33, 29.05)
E-PST  SA                9  21.66  14.95  ( 15.80, 27.52)
F-PST  SA                9  18.13  10.60  ( 12.27, 23.99)
```

Table E.8 ANOVA performed on the electrical tape of the tape test against the 6 commercial grades of paper.

```
Analysis of Variance
Source  DF  Adj SS  Adj MS  F-Value  P-Value
Factor   5   12661    2532     2.47    0.057
Error   27   27648    1024
Total   32   40308

Model Summary
      S    R-sq  R-sq(adj)  R-sq(pred)
31.9997  31.41%     18.71%       0.00%

Means
Factor            N   Mean  StDev      95% CI
A-ETape S         5   95.0   26.2  ( 65.6, 124.3)
B-ETape S         6   59.1   47.8  ( 32.3,  85.9)
C-ETape S         6   56.0   29.9  ( 29.2,  82.8)
D-Etape S         6  71.26  16.43  (44.45, 98.06)
E-Etape S         4   92.7   43.2  ( 59.9, 125.5)
F-ETape S         6  38.40  20.30  (11.59, 65.20)
```

Table E.9: Correlation of the relationship of the ash value, the tensile index and the surface roughness.

	Ash	Tensile Index
Tensile Index	-0.976	
	0.000	
Surface Roughness	-0.860	0.815
	0.003	0.007

Table E.10: Correlation of the ash value, the surface roughness and the results from studies 1-3.

	Ash	Surface Roughness
Bending Test	0.800	-0.863
	0.010	0.003
Abrasive Test	0.834	-0.799
	0.005	0.010
Edge Effect Test	0.559	-0.492
	0.118	0.179

Cells Contents: Pearson correlation
P-Value

Table E.11: Correlation of the laser printer test, the industrial tester and the results from studies 1-3.

	Laser SA	Industrial	
Industrial Tester	-0.050		
	0.812		
Bending Test SA	0.316	0.065	
	0.124	0.758	
Abrasive Test SA	0.112	0.196	
	0.593	0.347	
Edge Effect SA	-0.123	-0.476	
	0.559	0.016	
Bending Test 40+µm	0.239	0.448	
	0.250	0.025	
Abrasive Test 40+µm	-0.103	0.428	0.839*
	0.623	0.033	0.037*
Edge Effect Test 40+µm	-0.210	-0.320	
	0.314	0.119	

* using only the average of the 3 points per grade to correlate the 6 grades.

Cells Contents: Pearson correlation
P-Value

Table E.12: Correlation of the laser printer test, the industrial tester and study 4, tape test results.

	Printer Test	Industrial
Electrical Tape SA	0.310	0.132
	0.085	0.473
Paper Safe Tape SA	0.013	-0.659
	0.928	0.000

Cell Contents: Pearson correlation
P-Value

Table E.13: Correlation of the laser printer test, the industrial tester and the paper properties.

	Printer Test	Industrial Teste
Industrial Teste	0.004	
	0.995	
Ash	-0.060	-0.974
	0.910	0.001
Taber Stiffness	0.216	-0.765
	0.681	0.076
Elastic Modulus	0.324	0.728
	0.532	0.101
Tensile Index	-0.506	0.560
	0.306	0.247
Air Resistance	0.258	-0.906
	0.621	0.013
Sheffield Surface	-0.423	0.600
Roughness	0.403	0.208
Basis Weight	0.321	-0.811
	0.535	0.050
Caliper	0.258	-0.824
	0.622	0.044
Paper Cost	0.286	-0.837
	0.583	0.038

Cells Contents: Pearson correlation
P-Value

Appendix F. ADDITIONAL MICROSCOPE IMAGES

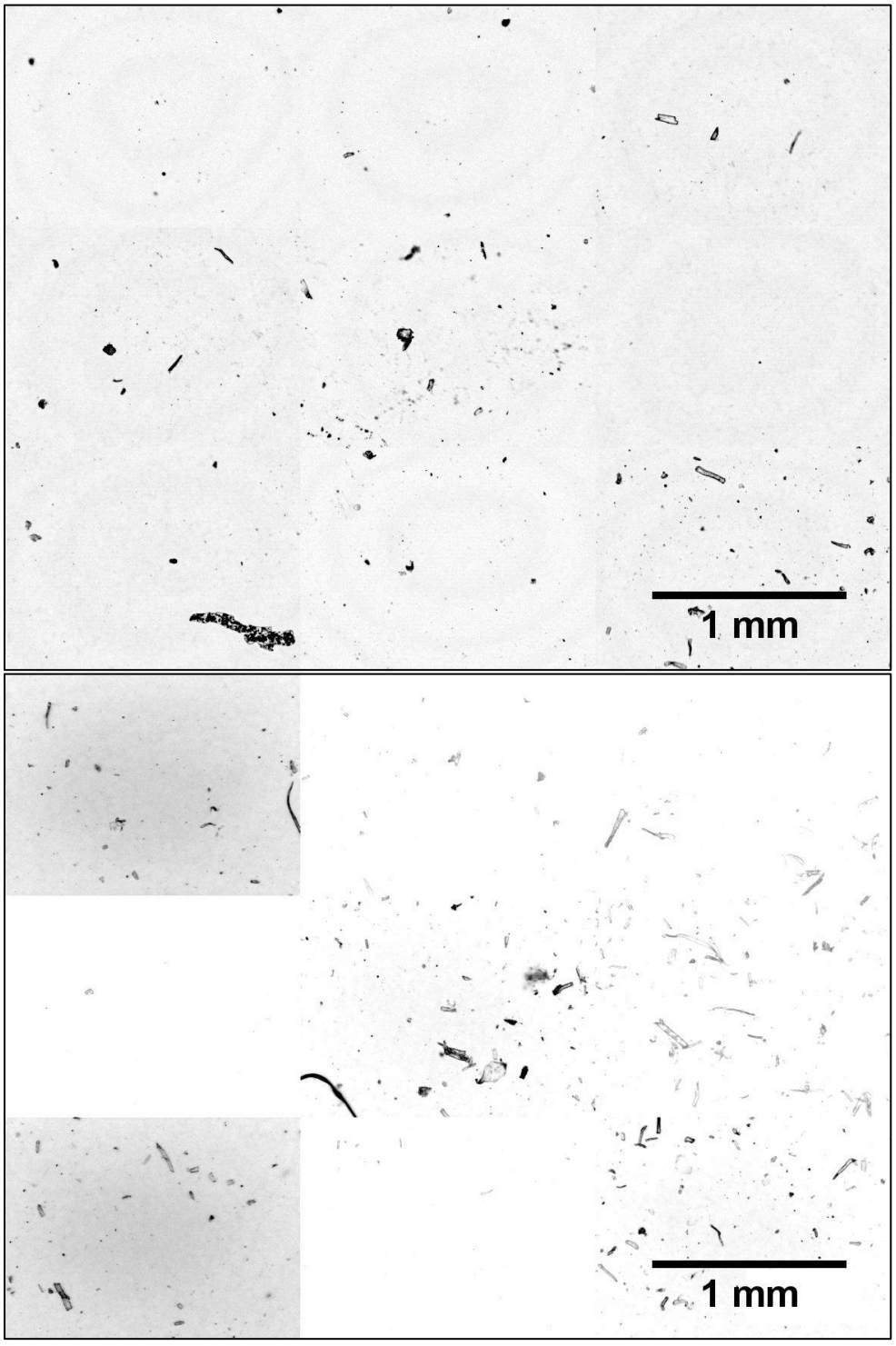

Figure F.1: Optical microscope image montoge of the Hp Color Laser Jet printer test, sample C (top) and sample E (bottom).

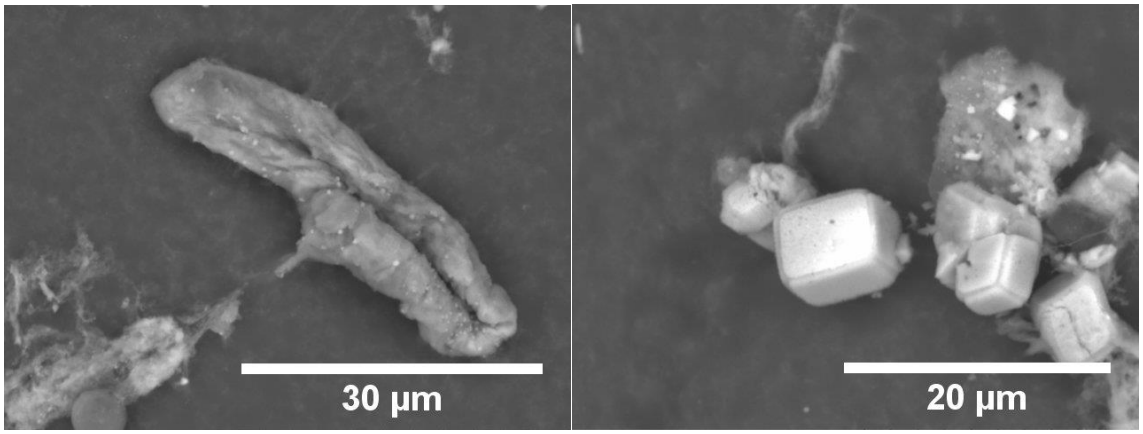

Figure F.2: Additional SEM images of the fibers and fillers of sample E after drying from the colloidal solution.

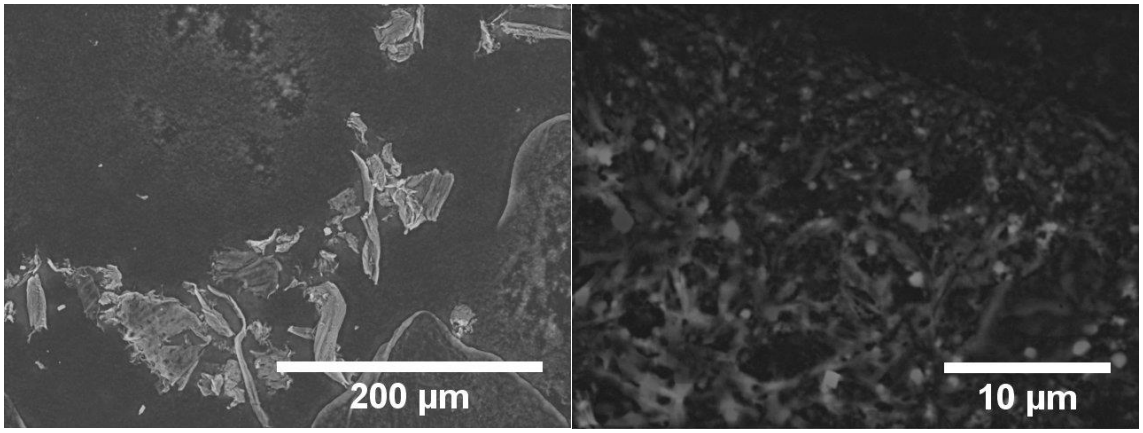

Figure F.3 Additional SEM images of the fibers and fillers for sample C after drying from the colloidal solution.

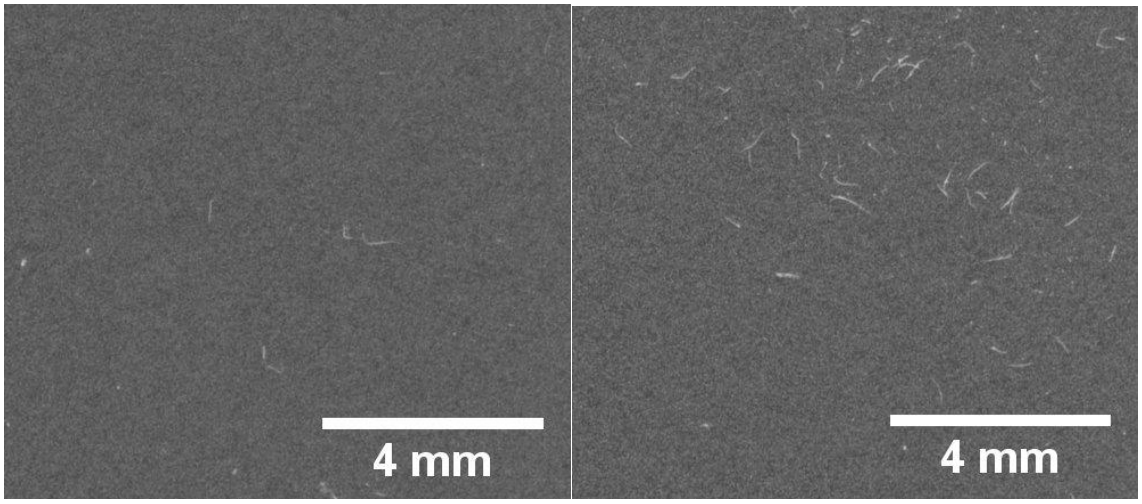

Figure F.4: Handsheet X-0(Left) and Z-33(Right) scanner samples from Study 3.

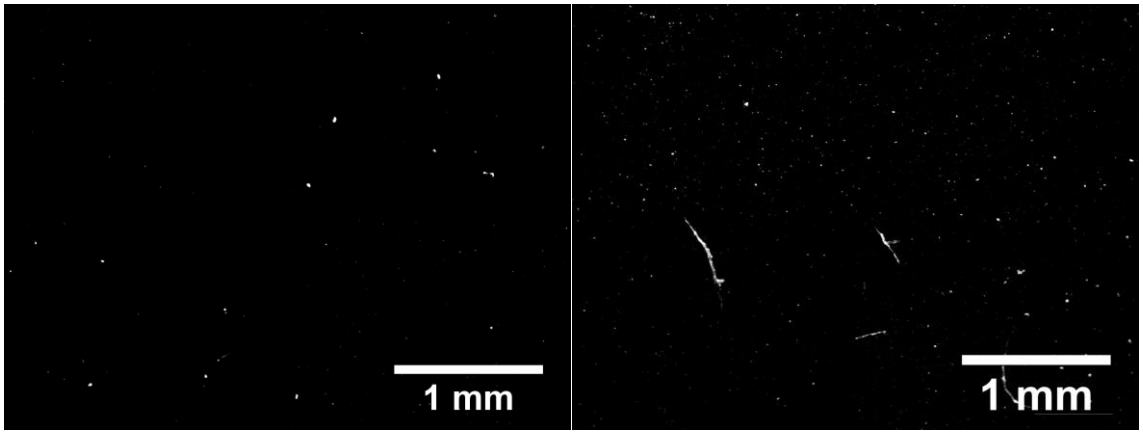

Figure F.5: Handsheet X-0(Left) and Z-33(Right) Microscope sample montage for Study 3.

Appendix G. INSTRUCTIONS FOR SCANNING PARTICLES

This section is the procedure that was used in this thesis to scan images from the scanner to the computer. It is comparable to most scanner programs but the image and the procedure is specific to the Epson Perfection V370 Photo Scanner.

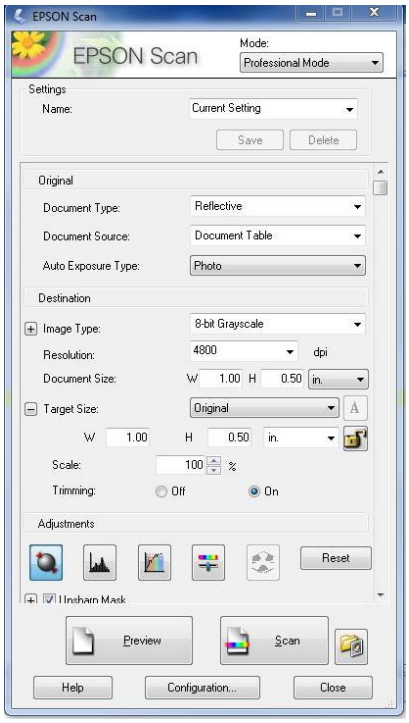

Note: There is a size restriction for the samples imaged at 4800DPI, 5in-wide x 6in-long is the maximum dimensions the scanner can scan at max settings.

1. Place painters tape or another low tack adhesive and low residual tape on the surface of the printer. Peel the tape off and place your sample face down on the scanner.
2. Open the scanner program and select professional mode
3. Select 8-bit gray scale and Select 4800 DPI
4. Press Preview
5. You can highlight the section of the sample on the preview panel or go to size and create the dimensions of the scanned section. Once after, you can move the selection on the preview panel by holding the section and dragging it. You can also make duplicates of the selection by activating the copy function on the left hand side
6. For all samples, it is advised that you hit the reset button which removes any auto exposure function. This should give more repeatable results between samples.
7. Once done, Hit scan and designate the location and name of the scan. Hit Ok once done.

ImageJ Particle Detection Without the Macros

ImageJ is a powerful tool used to analyze images. There are several built in tools that are capable of editing images, reducing background noise and separating the particles from the background within ImageJ. This document will go through a step by step procedure of how to quantify particle data from an image as used in this thesis.

Open ImageJ so that the main panel is assessable. Go to open and select the image.

1. **Gray Scale Conversion**: Thresholding requires the image to be gray scale.
    a. Go to Images → Tools → 8-bit.
2. (Optional) DespecklingDepending on the image, speckles or small, bright random pixels may exist. A function "Despeckling" will use a built in algorithm to remove speckles. This function can be performed several times to reduce the speckles.
    a. Go to Process → Noise → Despeckle
3. (Optional) Smoothing: Smoothing can help increase the efficiency of the thresholding by averaging a pixel with the surrounding pixels using a build in algorithm. This function can help retain particles that are split by using an excessive threshold. This function can also help reduce background noise in small amounts. This function can also be used several times to increase the effectiveness but too much can blur the picture.
    a. Go to Process → Smooth

4. (Optional)Subtract Background: When an image has an uneven backlight due to an inconsistent aperture of a microscope or various sources, the threshold cannot distinguish the unevenness. Subtract Background removes the unevenness of the background.

a. Go to Processes → Subtract Background…

b. Select rolling ball radius: 50 pixels is standard. Select less for images that contains items that must be removed in the background.

c. Light background: Select if the background is light and deselect if the background is desired black.

5. **Thresholding:** Go to Images → Adjust → Threshold…

a. Select Dark Background if the background should be dark and deselect dark background if the background should be white

b. Manually Thresholding

i. If the background should be dark. Move the upper scroll bar to the right. This bar restricts darker pixels and falsifies pixels under the numeric value. Keep the lower bar at 255

ii. If the background is bright, move the lower scroll bar to the left. This bar restricts brighter pixels and falsifies pixels over the numeric value. Keep the upper bar at 0.

iii. As the scroll bars move, you should be able to watch the image adapt to the changes. Select a value that best represents the particles. Restrictive thresholds ranges are between 0.5% to 2% brightness (as seen on the threshold screen). Less restrictive can rise above this percent.

c. Auto Threshold

i. Under the scroll bar, A drop down list exists. The list contains names of the auto threshold methods. Select one that best describes your particles in the image. Typical auto methods are Otsu, Yen and Triangle.

d. Select “Apply” once finished.

6. Select Scale and Measurements

a. Go to Analyze → Set Scale

i. Distance in Pixels: calculate the number of pixels it would take to measure 1μm (or any unit desired). Place in this box

ii. Place 1 in known distance

iii. Place 1 in pixel ratio unless known otherwise

iv. Select global if going to perform multiple images

b. Go to Analyze → Set Measurements

i. Select measurements that you wish ImageJ to output.

7. Analyze Particles : Select Analyze → Analyze Particles … → Ok

8. You can select all of the results page and paste it into a spreadsheet.

9. Distribution (Optional): Go to Analyze → Distribution.

a. Select the measurement that is desired and select the range set that is desired.

APPENDIX H. RAW DATA

$$CF_{Scanner} = \frac{1}{A_{Scanner}} * \frac{1}{N * I} * \frac{11}{L} * 8.5$$

$$CF_{Microscope} = CF_{Scanner} * \frac{1}{A_{Microscope}}$$

Where

- $CF_{Scanner}$ = Conversion Factor
- $A_{Scanner}$ = Imaged area of the scanner (in^2)
- $A_{Microscope}$ = Imaged area of the microscope (in^2)
- N = the number of sheets used to test
- I = Number of iterations per sheet
- L = the length of the tested sheet (in)

11/L is the scaling factor to convert from a length of L to the standard length of a sheet (11).

The conversion factor is used to convert the data from the area taken to the dusting value for a single side of a sheet. The collection of dust for the scanner is typically 0.5in in width by 1in. The calculation assumes that the sample already consists of the length of the paper but a scaling number (11/L) will scale the tested length against the actual length. For Test Method 1, the depth length of the scan is 1inch and the width is determined typically by ½inch but sometimes 1inch. The N and I normalizes the data from to form a single sheet and a single iteration per test.

Table H.1: Data table for laser printer test

Above 10μm (per sheet)						
Particle Count				Surface Area(mm^2)		
Average	Lower CI	Upper CI		Average	Lower CI	Upper CI
135.73	124.72	146		0.1722	0.152	0.1923
88.41	78.5	98		0.1088	0.09067	0.12693
40.12	31	49.23		0.06915	0.05248	0.08582
81.73	70.3	93.16		0.09433	0.07343	0.11524
98.69	87.42	109.96		0.1439	0.1232	0.1645
96	84.79	107.22		0.13073	0.11022	0.15124

Below 10μm (per sheet)						
Particle Count				Surface Area (mm^2)		
Average	Lower CI	Upper CI		Average	Lower CI	Upper CI
2424	2167	2681		0.0494	0.04426	0.05453
2137	1961	2314		0.04106	0.03754	0.04457
1332	1146	1518		0.02426	0.02056	0.02797
1938	1716	2160		0.03918	0.03475	0.04362
2430	2473	2686		0.048	0.04288	0.05311
2015	1806	2225		0.03873	0.03454	0.04292

Table H.2: Data Tables for Test Method 1, Configuration 1: Parameter Determination

Gravity Data					
	1	2	3	4	5
1 - PC	250	151	124		
1 - SA	29489018	23418282	16797769		
2 - PC	93	134	178		
2 - SA	9726894	18299712	21575542		
3 - PC	133	108	125		
3 - SA	18652683	12543594	16246026		
4 - PC	88	69	43		
4 - SA	10068870	8161989	6550024		
Blank - PC	6	8	14		
Blank - SA	575107.8	653320.4	974024.6		
Electrostatic Attraction Data					
1 - PC	170	70	119	46	83
1 - SA	14864249	6437189	11743797	4621414	8652732
2 - PC	25	33	36	110	
2 - SA	2223331	3147679	3239375	115	
3 - PC	21	41	13		
3 - SA	2303442	4541303	1598874		
4 - PC	11	8	0	13	24
4 - SA	1374447	1114545	0	1056426	2371183
Blank - PC	6	8	14		
Blank - SA	575107.8	653320.4	974024.6		
Filtration Data					
1 - PC	464	715	334		
1 - SA	61918108	75231981	41302191		
2 - PC	36	30	92		
2 - SA	6069884	4450197	9474062		
3 - PC	110	105	0		
3 - SA	13981920	14705403	0		
4 - PC	22	48	39		
4 - SA	2167568	5433843	4733529		
Blank - PC	27	26	19		
Blank - SA	3090084	2730437	2277655		

Table H.3: Data tables for capture method: electrical tape.

	1		2		3		4		5	
Threshold	PC	SA	PC	SA	PC	SA	PC	SA	PC	SA
1.5	91546	37559706	147964	40078934	147234	39086254	94397	35629916	90294	36558429
1.6	81889	33233396	123604	34219380	132739	34853629	84186	31663809	78918	32205571
1.7	81119	30218049	123604	34219380	132739	34853629	75567	28253584	78918	32205571
1.8	81119	30218049	106505	30361807	110669	30163000	73683	25545084	73229	28589844
1.9	75432	27009054	100470	26629677	89659	26121861	67081	22993342	70842	25912790
2	67559	24120245	100470	26629677	89659	26121861	59486	21315585	63601	23108130
2.1	59777	21561547	87417	23140982	83599	23151247	53536	19223046	63601	23108130
2.2	58836	19639026	74355	20144888	76227	20783618	49782	17426723	57692	20643560
2.3	53351	17702984	67429	18097550	64623	18268715	45130	15811492	52817	18527599
2.4	47248	16362477	67429	18097550	64623	18268715	40944	14793802	50344	17351119
2.5	47248	16362477	61135	15995944	54960	16092886	36693	13460303	45352	15630088
2.6	42296	14783173	52787	14083584	50207	14337101	33569	12277544	45352	15630088
2.7	39900	13461137	52787	14083584	50207	14337101	30385	11275746	41104	14100648
2.8	36010	12205378	45774	12440086	47130	12917446	28865	10545311	37235	12735469
2.9	32649	11381180	42973	11229711	41151	11502064	28865	10545311	35230	11959208
3	29290	10342987	37535	10297812	36208	10252819	26256	9665230.1	35230	11959208
3.1	27080	9440605.1	37535	10297812	36208	10252819	23935	8866094.6	31867	10851975
3.2	27080	9440605.1	32941	9168590.6	32754	9192037.9	21736	8223743.3	28790	9853511.7
3.3	24615	8608044.2	28905	8181121.3	30339	8302995.1	21039	7673175.1	26182	8943653
3.4	22947	8095486.7	28905	8181121.3	30339	8302995.1	19061	7067870.5	26182	8943653
3.5	20739	7400405	27080	7396314.8	26628	7642928.1	17310	6520480.6	25251	8352963.9
3.6	19026	6771418.7	23970	6872137.8	23656	6875420.4	15636	6129536.3	23020	7616901.6
3.7	17359	6207459.4	21188	6218349.4	21095	6249820.8	14922	5694198.4	20958	6968427.9
3.8	16590	5838946.3	21188	6218349.4	21095	6249820.8	13630	5270688.4	19157	6342802.3
3.9	16590	5838946.3	18949	5592932.2	19151	5643526.2	12427	4882323.3	19157	6342802.3
4	15032	5363357.3	17237	5044135.6	16970	5258912.7	11287	4645453.6	18693	5881776.7
4.1	13664	4935600.7	17237	5044135.6	16970	5258912.7	10529	4321855.1	17130	5374090.9
4.2	12384	4552394	16034	4700242.1	15245	4756046.6	10529	4321855.1	15538	4943546.7
4.3	11742	4297053.1	14126	4308021.2	13572	4376122.5	9642	4028269.1	15538	4943546.7
4.4	10687	3969338.2	14126	4308021.2	13572	4376122.5	8795	3761412.9	14244	4522433.6
4.5	10687	3969338.2	12579	3897824	12320	3961887.2	8107	3607494.6	13706	4157020.7
4.6	9766	3672834.3	11318	3537387.2	11232	3703472.1	7394	3371432.5	12520	3800101
4.7	8945	3409312.9	10831	3276679.5	10139	3365544.7	6823	3156499.1	11400	3525481.2
4.8	8289	3228534.4	10831	3276679.5	10139	3365544.7	6294	2964075.1	11400	3525481.2
4.9	7580	2995390.2	9589	3041894	9034	3134406.6	5990	2853403.9	10403	3239111.7
5	6955	2785719.4	8641	2769384.5	8213	2851554.2	5466	2682499.3	9687	2969441.9
5.1	6406	2603143.3	8641	2769384.5	8213	2851554.2	4982	2527148	8901	2716888.6
5.2	6406	2603143.3	7799	2522719.1	7865	2654180.2	4607	2387298	8901	2716888.6
5.3	5991	2472568	7457	2324589.6	7138	2419238.4	4452	2308619.4	8126	2545046.1
5.4	5490	2304841.7	6704	2187813.8	6451	2271364.2	4077	2187735.6	7477	2354888.7
5.5	5055	2146833.1	6704	2187813.8	6451	2271364.2	4077	2187735.6	6879	2159963.6
5.6	4625	2015788.9	6107	2010187.6	5860	2074928.1	3736	2075866	6305	1980357.4
5.7	4425	1918170	5567	1841002.4	5690	1920306.3	3440	1971030.6	6305	1980357.4
5.8	4141	1795879.4	5567	1841002.4	5690	1920306.3	3304	1902278	5823	1870415.7
5.9	4141	1795879.4	5177	1690705.3	5183	1757634.3	3031	1813100.1	5320	1742602

Table H.4: Data table capture method: paper safe tapes.

	1		2		3		4		5	
	PC	SA	PC	SA	PC	SA	PC	SA	PC	SA
1.5	77622	43502576	81106	41372234	79815	43625205	80740	44110876	82152	41799469
1.6	69990	35992125	74644	36277869	72278	38448071	74604	39074999	75547	37218079
1.7	63377	31783233	63197	29706273	64371	31663470	66353	32413366	66520	30601360
1.8	55605	26440692	57445	26306313	59196	28145935	60784	28784587	59762	27080673
1.9	50117	23105082	50869	22821995	53046	24502592	52158	23763768	51414	22446838
2	43157	19185660	43166	18795628	45396	20288099	47635	20838251	45924	19620607
2.1	38746	16786899	38287	16379594	40873	17896555	40864	17266188	38963	16246387
2.2	34591	14870188	31414	13495578	34681	14619667	36362	15057923	34568	14216139
2.3	29685	12339523	27946	11940346	31470	12932140	30683	12468092	29099	11780305
2.4	26195	10809822	24135	10480388	26671	10646264	27279	11033014	26283	10397723
2.5	22235	8992319.1	19869	8735623.5	23684	9316881.6	22697	9062608.9	21642	8555313.9
2.6	19637	7932762.5	17269	7746903.7	20125	7690968.9	20290	8038822.4	19286	7591682.7
2.7	16510	6606610.3	14221	6526212.2	17635	6749195.8	16872	6680078.5	16056	6271809.2
2.8	14843	5884668.5	12588	5830531.3	15759	5948367	14926	5890738.8	13939	5555833.4
2.9	12404	4917311.8	10954	5230020.4	13336	4927029.4	12610	4923173.6	11554	4653503.9
3	11108	4374194.6	9100	4440420.2	11852	4329749	11107	4371719.6	10077	4107494.8
3.1	9317	3686746.4	7927	4013367	9911	3594155.7	9341	3648761.8	8445	3463684.6
3.2	8251	3284860	6612	3461391.9	8759	3186980.6	7769	3070760.2	7377	3072245.2
3.3	6884	2787751.5	5891	3133651.1	7359	2640711	6832	2750105.6	6160	2602413.8
3.4	6123	2511959.4	5237	2862496.3	6560	2348922.6	5738	2322036.4	5487	2343373.4
3.5	5067	2130211.6	4336	2481165.3	5785	2075292.9	5121	2089361.2	4790	2094675.9
3.6	4564	1930284.4	3827	2274594.8	4795	1746040.9	4301	1786344.2	4054	1790173.9
3.7	3870	1662829.1	3264	2004898.9	4249	1566669.2	3850	1600146.7	3537	1608535.6
3.8	3446	1498203.2	2924	1839934.3	3513	1316460.7	3253	1374349.4	2955	1392325.6
3.9	2964	1300308.1	2448	1631748.4	3132	1188178	2901	1234707.8	2639	1261932.7
4	2640	1179424.3	2199	1505107.1	2629	1016335.5	2461	1064715	2196	1094258.6
4.1	2275	1025427.8	2017	1395425.9	2384	912437.94	2236	969180.37	1961	999114.73
4.2	2047	936302.07	1746	1247291.2	2138	828392.46	1903	829095.88	1636	877631.76
4.3	1743	815183.83	1587	1157019.1	1771	711911.58	1721	752840.11	1491	806039.39
4.4	1607	745519.35	1350	1040642.5	1604	647066.82	1487	649750.23	1232	709983.69
4.5	1342	651938.64	1209	972124.3	1373	561692.66	1355	590220.19	1090	657774.41
4.6	1225	594544.91	1107	909728.48	1234	510838.11	1178	509639.7	922	590506.76
4.7	1084	521702.02	959	825005.63	1057	443909.15	1075	463422.5	837	548041.13
4.8	989	480356.65	876	774724.24	961	404205.09	919	403918.51	696	491871.87
4.9	848	418820.56	754	705945.55	823	354575.01	803	367002.06	637	458420.41
5	768	386228.84	707	666267.54	737	324796.96	679	320602.5	552	417491.88
5.1	667	342721.1	642	629090.57	657	297129.17	619	292674.18	515	392299.08
5.2	600	315496.2	546	578392.34	577	260421.14	536	257268.79	453	355851.58
5.3	519	281341.33	506	546608.24	514	238745.43	487	236791.49	408	335139.81
5.4	479	260369.04	440	504324.98	434	212093.69	420	207638.71	348	305778.61
5.5	414	231138.09	396	478871.65	401	194586.39	382	191538.24	318	288141.04
5.6	373	215454.47	366	454981.48	348	173353.57	334	169159.11	272	265605.6
5.7	329	192866.92	297	423093.17	313	161577.82	299	156054.69	251	250651.44
5.8	308	179944.86	272	402746.14	273	149359.19	256	138651.59	217	232258.35
5.9	257	162463.61	229	374869.93	235	134352.92	230	128386.89	191	220638.92
6	237	151625.76	220	358613.15	206	125390.85	188	114709.31	164	204746.88

Table H.5: Data table capture method data: membranes.

	1		2		3		4		5	
Thres	PC	SA	PC	SA	PC	SA	PC	SA	PC	SA
1.50	46823	19417476	57057	21344451	56749	22015200	49883	18271685	67073	23117405
1.60	40859	15207334	54109	18768116	49963	17067797	42656	14409788	60553	18191365
1.70	38125	13433990	47282	14319880	46384	14953686	36442	11300131	53674	14127170
1.80	35049	11845541	44714	12526919	39643	11365705	36442	11300131	46369	10833660
1.90	29420	9155903	41267	10859166	36223	9863099	30938	8815709	46369	10833660
2.00	26683	8042574	34003	8044241	29894	7369585	25960	6853145	39434	8202823
2.10	21712	6179036	31081	6907178	26930	6323628	21535	5297444	32627	6152306
2.20	19598	5417573	24810	5013315	21914	4628077	17524	4074643	26643	4542416
2.30	15551	4162049	21962	4251044	19538	3937893	17524	4074643	26643	4542416
2.40	13784	3649595	16997	3030822	15324	2823365	14174	3119192	21236	3309323
2.50	10816	2815445	14733	2554581	13501	2386256	11318	2392378	16655	2388132
2.60	9384	2475408	12708	2147667	11802	2001877	8991	1829982	12894	1715325
2.70	7086	1945812	9474	1513548	8953	1402799	7114	1407957	12894	1715325
2.80	6149	1739762	8057	1267534	7703	1168196	7114	1407957	9675	1217227
2.90	4523	1402330	5752	895764	5676	812058	5525	1083499	7123	853924
3.00	3835	1267508	4839	754664	4743	673849	4196	841210	5219	595978
3.10	3204	1156342	3410	540304	3350	462563	3238	659937	5219	595978
3.20	2254	983613	2839	461156	2836	382217	2397	524177	3783	415017
3.30	1907	913715	2376	393445	2020	266700	2397	524177	2776	293612
3.40	1392	804112	1635	293117	1653	222020	1792	420514	1963	209645
3.50	1196	760890	1338	256487	1364	186979	1375	343086	1963	209645
3.60	892	683384	925	198989	929	134092	1039	285301	1342	150584
3.70	787	649490	773	178486	767	115439	774	241377	884	108066
3.80	598	594467	529	146155	526	86260	583	206961	607	80893
3.90	540	569222	448	133858	436	75266	583	206961	607	80893
4.00	462	527095	370	123098	288	59530	447	177756	391	62787
4.10	416	505784	261	106503	239	53121	347	154934	283	50750
4.20	366	464152	221	100406	177	43846	288	137036	173	41606
4.30	335	447973	160	88839	138	39652	245	122317	173	41606
4.40	308	410927	145	84957	113	36161	245	122317	127	36369
4.50	297	394566	104	76985	84	31107	204	109030	90	31862
4.60	289	380028	102	73989	77	29387	165	97332	72	28866
4.70	278	351709	97	71071	60	26026	151	86885	72	28866
4.80	270	337224	78	64923	56	24568	127	77298	57	26053
4.90	241	312943	73	62630	43	21884	127	77298	46	23630
5.00	239	300933	61	57680	43	20634	124	69899	41	21962
5.10	230	275975	56	55310	33	18628	101	62735	41	21962
5.20	218	263626	53	53434	29	17872	92	56795	34	20503
5.30	202	240309	50	49682	25	16205	84	51323	32	18836
5.40	201	230122	49	47937	23	15241	84	51323	29	16595
5.50	193	210661	43	44498	23	14485	77	45722	29	16595
5.60	187	200995	42	43404	21	13235	82	41111	28	15788
5.70	187	182863	39	40668	19	12688	72	36682	26	14954
5.80	191	173979	38	39131	19	11489	69	33165	23	14042
5.90	182	159806	34	37646	19	10968	64	29570	23	14042
6.00	169	152485	35	34363	18	10291	64	29570	21	13261

Table H.5: Data table capture method data: membranes continued.

Thres	6		7		8		9		10	
	PC	SA	PC	SA	PC	SA	PC	SA	PC	SA
1.50	49738	19100208	51122	20765460	47062	21245191	59832	17196002	49701	19996024
1.60	46873	16665025	45560	16357006	42607	16482840	59832	17196002	45448	17033174
1.70	40549	12578711	42603	14460434	40070	14432974	50661	12983099	41130	14479921
1.80	37429	10861068	36819	11198265	34988	10909395	41254	9746410	36904	12264856
1.90	34076	9346503	34063	9804689	32114	9435525	32944	7284445	32875	10370290
2.00	27896	6856741	28760	7469887	26846	6981845	32944	7284445	29078	8760973
2.10	24980	5848508	26189	6493829	24121	5968740	25514	5455714	25351	7405355
2.20	19621	4204462	21427	4874169	18984	4317556	19603	4087955	22019	6261492
2.30	17315	3552941	19204	4195604	14572	3107312	14920	3071776	19008	5307996
2.40	15126	2997553	15435	3088554	12654	2632036	14920	3071776	16199	4501956
2.50	11497	2115179	13704	2643629	9510	1878205	11186	2333395	13710	3835767
2.60	9919	1769071	10726	1921427	8155	1593295	8392	1796062	11392	3284625
2.70	7398	1231998	9444	1637272	5970	1135604	6175	1409364	9566	2839127
2.80	6312	1026939	7123	1178903	5102	961365	6175	1409364	7954	2457249
2.90	5361	853064	5388	841783	3603	705346	4544	1123802	6522	2147693
3.00	3732	594701	4666	711338	3041	604106	3304	914783	5272	1891518
3.10	3105	500313	3412	507816	2030	462485	2423	765710	4333	1685599
3.20	2114	360385	2890	430466	1681	405221	2423	765710	3489	1513444
3.30	1694	311640	1991	313516	1071	320967	1722	650480	2837	1369660
3.40	1380	270477	1695	268862	897	297676	1236	562657	1881	1147510
3.50	894	210791	1152	200370	593	250704	932	496952	1521	1064220
3.60	733	189767	951	176115	447	231789	932	496952	1265	995754
3.70	482	159415	660	139642	304	208707	708	444326	1086	928903
3.80	394	146728	551	123958	247	198390	540	399985	926	870155
3.90	327	135708	381	101162	171	183410	439	359291	817	816226
4.00	233	121014	325	92773	119	170514	439	359291	749	768446
4.10	198	115230	234	80268	110	164886	358	326308	700	722463
4.20	146	104366	196	74641	85	155534	305	296165	644	680284
4.30	126	100354	144	65913	72	150375	273	269435	596	640762
4.40	120	95821	123	61797	66	141205	273	269435	551	601240
4.50	99	84045	93	56534	62	137271	235	246040	516	567216
4.60	98	80841	85	53772	61	129533	224	223192	490	535380
4.70	81	75396	70	49682	54	125495	208	203314	465	505081
4.80	77	72452	62	47859	47	118252	208	203314	453	474677
4.90	71	70081	54	43091	45	114918	194	184322	444	445290
5.00	68	64636	43	40981	48	107597	190	167075	432	418560
5.10	61	62448	37	39782	46	104471	170	151678	420	394566
5.20	56	58410	36	37229	45	97332	170	151678	386	369581
5.30	51	56247	32	35952	44	94440	159	135682	370	346108
5.40	52	54059	31	33816	41	89152	139	124792	345	324015
5.50	46	50021	28	32826	42	86286	122	113850	328	303486
5.60	45	48171	25	30664	43	81727	122	113850	316	285640
5.70	42	45175	25	29622	41	76360	119	104184	297	268107
5.80	40	43534	25	27590	40	73963	119	95483	293	251277
5.90	40	41762	22	26730	36	68388	102	86599	285	234759
6.00	35	39365	20	25193	39	66173	102	86599	257	218919

Table H.6: Data tables for study 1.

Test Method 1 Configuration 1-Bending Stressing							
Microscope Sample							
Data Set	1	2	3	4	5	CF	A2
X - PC Lower	0	0.65	0.65			21.70831667	0.004233
X - PC Upper	0	0.65	0.65			21.70831667	0.004233
X - SA Lower	0	73.2861	44.0636			2.17083E-05	0.004233
X - SA Upper	0	73.2861	44.0636			2.17083E-05	0.004233
Y - PC Lower	17.502073	11.05	18			21.70831667	0.004233
Y - PC Upper	19.243739	11.05	24			21.70831667	0.004233
Y - SA Lower	0.0236335	521.7615	2415.7926			2.17083E-05	0.004233
Y - SA Upper	0.0247592	521.7615	2415.7926			2.17083E-05	0.004233
Z - PC Lower	78.179108	3.5	8.6			28.94442222	0.004233
Z - PC Upper	350.41224	3.5	8.6			28.94442222	0.004233
Z - SA Lower	0.0183812	399.5999	1036.5755			2.89444E-05	0.004233
Z - SA Upper	0.1049009	399.5999	1036.5755			2.89444E-05	0.004233

Test Method 1 Configuration 1-Bending Stressing										
Scanner Sample										
	1	2	3	4	5	CF	A	N	I	L
X - PC Lower	1.05	26	44			0.091666667	0.5	1	30	4
X - PC Upper	1.05	37	56			0.091666667	0.5	1	30	4
X - SA Lower	146.4371	203157.67	209488.44			9.16667E-08	0.5	1	30	4
X - SA Upper	146.4371	240464.9	259665.62			9.16667E-08	0.5	1	30	4
Y - PC Lower	78.179108	3.5	8.6			0.091666667	0.5	1	30	4
Y - PC Upper	350.41224	3.5	8.6			0.091666667	0.5	1	30	4
Y - SA Lower	0.0183812	399.5999	1036.5755			9.16667E-08	0.5	1	30	4
Y - SA Upper	0.1049009	399.5999	1036.5755			9.16667E-08	0.5	1	30	4
Z - PC Lower	6.65	80	84			0.122222222	0.5	1	30	3
Z - PC Upper	6.65	88	128			0.122222222	0.5	1	30	3
Z - SA Lower	799.9027	419966.87	550385.86			1.22222E-07	0.5	1	30	3
Z - SA Upper	799.9027	492445.02	680778.8			1.22222E-07	0.5	1	30	3

Table H.6: Data tables for study 1 continued.

Test Method 1 Configuration 1-Bending Stressing							
Microscope Sample							
Data Set	1	2	3	4	5	CF	A2
A - PC Lower	3.7	3.967	6.6			92.2603458	0.004233
A - PC Upper	N/A	N/A	N/A			92.2603458	0.004233
A - SA Lower	720.9	644.8	993.1			9.226E-05	0.004233
A - SA Upper	720.9	644.8	993.1			9.226E-05	0.004233
B - PC Lower	4.1	2.967	2.5	1.85	2.15	92.2603458	0.004233
B - PC Upper	4.1	2.967	2.5	N/A	N/A	92.2603458	0.004233
B - SA Lower	917.2	423.5	429.6	156.5	290.9	9.226E-05	0.004233
B - SA Upper	917.2	423.5	429.6	N/A	N/A	9.226E-05	0.004233
B - PC Lower	2	3	3.25	1.3	5.167	92.2603458	0.004233
B - PC Upper	N/A	3	3.25	1.3	5.167	92.2603458	0.004233
B - SA Lower	154.6	453	361.6	129.8	880.2	9.226E-05	0.004233
B - SA Upper	N/A	453	N/A	N/A	880.2	9.226E-05	0.004233
C - PC Lower	3.933	3.1	3.5			92.2603458	0.004233
C - PC Upper	N/A	N/A	N/A			92.2603458	0.004233
C - SA Lower	686.9	455	503.9			9.226E-05	0.004233
C - SA Upper	686.9	455	503.9			9.226E-05	0.004233
D - PC Lower	2.933	2.433	2.933			92.2603458	0.004233
D - PC Upper	N/A	N/A	N/A			92.2603458	0.004233
D - SA Lower	373.1	396	421			9.226E-05	0.004233
D - SA Upper	373.1	396	421			9.226E-05	0.004233
E - PC Lower	2.933	3.1	2.4			92.2603458	0.004233
E - PC Upper	N/A	N/A	N/A			92.2603458	0.004233
E - SA Lower	419.2	606	342.4			9.226E-05	0.004233
E - SA Upper	419.2	606	342.4			9.226E-05	0.004233
F - PC Lower	2.2	3.3	4.9			92.2603458	0.004233
F - PC Upper	N/A	N/A	N/A			92.2603458	0.004233
F - SA Lower	570	474.4	610.7			9.226E-05	0.004233
F - SA Upper	570	474.4	610.7			9.226E-05	0.004233

Table H.6: Data tables for study 1 continued.

Scanner Sample										
	1	2	3	4	5	CF	A	N	I	L
A - PC Lower	32	36	21	9	27	0.3896	0.5	3	20	8
A - PC Upper	45	42	26	11	32	0.3896	0.5	3	20	8
A - SA Lower	112469	171530	86130	31367	74823	0.3896	0.5	3	20	8
A - SA Upper	146806	197504	106529	37385	92877	0.3896	0.5	3	20	8
B - PC Lower	13	20	10	16	16	0.3896	0.5	3	20	8
B - PC Upper	16	28	11	17	22	0.3896	0.5	3	20	8
B - SA Lower	57863	68518	30820	112912	70550	0.3896	0.5	3	20	8
B - SA Upper	69326	86729	37333	128100	87484	0.3896	0.5	3	20	8
B - PC Lower	14	5	15	37	40	0.3896	0.5	3	20	8
B - PC Upper	17	11	15	43	47	0.3896	0.5	3	20	8
B - SA Lower	70264	14563	75266	144800	179033	0.3896	0.5	3	20	8
B - SA Upper	79747	29726	83134	167361	213605	0.3896	0.5	3	20	8
C - PC Lower	14	14	11	42	5	0.3896	0.5	3	20	8
C - PC Upper	18	19	14	48	5	0.3896	0.5	3	20	8
C - SA Lower	72035	66434	24385	154856	25479	0.3896	0.5	3	20	8
C - SA Upper	89464	82821	33295	182524	27173	0.3896	0.5	3	20	8
D - PC Lower	8	11	10	6	9	0.3896	0.5	3	20	8
D - PC Upper	9	14	13	8	11	0.3896	0.5	3	20	8
D - SA Lower	25063	57237	52548	27694	45618	0.3896	0.5	3	20	8
D - SA Upper	31445	68258	60572	33087	54293	0.3896	0.5	3	20	8
E - PC Lower	4	17	16	14	10	0.3896	0.5	3	20	8
E - PC Upper	5	22	21	19	16	0.3896	0.5	3	20	8
E - SA Lower	19305	54346	186745	51271	43221	0.3896	0.5	3	20	8
E - SA Upper	22874	71410	215272	67059	57420	0.3896	0.5	3	20	8
F - PC Lower	17	12	33	9	7	0.3896	0.5	3	20	8
F - PC Upper	23	13	38	10	9	0.3896	0.5	3	20	8
F - SA Lower	52861	40147	103376	33530	50073	0.3896	0.5	3	20	8
F - SA Upper	72009	46061	135864	39470	59087	0.3896	0.5	3	20	8

Table H.7: Data tables for study 2.

Test Method 1 Configuration 1-Edge Effects							
Microscope Sample							
Data Set	1	2	3	4	5	CF	A2
X - PC Lower	0	0.65	0.65			21.70831667	0.004233
X - PC Upper	0	0.65	0.65			21.70831667	0.004233
X - SA Lower	0	73.2861	44.0636			2.17083E-05	0.004233
X - SA Upper	0	73.2861	44.0636			2.17083E-05	0.004233
Y - PC Lower	17.502073	11.05	18			21.70831667	0.004233
Y - PC Upper	19.243739	11.05	24			21.70831667	0.004233
Y - SA Lower	0.0236335	521.7615	2415.7926			2.17083E-05	0.004233
Y - SA Upper	0.0247592	521.7615	2415.7926			2.17083E-05	0.004233
Z - PC Lower	78.179108	3.5	8.6			28.94442222	0.004233
Z - PC Upper	350.41224	3.5	8.6			28.94442222	0.004233
Z - SA Lower	0.0183812	399.5999	1036.5755			2.89444E-05	0.004233
Z - SA Upper	0.1049009	399.5999	1036.5755			2.89444E-05	0.004233

Test Method 1 Configuration 1-Edge Effects										
Scanner Sample										
	1	2	3	4	5	CF	A	N	I	L
X - PC Lower	1.05	26	44			0.091666667	0.5	1	30	4
X - PC Upper	1.05	37	56			0.091666667	0.5	1	30	4
X - SA Lower	146.4371	203157.67	209488.44			9.16667E-08	0.5	1	30	4
X - SA Upper	146.4371	240464.9	259665.62			9.16667E-08	0.5	1	30	4
Y - PC Lower	78.179108	3.5	8.6			0.091666667	0.5	1	30	4
Y - PC Upper	350.41224	3.5	8.6			0.091666667	0.5	1	30	4
Y - SA Lower	0.0183812	399.5999	1036.5755			9.16667E-08	0.5	1	30	4
Y - SA Upper	0.1049009	399.5999	1036.5755			9.16667E-08	0.5	1	30	4
Z - PC Lower	6.65	80	84			0.122222222	0.5	1	30	3
Z - PC Upper	6.65	88	128			0.122222222	0.5	1	30	3
Z - SA Lower	799.9027	419966.87	550385.86			1.22222E-07	0.5	1	30	3
Z - SA Upper	799.9027	492445.02	680778.8			1.22222E-07	0.5	1	30	3

Table H.7: Data table for study 2 continued.

Test Method 1 Configuration 1-Edge Effects Factory Cut							
Microscope Sample							
Data Set	1	2	3	4	5	CF	A2
A - PC Lower	4.75	6.3	6.75			5.4270792	0.004233
A - PC Upper	N/A	N/A	N/A			5.4270792	0.004233
A - SA Lower	978.31	924.0647	1397.221			5.427E-06	0.004233
A - SA Upper	N/A	N/A	N/A			5.427E-06	0.004233
B - PC Lower	4.95	4.1	3.3	2.45	2.45	5.4270792	0.004233
B - PC Upper	N/A	N/A	N/A	N/A	N/A	5.4270792	0.004233
B - SA Lower	1033.98	1020.0043	626.1083	695.1773	600.0487	5.427E-06	0.004233
B - SA Upper	N/A	N/A	N/A	N/A	N/A	5.427E-06	0.004233
B - PC Lower	2.45	2.45	3.91875	7.25	5.7	5.4270792	0.004233
B - PC Upper	N/A	N/A		N/A	N/A	5.4270792	0.004233
B - SA Lower	749.976	1588.2894	1297.2535	273707.94	213370.26	5.427E-06	0.004233
B - SA Upper	#DIV/0!	N/A	N/A	307888.86	253699.59	5.427E-06	0.004233
C - PC Lower	2.9	8.3	7.4			5.4270792	0.004233
C - PC Upper	N/A	N/A	N/A			5.4270792	0.004233
C - SA Lower	383.70	1563.7435	1539.6843			5.427E-06	0.004233
C - SA Upper	N/A	N/A	N/A			5.427E-06	0.004233
D - PC Lower	8.1		10.65	10.7		5.4270792	0.004233
D - PC Upper	N/A		N/A	N/A		5.4270792	0.004233
D - SA Lower	1652.65		2559.175	2560.9321		5.427E-06	0.004233
D - SA Upper	N/A		N/A	N/A		5.427E-06	0.004233
E - PC Lower	8.85	6.85	8.3			5.4270792	0.004233
E - PC Upper	N/A	N/A	N/A			5.4270792	0.004233
E - SA Lower	2687.36	1320.0962	1494.7286			5.427E-06	0.004233
E - SA Upper	N/A	N/A	N/A			5.427E-06	0.004233
F - PC Lower	5.05	4.4	4.25			5.4270792	0.004233
F - PC Upper	N/A	N/A	N/A			5.4270792	0.004233
F - SA Lower	1134.8	587.7487	846.8858			5.427E-06	0.004233
F - SA Upper	N/A	N/A	N/A			5.427E-06	0.004233

Table H.7: Data table for study 2 continued.

Test Method 1 Configuration 1-Edge Effects Factory Cut										
Scanner Sample										
	1	2	3	4	5	CF	A	N	I	L
A - PC Lower	28	24	41			0.0229167	0.5	3	20	8
A - PC Upper	36	30	48			0.0229167	0.5	3	20	8
A - SA Lower	161760.192	106997.76	149619.71			0.0229167	0.5	3	20	8
A - SA Upper	188542.198	123619.28	173405.68			0.0229167	0.5	3	20	8
B - PC Lower	75	55	43	36	39	0.0229167	0.5	3	20	8
B - PC Upper	81	68	50	45	44	0.0229167	0.5	3	20	8
B - SA Lower	273707.936	213370.26	199119.53	129715.57	120284.56	0.0229167	0.5	3	20	8
B - SA Upper	307888.862	253699.59	236557.02	161213.09	138807.91	0.0229167	0.5	3	20	8
B - PC Lower	31	93	96	60	38	0.0229167	0.5	3	20	8
B - PC Upper	36	116	106	73	53	0.0229167	0.5	3	20	8
B - SA Lower	103793.301	444299.94	486036.1	263703.76	155325.22	0.0229167	0.5	3	20	8
B - SA Upper	124374.803	521806.23	550880.86	324588.54	203027.41	0.0229167	0.5	3	20	8
C - PC Lower	59	80	52			0.0229167	0.5	3	20	8
C - PC Upper	65	104	65			0.0229167	0.5	3	20	8
C - SA Lower	269643.74	197217.69	154152.85			0.0229167	0.5	3	20	8
C - SA Upper	304033.087	257008.26	187500.1			0.0229167	0.5	3	20	8
D - PC Lower	207		151	120		0.0229167	0.5	3	20	8
D - PC Upper	248		170	127		0.0229167	0.5	3	20	8
D - SA Lower	913844.78		583316.27	418247.4		0.0229167	0.5	3	20	8
D - SA Upper	1071618.93		675307.77	452428.33		0.0229167	0.5	3	20	8
E - PC Lower	74	90	102			0.0229167	0.5	3	20	8
E - PC Upper	86	114	123			0.0229167	0.5	3	20	8
E - SA Lower	274776.09	392768.02	381487.27			0.0229167	0.5	3	20	8
E - SA Upper	320706.709	476579.03	453600.69			0.0229167	0.5	3	20	8
F - PC Lower	37	30	36			0.0229167	0.5	3	20	8
F - PC Upper	43	34	40			0.0229167	0.5	3	20	8
F - SA Lower	126823.742	92564.658	124426.91			0.0229167	0.5	3	20	8
F - SA Upper	148707.871	108482.76	212015.53			0.0229167	0.5	3	20	8

Table H.7: Data table for study 2 continued.

Test Method 1 Configuration 1-Edge Effect Benchtop Cut							
Microscope Sample							
Data Set	1	2	3	4	5	CF	A2
A - PC Lower	13.9	16.85	10.65	20.3		2.470027083	0.009301
A - PC Upper	N/A	N/A	N/A	N/A		2.470027083	0.009301
A - SA Lower	3081.3504	3563.706	2152.5143	4806.3316		2.47003E-06	0.009301
A - SA Upper	N/A	N/A	N/A	N/A		2.47003E-06	0.009301
B - PC Lower	6.55	10.65	11.15	20		2.470027083	0.009301
B - PC Upper	N/A	N/A	N/A	N/A		2.470027083	0.009301
B - SA Lower	1132.7428	5894.3861	2112.2438	5894.3861		2.47003E-06	0.009301
B - SA Upper	N/A	N/A	N/A	N/A		2.47003E-06	0.009301
B - PC Lower						5.427079167	0.004233
B - PC Upper						5.427079167	0.004233
B - SA Lower						5.42708E-06	0.004233
B - SA Upper						5.42708E-06	0.004233
C - PC Lower	4.95	4.6	5.45	2.7		5.427079167	0.004233
C - PC Upper	N/A	N/A	N/A	N/A		5.427079167	0.004233
C - SA Lower	1004.947	763.3813	904.7902	460.3428		5.42708E-06	0.004233
C - SA Upper	N/A	N/A	N/A	N/A		5.42708E-06	0.004233
D - PC Lower	20.85	15.85	8.9	11.3		5.427079167	0.004233
D - PC Upper	N/A	N/A	N/A	N/A		5.427079167	0.004233
D - SA Lower	4512.6244	3406.0878	1794.0636	2332.4773		5.42708E-06	0.004233
D - SA Upper	N/A	N/A	N/A	N/A		5.42708E-06	0.004233
E - PC Lower	4.85	6	2.9	13.95		5.427079167	0.004233
E - PC Upper	N/A	N/A	N/A	N/A		5.427079167	0.004233
E - SA Lower	865.6737	913.2515	527.7357	2750.1622		5.42708E-06	0.004233
E - SA Upper	N/A	N/A	N/A	N/A		5.42708E-06	0.004233
F - PC Lower	7.2	5.65	10.15	9.45		5.427079167	0.004233
F - PC Upper	N/A	N/A	N/A	N/A		5.427079167	0.004233
F - SA Lower	1492.7552	912.6838	1647.3832	2399.0593		5.42708E-06	0.004233
F - SA Upper	N/A	N/A	N/A	N/A		5.42708E-06	0.004233

Table H.7: Data table for study 2 continued.

Test Method 1 Configuration 1-Edge Effect Benchtop Cut										
Scanner Sample										
	1	2	3	4	5	CF	A	N	I	L
A - PC Lower	86	94	142	211		0.0229167	0.5	3	20	8
A - PC Upper	115	114	170	253		0.0229167	0.5	3	20	8
A - SA Lower	443857.04	478689.28	776391.6	857024.2		0.0229167	0.5	3	20	8
A - SA Upper	548119.29	563177.66	899020.89	1007607.9		0.0229167	0.5	3	20	8
B - PC Lower	0	0	0	0		0.0229167	0.5	3	20	8
B - PC Upper	0	0	0	0		0.0229167	0.5	3	20	8
B - SA Lower	2112.2438	9942.9501	0	0		0.0229167	0.5	3	20	8
B - SA Upper	N/A	N/A	0	0		0.0229167	0.5	3	20	8
B - PC Lower						0.0229167	0.5	3	20	8
B - PC Upper						0.0229167	0.5	3	20	8
B - SA Lower						0.0229167	0.5	3	20	8
B - SA Upper						0.0229167	0.5	3	20	8
C - PC Lower	173	65	149	110		0.0229167	0.5	3	20	8
C - PC Upper	192	79	172	125		0.0229167	0.5	3	20	8
C - SA Lower	872890.19	409050.86	1114553.5	520581.76		0.0229167	0.5	3	20	8
C - SA Upper	1006175	472280.36	1284702.6	596785.43		0.0229167	0.5	3	20	8
D - PC Lower	10.7	262	178	453		0.0229167	0.5	3	20	8
D - PC Upper	N/A	297	221	519		0.0229167	0.5	3	20	8
D - SA Lower	2560.9321	1179111.7	1218893.9	2180623.3		0.0229167	0.5	3	20	8
D - SA Upper	N/A	1336729.5	1389043	2517065.7		0.0229167	0.5	3	20	8
E - PC Lower	136	54	64	190		0.0229167	0.5	3	20	8
E - PC Upper	156	66	77	235		0.0229167	0.5	3	20	8
E - SA Lower	592252.28	190548.24	367080.22	753804.06		0.0229167	0.5	3	20	8
E - SA Upper	676297.76	227047.85	424838.69	908842.69		0.0229167	0.5	3	20	8
F - PC Lower	104	92	120	174		0.0229167	0.5	3	20	8
F - PC Upper	121	113	155	212		0.0229167	0.5	3	20	8
F - SA Lower	479627.17	496561.32	802496.24	654309.42		0.0229167	0.5	3	20	8
F - SA Upper	553095.32	568752.9	957534.88	832873.5		0.0229167	0.5	3	20	8

Table H.8: Data table for study 3.

Test Method 1 Configuration 1-Abrasive Test							
Microscope Sample							
Data Set	1	2	3	4	5	CF	A2
X - PC Lower	2.8	0.9	1.6			369.04138	0.004233
X - PC Upper	2.8	0.9	1.6			369.04138	0.004233
X - SA Lower	586.8837	126.676	295.3071			369.04138	0.004233
X - SA Upper	586.8837	126.676	295.3071			369.04138	0.004233
Y - PC Lower	10.25	4.95	2.8			369.04138	0.004233
Y - PC Upper	10.25	4.95	2.8			369.04138	0.004233
Y - SA Lower	1619.7286	849.2106	429.4712			369.04138	0.004233
Y - SA Upper	1619.7286	849.2106	429.4712			369.04138	0.004233
Z - PC Lower	8	29.05	16.65			369.04138	0.004233
Z - PC Upper	8	29.05	16.65			369.04138	0.004233
Z - SA Lower	902.8439	4591.1008	1921.6047			369.04138	0.004233
Z - SA Upper	902.8439	4591.1008	1921.6047			369.04138	0.004233

Test Method 1 Configuration 1-Abrasive Test										
Scanner Sample										
	1	2	3	4	5	CF	A	N	I	L
X - PC Lower	25	18	42			1.5583333	0.5	1	30	4
X - PC Upper	28	21	54			1.5583333	0.5	1	30	4
X - SA Lower	190704.56	48171.138	291189.19			1.5583333	0.5	1	30	4
X - SA Upper	215324.2	64975.023	348374.5			1.5583333	0.5	1	30	4
Y - PC Lower	117	102	271			1.5583333	0.5	1	30	4
Y - PC Upper	138	139	311			1.5583333	0.5	1	30	4
Y - SA Lower	704564.76	605877.76	1725928.4			1.5583333	0.5	1	30	4
Y - SA Upper	835192.18	765866.38	2096708			1.5583333	0.5	1	30	4
Z - PC Lower	226	278	192			1.5583333	0.5	1	30	4
Z - PC Upper	294	376	212			1.5583333	0.5	1	30	4
Z - SA Lower	1191799.3	1632608.2	1108561.4			1.5583333	0.5	1	30	4
Z - SA Upper	1476397.2	2117758.5	1347723.7			1.5583333	0.5	1	30	4

Table H.8: Data table for study 3 continued.

Test Method 1 Configuration 1-Abrasive Test							
Microscope Sample							
Data Set	1	2	3	4	5	CF	A2
A - PC Lower	2.8	2.45	2.45			246.02759	0.004233
A - PC Upper	N/A	N/A	N/A			246.02759	0.004233
A - SA Lower	446.9345	361.835	267.7065			0.000246	0.004233
A - SA Upper	N/A	N/A	N/A			0.000246	0.004233
B - PC Lower	2.65	1.45	1.6	1.15	0.95	246.02759	0.004233
B - PC Upper	N/A	N/A	N/A	N/A	N/A	246.02759	0.004233
B - SA Lower	483.9695	308.6613	128.1358	185.7158	164.5221	0.000246	0.004233
B - SA Upper	N/A	N/A	N/A	N/A	N/A	0.000246	0.004233
B - PC Lower	1.15	0.95	1.7	1.55	3.35	246.02759	0.004233
B - PC Upper	N/A	N/A	N/A	N/A	N/A	246.02759	0.004233
B - SA Lower	98.8051	137.8947	395.2476	15501.259	43846.417	0.000246	0.004233
B - SA Upper	N/A	N/A	N/A	24723.856	52756.384	0.000246	0.004233
C - PC Lower	1.45	1.9	2.05			246.02759	0.004233
C - PC Upper	N/A	N/A	N/A			246.02759	0.004233
C - SA Lower	185.9862	395.3558	265.3547			0.000246	0.004233
C - SA Upper	N/A	N/A	N/A			0.000246	0.004233
D - PC Lower	1.3	1.6	1.25			246.02759	0.004233
D - PC Upper	N/A	N/A	N/A			246.02759	0.004233
D - SA Lower	149.3296	131.6501	203.8549			0.000246	0.004233
D - SA Upper	N/A	N/A	N/A			0.000246	0.004233
E - PC Lower	1.25	2.15	1.7			246.02759	0.004233
E - PC Upper	N/A	N/A	N/A			246.02759	0.004233
E - SA Lower	177.8493	295.3612	263.5435			0.000246	0.004233
E - SA Upper	N/A	N/A	N/A			0.000246	0.004233
F - PC Lower	2.35	3.05	3			246.02759	0.004233
F - PC Upper	N/A	N/A	N/A			246.02759	0.004233
F - SA Lower	400.3028	428.9306	609.0506			0.000246	0.004233
F - SA Upper	N/A	N/A	N/A			0.000246	0.004233

Table H.8: Data table for study 3 continued.

Test Method 1 Configuration 1-Abrasive Test										
Scanner Sample										
	1	2	3	4	5	CF	A	N	I	L
A - PC Lower	25	8	13			1.0388889	0.5	3	20	8
A - PC Upper	30	8	13			1.0388889	0.5	3	20	8
A - SA Lower	86598.627	72842.889	46165.093			1.0388889	0.5	3	20	8
A - SA Upper	102881.46	83576.533	52678.226			1.0388889	0.5	3	20	8
B - PC Lower	6	11	30	8	19	1.0388889	0.5	3	20	8
B - PC Upper	11	14	36	11	24	1.0388889	0.5	3	20	8
B - SA Lower	15501.259	43846.417	145633.67	26234.903	71800.	1.0388889	0.5	3	20	8
B - SA Upper	24723.856	52756.384	167491.75	32617.774	95039.	1.0388889	0.5	3	20	8
B - PC Lower	15	12	8	4	13	1.0388889	0.5	3	20	8
B - PC Upper	17	17	9	7	18	1.0388889	0.5	3	20	8
B - SA Lower	38271.174	31653.83	28683.841	14797.84	42648	1.0388889	0.5	3	20	8
B - SA Upper	48014.823	44601.94	35509.606	22561.496	58774.	1.0388889	0.5	3	20	8
C - PC Lower	11	20	18			1.0388889	0.5	3	20	8
C - PC Upper	18	29	25			1.0388889	0.5	3	20	8
C - SA Lower	56638.212	53746.38	37958.544			1.0388889	0.5	3	20	8
C - SA Upper	72061.313	75995.245	52417.701			1.0388889	0.5	3	20	8
D - PC Lower	16	7	13			1.0388889	0.5	3	20	8
D - PC Upper	19	12	16			1.0388889	0.5	3	20	8
D - SA Lower	66433.965	21154.659	58149.259			1.0388889	0.5	3	20	8
D - SA Upper	76281.823	35275.133	78704.709			1.0388889	0.5	3	20	8
E - PC Lower	3	5	3			1.0388889	0.5	3	20	8
E - PC Upper	4	8	4			1.0388889	0.5	3	20	8
E - SA Lower	7034.1845	10186.541	11567.326			1.0388889	0.5	3	20	8
E - SA Upper	11567.326	15865.994	15996.257			1.0388889	0.5	3	20	8
F - PC Lower	10	8	13			1.0388889	0.5	3	20	8
F - PC Upper	13	9	15			1.0388889	0.5	3	20	8
F - SA Lower	30377.256	19539.402	47337.457			1.0388889	0.5	3	20	8
F - SA Upper	37411.441	23812.017	59503.991			1.0388889	0.5	3	20	8

Table H.9: Data table for study 4.

Electrical Tape											
Scanner Samples											
ID	1	2	3	4	5	6	CF	A	N	I	L
A - PC Lower	27	40		46	37	37	93.5	0.5	1	1	1
A - PC Upper	47	68		64	83	83	93.5	0.5	1	1	1
A - SA Lower	574093.7	473921.7		1102074	482649.3	482649.3	93.5	0.5	1	1	1
A - SA Upper	789027.1	785744.5		1474495	1014434	1014434	93.5	0.5	1	1	1
B - PC Lower	47	7	74	10	15	39	93.5	0.5	1	1	1
B - PC Upper	82	21	98	25	38	96	93.5	0.5	1	1	1
B - SA Lower	401183	50463.76	930231.8	130106.4	121144.3	395190.9	93.5	0.5	1	1	1
B - SA Upper	729028.1	146180.8	1477700	248593.3	279595.8	908764.5	93.5	0.5	1	1	1
C - PC Lower	8	42	34	32	10	21	93.5	0.5	1	1	1
C - PC Upper	25	75	57	54	37	51	93.5	0.5	1	1	1
C - SA Lower	124296.6	511072.6	682941.2	426584.2	98921.48	180309.6	93.5	0.5	1	1	1
C - SA Upper	236531	939219.9	977569.3	680883	288662.1	471108	93.5	0.5	1	1	1
D - PC Lower	36	24	16	22	32	34	93.5	0.5	1	1	1
D - PC Upper	86	72	51	41	87	86	93.5	0.5	1	1	1
D - SA Lower	413662.2	331388.2	156914.4	604470.9	393054.6	443857	93.5	0.5	1	1	1
D - SA Upper	885786.2	699797.2	429371.8	852386.8	855643.4	849729.5	93.5	0.5	1	1	1
E - PC Lower	18	47	34	30		0	93.5	0.5	1	1	1
E - PC Upper	32	79	65	53		0	93.5	0.5	1	1	1
E - SA Lower	189167.5	835452.7	838631.1	739397		0	93.5	0.5	1	1	1
E - SA Upper	316850.9	1280691	1298875	1068883		0	93.5	0.5	1	1	1
F - PC Lower	23	14	9	15	11	19	93.5	0.5	1	1	1
F - PC Upper	33	26	23	24	20	36	93.5	0.5	1	1	1
F - SA Lower	582456.5	442059.4	183409.8	176089.1	118721.4	238667.3	93.5	0.5	1	1	1
F - SA Upper	760786.1	575161.8	296686.3	256956.2	189610.4	384848.1	93.5	0.5	1	1	1

Table H.9: Data table for study 4 continued.

Paper Safe Tape														
Scanner Sample														
ID	1	2	3	4	5	6	7	8	9	CF	A	I	N	L
A - PC (L)	18	12	24	33	13	21	20	9	20	18.7	1	5	1	1
A - PC (U)	26	21	30	45	15	25	25	12	25	18.7	1	5	1	1
A - SA (L)	96472.	55648.22	91991.5	27123 2.9	74171.57	10590 3.6	13156 5.3	82612.59	15001 0.5	18.7	1	5	1	1
A - SA (U)	13844 3.2	92747.03	12390 5.9	34837 4.5	90532.56	13156 5.3	16788 2.5	10431 4.4	19062 6.4	18.7	1	5	1	1
B - PC (L)	97	37	20	27	41	9	39	15	29	18.7	1	5	1	1
B - PC (U)	124	55	31	36	50	20	51	24	33	18.7	1	5	1	1
B - SA (L)	66673 6.5	22603 1.8	13724 4.8	30353 8	24043 8.8	58540.05	33527 0.1	92799.13	18781 2.7	18.7	1	5	1	1
B - SA (U)	84319 0.3	32083 7	19026 1.7	36205 2.1	30752 4.1	10465 3	41569 4.3	13338 9	23246 6.8	18.7	1	5	1	1
C - PC (L)	69	20	26	22	16	26	44	13	35	18.7	1	5	1	1
C - PC (U)	109	29	30	27	23	27	51	16	43	18.7	1	5	1	1
C - SA (L)	48447 2.9	91887.29	14889 0.2	15600 2.6	12820 4.5	17892 8.8	33628 6.1	92720.97	17491 6.7	18.7	1	5	1	1
C - SA (U)	72597 9.9	13172 1.6	19515 9.5	19104 3.2	17134 7.5	20237 6.1	43419 1.6	12002 4	22478 1.3	18.7	1	5	1	1
D - PC (L)	154	81	231	108	61	143	141	95	145	18.7	1	5	1	1
D - PC (U)	232	137	357	182	90	211	252	174	250	18.7	1	5	1	1
D - SA (L)	83021 6.1	48163 3.2	14348 95	73460 3.3	39972 4	84702 0	10424 40	54270 0.4	12800 13	18.7	1	5	1	1
D - SA (U)	11909 92	73199 8.1	20675 03	11275 02	54004 3	11931 80	15899 60	87427 1	18449 10	18.7	1	5	1	1
E - PC (L)	109	53	51	199	199	74	165	24	148	18.7	1	5	1	1
E - PC (U)	185	80	70	317	317	106	228	21	232	18.7	1	5	1	1
E - SA (L)	63755 7.6	36700 2.1	23692 1.8	13895 38	13895 38	41676 2.4	13024 70	21581 9.2	10005 74	18.7	1	5	1	1
E - SA (U)	10759 96	52336 9.4	34574 3.2	22278 57	22278 57	59035 0.4	17551 07	17822 5.4	14999 23	18.7	1	5	1	1
F - PC (L)	45	143	157	202	132	50	22	136	138	18.7	1	5	1	1
F - PC (U)	68	295	261	364	216	76	40	216	198	18.7	1	5	1	1
F - SA (L)	22777 7.3	78353 0	94557 6.8	91994 1.1	69617 5.8	20175 0.8	99182	90748 8	60210 0.1	18.7	1	5	1	1
F - SA (U)	34582 1.4	14353 64	15047 94	16510 79	10950 66	31203 1.2	17296 2.8	13190 14	88818 3	18.7	1	5	1	1

- (L) = Lower and (U) = Upper

APPENDIX I. IMAGEJ PROGRAM FOR A SINGLE IMAGE

```
// Separate photos

//Ratio Analysis with the use of parimeters, area and feret diameters



//User Input Section



//Manual Calibration Section



PS = 0.1959183;

P1 = 0.9175;                    //Pixel Size Array, Replace the following with the first as
the default

P15 = 1.36;

P2 = 1.784;

P3 = 2.704;

P4 = 3.532;



PixelSize =newArray(6);

PixelSize[0] = PS;
```

```
PixelSize[1] = P1;

PixelSize[2] = P15;

PixelSize[3] = P2;

PixelSize[4] = P3;

PixelSize[5] = P4;



AdaptiveStep = true;

sig = 3.0;

sigGuess = 3.0;

sigLower = 0.4;

sigUpper = 0.8;



ThresholdRange = false;

sigT1 = 3.2;

sigT2 = 3.8;



Tsetfilter = 70;

Calibration = false;                    //Threshold Calibration  //Manual Mode Only
```

```
Sigstart2 = 1.5;                //Starting range for the minimum brightness threshold

Sigend = 6;                     //Ending range for the minimum brightness threshold

Sigstep = 0.1;                  //specific iterations based on start and end points of
brightness threshold

//Confidence Interval

Auto = false;                   //Autorun threshold

AutoMethod = "Yen"              //Chose autothreshold method

blackObjects = false;           //Black Objects on white background = True

SubBackground = false;          //Subtract the background

Nsm = 2;                        //Smoothing, # of times. Only in Auto Mode

N = 1;                          //Number of separate files to open

N2 = 1;                         //Despeckle iterations

P = 1;                          //Pixels per unit

R = 1;                          //Pixel Ratio

D = 1;                          //Distance

SRange1 = 0     ;               //Distribution starting range

SRange2 = 600;                  // Distribution ending range

SBins = 600     ;               //Bins within Distribution
```

```
SArea = true;

Split = 60;

SplitTop = true;

PrintDist = true;

PrintSphere = true;

////////////////////////////////////////////////////////////////////////////////////////////////////
/

//End User Input Section

//Do not touch



MicroA = true;

run("Open...");

Dialog.create("");

//Dialog.addCheckbox("Threshold Calibration",Calibration);

Dialog.addCheckbox("Adaptive Step ",AdaptiveStep);

Dialog.addCheckbox("Threshold Range"ThresholdRange);

Dialog.addMessage("xxxxxxxxx Additional Picks xxxxxxxxxxx");
```

```
//Dialog.addCheckbox("Click for Auto Method",Auto);

//          Dialog.addChoice("AutoMethod",newArray("Yen","Triangle"))

//Dialog.addCheckbox("Black Objects on White Background",blackObjects);

Dialog.addCheckbox("Subtract Background",SubBackground);

//Dialog.addNumber("Standard Deviation for Manual",sig);

Dialog.addNumber("Set Average Brightness to ",Tsetfilter);

Dialog.addMessage("xxxxxxxxxxx Fill in All Values xxxxxxxxxxxx");

Dialog.addNumber("Smoothing Iterations",Nsm);

//Dialog.addNumber("Number of Samples",N);

Dialog.addNumber("Despeckle Iterations",N2);

Dialog.addChoice("Pixel Size",PixelSize);

Dialog.addNumber("Lower Bin Range",SRange1);

Dialog.addNumber("Upper Bin Range",SRange2);

Dialog.addNumber("Number of Bins",SBins);

Dialog.addCheckbox(" Count only above ", SplitTop);

Dialog.addNumber("Count above",Split);

Dialog.addCheckbox("Include Sphericity in Calculation",PrintSphere);

Dialog.addCheckbox("Includes the particle size distribution",PrintDist);
```

```
Dialog.show();

debugMode = false;                  //Activate Log Input of specific locations

//Calibration = Dialog.getCheckbox();              // Activates the manual brightness calibration
for particle detection

AdaptiveStep = Dialog.getCheckbox();

ThresholdRange = Dialog.getCheckbox();

//Auto = Dialog.getCheckbox();                              //Autorun threshold

//        AutoMethod = Dialog.getChoice();        //chose autothreshold method

//blackObjects = Dialog.getCheckbox();            //Black Objects on white background = True

SubBackground = Dialog.getCheckbox();           //Subtract Background, Only in Auto Mode

//sig = Dialog.getNumber();                                 //Standard Deviation for only
single run

Tsetfilter = Dialog.getNumber();

Nsm = Dialog.getNumber();                                         //Smoothing, # of
times. Only in Auto Mode

//N = Dialog.getNumber();                           //Number of separate files to open

N2 = Dialog.getNumber();                          //Despeckle iterations

BW = false ;

P = Dialog.getChoice();                           //Pixels per unit
```

```
R = 1;                          //Pixel Ratio

D = 1;                          //Distance

SRange1 = Dialog.getNumber();       //Distribution starting range

SRange2 = Dialog.getNumber();       // Distribution ending range

SBins = Dialog.getNumber();         //Bins within Distribution

SplitTop = Dialog.getCheckbox();

Split = Dialog.getNumber();

PrintSphere = Dialog.getCheckbox();         // prints the sphericity at the end of the
document

PrintDist = Dialog.getCheckbox();           // prints the particle size distribution.



t5 =
newArray(100,12.706,4.303,3.182,2.776,2.571,2.447,2.365,2.306,2.262,2.228,2.201,2.179,2.160
,2.145,2.131,2.12,2.11,2.101,2.093,2.086,2.080,2.074,2.069,2.064,2.06,2.056,2.052,2.048,2.045,
2.042);

t10 =
newArray(6.314,2.920,2.353,2.132,2.015,1.943,1.895,1.860,1.833,1.812,1.796,1.782,1.771,1.76
1,1.753,1.746,1.740,1.734,1.729,1.725,1.721,1.717,1.714,1.711,1.708,1.706,1.703,1.701,1.699,1
.697);
```

```
if(Calibration == true)

{

Dialog.create("");

Dialog.addNumber("Starting Threshold Sigma",Sigstart2);

Dialog.addNumber("Ending Threshold Sigma",Sigend);

Dialog.addNumber("Threshold Interval",Sigstep);

Dialog.show();

Sigstart2 = Dialog.getNumber();              //Starting range for the minimum brightness threshold

Sigend = Dialog.getNumber();                          //Ending range for the minimum brightness
threshold

Sigstep = Dialog.getNumber();    //specific iterations based on start and end points of brightness
threshold

}

if(ThresholdRange == true)

{

Dialog.create("");

Dialog.addNumber("Sigma for lower Range",sigT1);

Dialog.addNumber("Sigma for upper Range",sigT2);
```

```
Dialog.show();

sigT1 = Dialog.getNumber();                //Starting range for the minimum brightness threshold

sigT2 = Dialog.getNumber();                        //Ending range for the minimum brightness

threshold

}

if(AdaptiveStep == true)

{

Dialog.create("");

Dialog.addNumber("Guess Value for Sigma",sigGuess);

Dialog.addNumber("Ending Threshold Sigma",sigLower);

Dialog.addNumber("Threshold Interval",sigUpper);

Dialog.show();

sigGuess = Dialog.getNumber();          //Starting range for the minimum brightness threshold

sigLower = Dialog.getNumber();                     //Ending range for the minimum brightness

threshold

sigUpper = Dialog.getNumber();

}

///(2)///          Dafult Parameter Sets and Introduction Calculations
```

```
// Determination of t

if(N > 29)

{

t55 = -0.000612821*N+2.049051282;

t1010 = -0.000386667*N+ 1.7016666;

}

else

{

t55 = t5[N];

t1010 = t10[N];

}



if(ThresholdRange == true)

{

AdaptiveLoop = 1;

}

Sigstart = Sigstart2 - Sigstep;

Sigiter = ((Sigend-Sigstart)/Sigstep);
```

```
if(MicroA == true)

{

Median = newArray(N);

}

// Failsafe for Calibration

if(Calibration == true)

{

N = Sigiter;

Auto = false;

SArea = false;

MicroA = false;

Nsm = 0;

N2 = 0;

}

x8 = 1;

kountrenew = 0;

AdaptiveFinal = 0;

AdaptiveMatrix = newArray(40);
```

```
AdaptiveMatrix[0] = 100000000000;

AdaptiveMatrix[1] = 100000000000;

AdaptiveT = newArray(4);

AdaptiveLoop = 0;

FirstMove = 0;

ParticleCountLower = "N/A";

areaCountLower = "N/A";

k6 = 2;

if(AdaptiveStep == false)

{

AdaptiveLoop = 2;

}

if(ThresholdRange == true)

{

AdaptiveLoop = 1;

}

///(3)///          Beginning of Loops and Imaging Adaptations

CalibrateCount = newArray(N+1);
```

```
CalibrateArea = newArray (N+1);

// Starting of Main Loop

while(AdaptiveLoop < 3)

{

if(AdaptiveLoop > 0)

{

AdaptiveStep = false;

AdaptiveFinal = 2;

}

for(x=0; x<N;x++)

{

if(AdaptiveStep == false)

{

AdaptiveFinal = 2;

}

while(AdaptiveFinal <3)

{

if(AdaptiveStep == false)
```

```
{
AdaptiveFinal = 3;
}
a = getTitle();
//Duplicating Step

run("Duplicate...","  ");
if(debugMode == true)
{
print("Duplicate");
}
//8 Bit Gray
run("8-bit");
if(debugMode == true)
{
print("8bit Gray");
}
//Subtract Background
```

```
if(SubBackground == true)

{

if(blackObjects == true)

{

xa2 = " light";

}

else

{

xa2 = " " ;

}

run("Subtract Background...", "rolling=50"+ xa2);

if(debugMode == true)

{

print("Sub Background");

}

}

//Measure Mean Brightness

if(Auto == false)
```

```
{

TempName = getTitle();

run("Set Measurements...", " mean standard skewness area perimeter feret's redirect=None
decimal=5");

run("Measure");

meanCount = getValue("results.count");

Tmean = getResult("Mean", meanCount-1 );

Skew = getResult("Skew",meanCount - 1);

Deviation = getResult("StdDev",meanCount - 1);

FindArea = getResult("Area",meanCount - 1);;

//Adapt Brightness of Image to Standard

if(Calibration == false)

{

Tdiff = round(Tmean - Tsetfilter);

setMinAndMax(Tdiff, 255+Tdiff);

call("ij.ImagePlus.setDefault16bitRange", 8);

run("Apply LUT");

Tmean = Tmean -Tdiff;
```

```
}

//print brightness for calibration

if(Calibration == true){if(x == 0)

{

print("Skewness = " + Skew);

print("Standard Deviation = "+Deviation);

print("Brightness Mean "+ Tmean);

}

}

//Hoopla

selectWindow("Results");

IJ.deleteRows(meanCount - 1, meanCount - 1);

selectWindow(TempName);

run("Set Measurements...", " mean standard skewness area perimeter feret's redirect=None
decimal=5");

if(debugMode == true)

{

print("Measure Mean Brightness");
```

```
}

}

// Smoothing a Nsm Incr and despeck N2 incr

if(AdaptiveStep == false)

{

for(xx = 0; xx<N2; xx++)

{

run("Despeckle"," ");

if(debugMode == true){print("Despeckle "+xx+1);}

}

for (xx = 0; xx <Nsm; xx++)

{

run("Smooth");

if(debugMode == true){print("Smoothing "+ xx+1);}

}

}

///(4)///          Threshold Determination and Analysis

//Auto Threshold
```

```
if (Auto == true)

{

rename("2");

if(blackObjects == true)

{

run("Auto Threshold", "method="+AutoMethod+" White_objects_on_black_Background");
                        //Auto Threshold Color

}

else

{

run("Auto Threshold", "method="+AutoMethod+" white");

}



if(debugMode == true){print("Auto Threshold");}

}

//Manual Threshold

else

{
```

```
Tad = 0;

T2=255;

if(Calibration == true)

{

sig=(Sigend-Sigstart)*x8/N + Sigstart;

x8++;

Tad = 0;

}

T = Tmean+sig*Deviation;

if(ThresholdRange == true)

{

AdaptiveT1 = Tmean+sigT1*Deviation;

AdaptiveT2 = Tmean + sigT2*Deviation;

}

//AutoAdaptive Section of Manual

if(AdaptiveFinal == 0 )

{

if(k6 == 2)
```

```
{
T = Tmean+sigGuess*Deviation;
}
if(k6 > 2)
{
T = AdaptiveT;
}
}
if(FirstMove >0)
{
if(AdaptiveLoop == 2)
{
T = AdaptiveT2;
}
}
if(AdaptiveLoop == 1)
{
T = AdaptiveT1;
```

```
}

//End of AutoAdaptive

T3 = T;

T = T3 - Tad;

if(blackObjects == true)

{

T2 = T-Tad;

T = 255 ;

}

setThreshold(T,T2);

Tdid = T;

T = T+ Tad;

rename("2");

if(debugMode == true)

{

print("Manual Threshold");

}

}
```

```
selectWindow("2");

//Analysis section, Set the measurements, set the scale and analyse the particles

run("Set Measurements...", " mean standard skewness area perimeter feret's redirect=None
decimal=5");

run("Set Scale...", "distance="+P+" known="+D+" pixel="+R+" unit=µm global");

run("Analyze Particles...", "display");

if(debugMode == true){print("Analyze Particles");}



//Standard Analysis

if(MicroA == true)

{

Tol = 1;

kount19 = 0;

Kount = getValue("results.count");

X1 = newArray(Kount-kountrenew);

X2 = newArray(Kount-kountrenew);

//Segregation of particle size range in the calculation of Confidence Interval

for (x5 = kountrenew; x5<(Kount);x5++)
```

```
{
x44 = x5-kountrenew;
X2[x44] = getResult("Area",x5);
X1[x44] = sqrt(X2[x44]*4/3.1415);
if(SplitTop == true)
{
if(X1[x44] > Split)
{
kount19++;
}
}
else
{
if(X1[x44]<Split)
{
kount19++;
}
}
```

```
}

X3 = newArray(kount19+1);

kount19 = 0;

for (x5 = 1; x5<(Kount-kountrenew);x5++)

{

if(SplitTop == true)

{

if(X1[x5] > Split)

{

kount19++;

X3[kount19] = X1[x5];

}

}

else

{

if(X1[x5]<Split)

{

kount19++;
```

```
X3[kount19] = X1[x5];

}

}

}

//Sorting from smallest to largest

if(AdaptiveLoop > 1)

{

while( Tol > 0)

{

Tol = 0;

for(x5 = 1; x5<kount19-1;x5++)

{

if(X3[x5]>X3[x5+1])

{

switch1 = X3[x5];

switch2 = X3[x5+1];

X3[x5] = switch2;

X3[x5+1] = switch1;
```

```
Tol++;

}

}

}

Kount12 = kount19/2;

KountPick=round(Kount12);

Median[x] = X3[KountPick];

}

else

{

Median[x] = 1;

}

//AutoAdaptive New Threshold Calculation

if(AdaptiveFinal == 0 )

{

adaptSum = 0;

for(k5 = kountrenew; k5 < Kount; k5++)

{
```

```
adaptSum = getResult("Area",k5)+ adaptSum;

}

AdaptiveMatrix[k6] = adaptSum/(Kount-kountrenew);

if(AdaptiveMatrix[k6-1]<AdaptiveMatrix[k6])

{

if(AdaptiveMatrix[k6 - 2]< AdaptiveMatrix[k6])

{

if(AdaptiveMatrix[k6 - 3]< AdaptiveMatrix[k6])

{

if(AdaptiveMatrix[k6 - 4] < AdaptiveMatrix[k6])

{

AtaptiveStep = true;

AdaptiveFinal = 3;

AdaptiveTFinal = T+3;

AdaptiveT1 = Deviation*sigLower+AdaptiveTFinal;

AdaptiveT2 = Deviation*sigUpper+AdaptiveTFinal;

}

}
```

```
else

{

AdaptiveT = T-1;

}

}

else

{

AdaptiveT = T-1;

}

}

else

{

AdaptiveT = T-1;

}

k6++;

}

kountrenew = Kount;

}
```

```
////((5))///                    Section on results stacking and Closing

//Close Exisiting Windows and Open Next Selection

selectWindow("2");

run("Close");

selectWindow(a);

if(debugMode == true)

{

print(x+" Finished");

}

if(AdaptiveLoop > 1)

{

if (x < N-1)

{

run("Open Next");

}

else

{

selectWindow(a);
```

```
run("Close");

}

}

}

};

// End of Main Loop

//Standard Analysis for Stacked

if(MicroA == true)

{

x22 = 0;

for (x7 = 0; x7 <N;x7++)

{

x22 = Median[x7]+x22;

}

//Find the Standard Deviation of all the Median Values

MedianAv = x22/N;

for (x7 = 0; x7 <N;x7++)

{
```

```
x23 = (Median[x7]-MedianAv)*(Median[x7]-MedianAv)+x23;

}

MedianSTDEV = sqrt(x23/N);

E = MedianAv * 0.05;

Num = (t55*MedianSTDEV/E)*(t55*MedianSTDEV/E);

E = MedianAv * 0.1;

Num2 = (t1010*MedianSTDEV/E)*(t1010*MedianSTDEV/E);

EE = t55*MedianSTDEV/sqrt(N);

if(debugMode == true)

{

print("External Microscope Analysis Complete");

}

}

// Stacked Distribution Formulation

if(Calibration == false)

{

//Results Section

selectWindow("Results");
```

```
if(SArea == true)

{

kount2 = getValue("results.count");

SurfaceArea = newArray(kount2+1);

AreaFeret = newArray(kount2+1);

effArea = newArray(kount2+1);

Volume = newArray(kount2+1);

eps = newArray(kount2+1);

ActualVolume = newArray(kount2+1);

alpha = newArray(kount2+1);

aDiameter = newArray(kount2+1);

kk2 = newArray(kount2+1);

Sphericity = newArray(kount2+1);

ShortFeret = newArray(kount2+1);

CumVol = newArray(SRange2);

CumSphere = newArray(SRange2);

Index = 0;

areaCountUpper = 0;
```

```
Sum7 = 0;

particleCountUpper = 0;

nTop = 0;

TopVolume = 0;

FiberVol = 0;

kount5 = 0;

TVolume = 0;

if(SplitTop == true)

{

Stringg = "above";

for(x40 = 1; x40<kount2;x40++)

{

SurfaceArea[x40] = getResult("Area",x40);

AreaFeret[x40] = getResult("Feret",x40);

Index = SurfaceArea[x40] + Index;

ShortFeret[x40] = getResult("MinFeret",x40);

aDiameter[x40] = sqrt(SurfaceArea[x40]*4/3.1415);

if(aDiameter[x40]<SRange2)
```

```
{
if(aDiameter[x40]>Split)
{
alpha[x40] = SurfaceArea[x40]/(ShortFeret[x40]*AreaFeret[x40]);
aDiameter[x40] = sqrt(SurfaceArea[x40]*4/3.1415);
Volume[x40] = 4*3.1415*aDiameter[x40]*aDiameter[x40]*aDiameter[x40]/24;
kk2[x40] = AreaFeret[x40]/ShortFeret[x40];
Sphericity[x40] = (2*kk2[x40])/(1+2*kk2[x40]);
Darray = round(aDiameter[x40]);
if(Darray < SRange2)
{
CumVol[Darray]++;
kount5++;
CumSphere[Darray] = CumSphere[Darray]+kk2[x40];
}
nTop = aDiameter[x40]+nTop;    // mean Top
Sum7 = SurfaceArea[x40]*aDiameter[x40]+Sum7; ///Surface Top
TopVolume = Volume[x40]*aDiameter[x40]+TopVolume;          //Top Volume
```

```
areaCountUpper=SurfaceArea[x40]+areaCountUpper;  // Total Surface Vol

TVolume = Volume[x40] +TVolume; //Volume Total

if(kk2[x40]>2.3)

{

FiberVol = SurfaceArea[x40]+FiberVol;

}

if(alpha[x40]<0.35)

{

if(kk2[x40]<2.3)

{

FiberVol = SurfaceArea[x40]+FiberVol;

}

}

particleCountUpper++;

}

}

}

}
```

```
else

{

Stringg = "below";

for(x40 = 1; x40<kount2;x40++)

{

SurfaceArea[x40] = getResult("Area",x40);

AreaFeret[x40] = getResult("Feret",x40);

Index = SurfaceArea[x40] + Index;

ShortFeret[x40] = getResult("MinFeret",x40);

aDiameter[x40] = sqrt(SurfaceArea[x40]*4/3.1415);

if(aDiameter[x40]<Split+1)

{

alpha[x40] = SurfaceArea[x40]/(ShortFeret[x40]*AreaFeret[x40]);

Volume[x40] = 4*3.1415*aDiameter[x40]*aDiameter[x40]*aDiameter[x40]/24;

kk2[x40] = AreaFeret[x40]/ShortFeret[x40];

Sphericity[x40] = (2*kk2[x40])/(1+2*kk2[x40]);

Darray = round(aDiameter[x40]);

if(Darray < SRange2)
```

```
{
CumVol[Darray]++;
kount5++;
CumSphere[Darray] = CumSphere[Darray]+kk2[x40];
}
nTop = aDiameter[x40]+nTop;                                          // mean Top
Sum7 = SurfaceArea[x40]*aDiameter[x40]+Sum7;          ///Surface Top
TopVolume = Volume[x40]*aDiameter[x40]+TopVolume;     //Top Volume
areaCountUpper=SurfaceArea[x40]+areaCountUpper;    // Total Surface Vol
TVolume = Volume[x40] +TVolume;                                      //Volume Total
if(kk2[x40]>2.3)
{
FiberVol = SurfaceArea[x40]+FiberVol;
}
if(alpha[x40]<0.35)
{
if(kk2[x40]<2.3)
{
```

```
FiberVol = SurfaceArea[x40]+FiberVol;

}

}

particleCountUpper++;

}

}

}

areaCountUpper = areaCountUpper/N;

TVolume2 = TVolume/N;

particleCountUpper=particleCountUpper/N;

meanSurfaceDiameter = Sum7/areaCountUpper;

FiberVol2 = FiberVol/N;

nTop2 = nTop/N;

TopVolume2 = TopVolume / N;

STop = Sum7/N;

MeanCount2 = nTop2/particleCountUpper;

MeanSurface = STop/areaCountUpper;

MeanVolume = TopVolume2/TVolume;
```

```
if(AdaptiveLoop == 1)

{

areaCountLower = areaCountUpper;

ParticleCountLower = particleCountUpper;

}

if(AdaptiveLoop <2)

{

run("Clear Results");

kountrenew = 0;

}

AdaptiveLoop++;

}

}

FirstMove++;

}

if(Calibration == false)

{

if(SArea == true)
```

```
{

print("Distrubution in terms of um for particles "+Stringg+" " + Split+" um");

print("Total Particle Count per Image");

print(particleCountUpper);

print(ParticleCountLower);

print("Total Area per Image");

print(areaCountUpper);

print(areaCountLower);

print("Sigma used for upper and lower");

print((AdaptiveT1-Tmean)/Deviation+" and " + (AdaptiveT2-Tmean)/Deviation);

print("Mean Particle Diameter");

print(MeanCount2);

print("Mean Surface Particle Diameter");

print(MeanSurface);



if(PrintDist == true)

{

print("Particle Distribution ");
```

```
for(D11 = 0; D11<SRange2;D11++)

{

print(CumVol[D11]/N);

}

}

if(PrintSphere == true)

{

print("Sphericity");

for(D11 = 0; D11<SRange2; D11++)

{

print(CumSphere[D11]/(CumVol[D11]));

}

}

areaCountUpper = 0;

Sum7 = 0;

particleCountUpper = 0;

TVolume = 0;

TopVolume = 0;
```

```
nTop = 0;

FiberVol = 0;

}

}

run("Clear Results");

if(Calibration == true)

{

print("Count xxxxxxxxxxxxxxxxxxxxxxxxxxx");

for(x25 = 0; x25 < N; x25++)

{

print(CalibrateCount[x25]);

}

print("Area xxxxxxxxxxxxxxxxxxxxxxxxxxx");

for(x25 = 0; x25 < N; x25++)

{

print(CalibrateArea[x25]);

}

}
```

```
//selectWindow("Console");

//run("Close");

if(debugMode == true)

{

'Run Complete

}

selectWindow("Results");

run("Close"," ");
```

BIOGRAPHY OF THE AUTHOR

Gregory Kin Yum was born in Portland Maine and raised in Buxton Maine where he attended Bonny Eagle High School until 2009. He attended the University of Maine and graduated in December of 2013 with a degree in Chemical Engineering. He is a candidate for the Master of Science degree in Chemical Engineering from the University of Maine in August 2017.